Bounds on the maximal number of graph embeddings

Evangelos Bartzos

NATIONAL AND KAPODISTRIAN UNIVERSITY OF ATHENS

SCHOOL OF SCIENCES
DEPARTMENT OF INFORMATICS AND TELECOMMUNICATIONS

PROGRAM OF POSTGRADUATE STUDIES

PhD THESIS

Bounds on the maximal number of graph embeddings.

Evangelos Bartzos

ATHENS

ΕΘΝΙΚΟ ΚΑΙ ΚΑΠΟΔΙΣΤΡΙΑΚΟ ΠΑΝΕΠΙΣΤΗΜΙΟ ΑΘΗΝΩΝ

ΣΧΟΛΗ ΘΕΤΙΚΩΝ ΕΠΙΣΤΗΜΩΝ
ΤΜΗΜΑ ΠΛΗΡΟΦΟΡΙΚΗΣ ΚΑΙ ΤΗΛΕΠΙΚΟΙΝΩΝΙΩΝ

ΠΡΟΓΡΑΜΜΑ ΜΕΤΑΠΤΥΧΙΑΚΩΝ ΣΠΟΥΔΩΝ

ΔΙΔΑΚΤΟΡΙΚΗ ΔΙΑΤΡΙΒΗ

Φράγματα του μέγιστου αριθμού εμβυθίσεων γράφων.

Ευάγγελος Μπάρτζος

ΑΘΗΝΑ

PhD THESIS

Bounds on the maximal number of graph embeddings.

Evangelos Bartzos

SUPERVISOR: Ioannis Z. Emiris, Professor ATHENA Research Center

THREE-MEMBER ADVISORY COMMITTEE:

Ioannis Z. Emiris, Professor ATHENA Research Center

Theoharis Theoharis, Professor NKUA

Laurent Busé, Research Director INRIA

SEVEN-MEMBER EXAMINATION COMMITTEE

Ioannis Z. Emiris,
Professor ATHENA Research Center

Theoharis Theoharis,
Professor NKUA

Laurent Busé,
Research Director INRIA

Zissimopoulos Vassilios,
Professor NKUA

Archontia Giannopoulou,

Assistant Professor NKUA

Josef Schicho,
Professor Johannes Kepler University

Skoutas Dimitrios,
Researcher B ATHENA Research Center

Examination Date: 28/04/2022

ΔΙΔΑΚΤΟΡΙΚΗ ΔΙΑΤΡΙΒΗ

Φράγματα του μέγιστου αριθμού εμβυθίσεων γράφων.

Ευάγγελος Μπάρτζος

ΕΠΙΒΛΕΠΩΝ ΚΑΘΗΓΗΤΗΣ: Ιωάννης Ζ. Εμίρης, Καθηγητής ”Αθηνά” Ερευνητικό Κέντρο

ΤΡΙΜΕΛΗΣ ΕΠΙΤΡΟΠΗ ΠΑΡΑΚΟΛΟΥΘΗΣΗΣ:

Ιωάννης Ζ. Εμίρης, Καθηγητής ”Αθηνά” Ερευνητικό Κέντρο

Θεοχάρης Θεοχάρης, Καθηγητής ΕΚΠΑ

Laurent Busé, Διευθυντής Έρευνας INRIA

ΕΠΤΑΜΕΛΗΣ ΕΞΕΤΑΣΤΙΚΗ ΕΠΙΤΡΟΠΗ

Ιωάννης Ζ. Εμίρης,
Καθηγητής ”Αθηνά” Ερευνητικό Κέντρο

Θεοχάρης Θεοχάρης,
Καθηγητής ΕΚΠΑ

Laurent Busé,
Διευθυντής Έρευνας INRIA

Ζησιμόπουλος Βασίλειος,
Καθηγητής ΕΚΠΑ

Γιαννοπούλου Αρχοντία ,

Επίκουρη Καθηγήτρια ΕΚΠΑ

Josef Schicho,
Καθηγητής Johannes Kepler University

Σκούτας Δημήτριος,
Ερευνητής Β ”Αθηνά” Ερευνητικό Κέντρο

Ημερομηνία Εξέτασης: 28/04/2022

ABSTRACT

Rigidity theory is the branch of mathematics that studies the embeddings (or equivalently realizations) of graphs in an euclidean space or a manifold. If the number of realizations satisfying edge length constraints is finite up to rigid motions, then the embedding is called rigid, otherwise it is called flexible. These embeddings can be related to the real solutions of certain algebraic systems and their complex solutions extend the notion of rigidity to $\mathbb{C}^d$.

One of the major open problems in rigidity theory is to find tight upper bounds on the numbers of rigid graph realizations in an embedding space for a given number of vertices. Given a minimally rigid graph $G(V, E)$, the upper bound of embeddings in $\mathbb{R}^d$ used to be $O\left(2^{d\cdot|V|}\right)$, while for the cases of $d = 2$ and $d = 3$ it has been proved that there are graphs with $\Omega\left(2.3003^{|V|}\right)$ and $\Omega\left(2.5198^{|V|}\right)$ realizations respectively. In this thesis, we display methods that reduce the gap between the existing upper bounds and asymptotic lower bounds on the maximal number of realizations on euclidean spaces or spheres.

We propose two methods to compute a bound on the number of realizations using the multihomogeneous Bézout (m-Bézout) bound of well-constrained algebraic systems. The first one relates the m-Bézout bound with the number of certain oudegree-constrained graph orientations, while the second uses matrix permanent formulation. Then, we examine the exactness of these bounds on the number of complex embeddings. First with computations indicating that the m-Bézout bounds are tight for certain classes of graphs. Consequently, we exploit Bernstein's second theorem on the exactness of mixed volume, and relate it to the m-Bézout bound by analyzing the associated Newton Polytopes.

Using these two methods, we improve the upper bounds on the number of graph embeddings. A first improvement is achieved for realizations of graphs in $d \geq 5$ and planar graphs in $\mathbb{C}^3$ applying existing bounds on permanents and orientations of planar graphs. Then we introduce an elimination technique on a graphical construction that further decreases these bounds in all dimensions. This approach gives $O\left(3.7764^{|V|}\right)$ and $O\left(6.8399^{|V|}\right)$ as bounds for $d = 2$ and $d = 3$ respectively, which is the first improvement on the asymptotic upper bound for these cases.

Finally, we try to find edge lengths that can maximize the number of real embeddings in the plane, space and on the sphere for certain graphs. In order to achieve that, we use methods that sample efficiently a vast space of parameters. Our results provide a full classification according to their maximal number of real embeddings of all 7-vertex graphs in $\mathbb{R}^2$ and $\mathbb{R}^3$, while for the previously untreated case of S^2 we give a full characterization for all 6-vertex graphs. We also establish new asymptotic lower bounds on the maximal number of realizations (or simply *lower bounds*) proving that in $\mathbb{R}^2, S^2$ and $\mathbb{R}^3$ there exist graphs with $\Omega\left(2.3780^{|V|}\right)$, $\Omega\left(2.5198^{|V|}\right)$ and $\Omega\left(2.6553^{|V|}\right)$ embeddings respectively.

SUBJECT AREA: Graph Rigidity

KEYWORDS: Minimally rigid graph, Multihomogeneous Bézout Bound, Distance Geometry, Asymptotic Bound, Mixed Volume

ΠΕΡΙΛΗΨΗ

Η *Θεωρία Άκαμπτων Γράφων* (Θ.Α.Γ.) είναι ο κλάδος των μαθηματικών που μελετά τις εμβυθίσεις γράφων (ή διαμορφώσεις) σε έναν ευκλείδιο χώρο ή μια πολλαπλότητα. Εφόσον ο αριθμός των εμβυθίσεων ως προς τις ευκλείδιες κινήσεις είναι πεπερασμένος για δεδομένα βάρη των ακμών του γράφου, που αντιστοιχούν σε αποστάσεις, τότε ο γράφος ονομάζεται άκαμπτος, αλλιώς ονομάζεται έυκαμπτος. Ο υπολογισμός του αριθμού αυτού μπορεί να γίνει συνδέοντας τις αποστάσεις μεταξύ κορυφών που βρίσκονται σε μία ακμή με αλγεβρικά συστήματα. Ως εκ τούτου ο αριθμός των πραγματικών ριζών αυτών των συστημάτων αντιστοιχεί στον αριθμό των διαμορφώσεων. Οι μιγαδικές ρίζες αυτών των συστημάτων επεκτείνουν την έννοια των άκαμπτων γράφων στους μιγαδικούς ευκλείδιους χώρους και τις αντίστοιχες πολλαπλότητες.

Ένα από τα βασικά ερωτήματα στην Θ.Α.Γ. είναι η αναζήτηση άνω φραγμάτων στον αριθμό των εμβυθίσεων για έναν δοσμένο αριθμό κορυφών που να μπορούν να πραγματωθούν. Το μέχρι τώρα γνωστό άνω φράγμα για κάθε ευκλείδιο χώρο διάστασης d για έναν άκαμπτο γράφο $G(V, E)$ ήταν της τάξης του $O\left(2^{d\cdot|V|}\right)$, ενώ το μέγιστο των εμβυθίσεων που έχουν βρεθεί για συγκεκριμένους γράφους είναι της τάξης του $\Omega\left(2.3003^{|V|}\right)$ στο επίπεδο και $\Omega\left(2.5198^{|V|}\right)$ στον χώρο. Σε αυτή την διατριβή, αναπτύσσονται μέθοδοι που μειώνουν το κενό αυτό μεταξύ των άνω φραγμάτων και των (υπολογισμένων) κάτω φραγμάτων του μεγίστου αριθμού των εμβυθίσεων.

Για αυτόν τον σκοπό, προτείνουμε δύο μεθόδους για τον υπολογισμό του πολυ-ομογενούς φράγματος Bézout (Π.Φ. Bézout) τετράγωνων αλγεβρικών συστημάτων. Αρχικά, συνδέουμε το φράγμα αυτό με τον αριθμό διαφορετικών προσανατολισμένων γράφων που μπορεί να προκύψει με βάση περιορισμούς στο βαθμό εξερχόμενων ακμών κάθε κορυφής ενός αρχικά μη προσανατολισμένου γράφου. Επιπλέον, χρησιμοποιούμε την permanent πινάκων που σχετίζονται με το αλγεβρικό σύστημα. Στην συνέχεια μελετάμε την ακρίβεια αυτού του φράγματος σε σχέση με τον αριθμό εμβυθίσεων σε μιγαδικούς χώρους. Βρίσκουμε ότι ο υπολογισμός του όριου για μια πλειάδα γράφων υποδεικνύει ότι για συγκεκριμένες κλάσεις αυτό μπορεί να είναι ακριβές. Αυτό μας παρακινεί να χρησιμοποιήσουμε το δεύτερο θεώρημα του Bernstein, που αφορά την ακρίβεια των μεικτών όγκων, και να αναλύσουμε τις συνθήκες των πολυτόπων του Newton οι οποίες καθιστούν το φράγμα μας ακριβές.

Το επόμενο βήμα είναι η βελτίωση των ασυμπτωτικών άνω φραγμάτων. Εφαρμόζοντας άμεσα υπάρχοντα φράγματα των permanent και των προσανατολισμών επίπεδων γραφημάτων, βρίσκουμε μια πρώτη βελτίωση σε συγκεκριμένες κατηγορίες άκαμπτων γράφων, δηλαδή αυτών που εμβυθίζονται σε μεγάλες διαστάσεις ($d \geq 5$), καθώς και επίπεδων γράφων που εμβυθίζονται στον χώρο. Έπειτα, αναπτύσσουμε μια μέθοδο που συνδέει τα άνω φράγματα στους προσανατολισμούς των γράφων με μια διαδικασία σταδιακής απαλοιφής κορυφών. Αυτή η μέθοδος μειώνει τα άνω φράγματα σε όλες τις κατηγορίες των γράφων που εξετάζουμε, σπάζοντας για πρώτη φορά τα τετριμμένα

φράγματα για τις εμβυθίσεις στο επίπεδο και το χώρο, αποδεικνείοντας ότι είναι της τάξης του $O\left(3.7764^{|V|}\right)$ και $O\left(6.8399^{|V|}\right)$ αντίστοιχα.

Το τελευταίο πρόβλημα που μας απασχολεί είναι η εύρεση κάτω φραγμάτων του μεγίστου αριθμού των εμβυθίσεων συγκεκριμένων γράφων. Αυτό επιτυγχάνεται με την αναζήτηση των αποστάσεων που ταυτίζουν των αριθμό των πραγματικών λύσεων των αλγεβρικών συστημάτων με αυτό των μιγαδικών. Τα αποτελέσματά μας ταξινομούν πλήρως ως προς τον μέγιστο αριθμό διαμορφώσεων όλους τους άκαμπτους γράφους με 7 κορυφές που εμβυθίζονται στο επίπεδο και τον χώρο, καθώς και τους γράφους με 6 κορυφές που εμβυθίζονται στην σφαίρα S^2. Επιπλέον βελτιώνουν τα υπάρχοντά κάτω φράγματα του μέγιστου αριθμού διαμορφώσεων σε $\Omega\left(2.3780^{|V|}\right)$ στο επίπεδο, $\Omega\left(2.5198^{|V|}\right)$ στην σφαίρα S^2 και $\Omega\left(2.6553^{|V|}\right)$ στον χώρο.

ΘΕΜΑΤΙΚΗ ΠΕΡΙΟΧΗ: Θεωρία Άκαμπτων Γράφων

ΛΕΞΕΙΣ ΚΛΕΙΔΙΑ: Ελαχιστικώς Άκαμπτος Γράφος, Πολυ-ομογενές Φράγμα Bézout, Γεωμετρία Αποστάσεων, Ασυμπτωτικό Όριο, Μεικτός Όγκος

ΣΥΝΟΠΤΙΚΗ ΠΑΡΟΥΣΙΑΣΗ ΤΗΣ ΔΙΔΑΚΤΟΡΙΚΗΣ ΔΙΑΤΡΙΒΗΣ

Η *Θεωρία Άκαμπτων Γράφων* (Θ.Α.Γ.- Rigidity theory) αποτελεί έναν ιδιαίτερα ενεργό κλάδο των μαθηματικών. Παρόλο που οι απαρχές της εντοπίζονται στα τέλη του 19ου αιώνα [53], υπάρχει ένα αυξανόμενο ενδιαφέρον τα τελευταία χρόνια που ωθείται από τις εφαρμογές της στην ρομποτική [47], την μοριακή βιολογία [32, 11, 50], την τεχνολογία του GPS [73] και την αρχιτεκτονική [2, 29]. Εκτός από τις εφαρμογές αυτές βέβαια η Θ.Α.Γ. έχει ερευνητικό ενδιαφέρον ως ανεξάρτητο μαθηματικό αντικείμενο που αλληλεπιδρά με την θεωρία γραφημάτων, την υπολογιστική άλγεβρα και την υπολογιστική γεωμετρία, όπως άλλωστε και με το συγγενικό πεδίο της Γεωμετρίας Αποστάσεων.

Η Θ.Α.Γ. ασχολείται με τις εμβυθίσεις γράφων σε ευκλείδιους χώρους ή σε άλλες πολλαπλότητες. Στην παρούσα διατριβή καταπιανόμαστε με τις εμβυθίσεις απλών και μη κατευθυνόμενων γράφων σε ευκλείδιους χώρους ($\mathbb{R}^d$) ή σφαίρες διάστασης d (S^d). Στην συνέχεια θα παραθέσουμε κάποιες βασικές έννοιες και ορισμούς της Θ.Α.Γ. χρησιμοποιώντας τους ευκλείδειους χώρους, που ισχύουν ανάλογα και για τις d-διάστατες σφαίρες. Η εμβύθιση ενός απλού μη κατευθυνόμενου γράφου $G = (V, E)$ σε έναν ευκλείδειο χώρο $\mathbb{R}^d$ είναι μια απεικόνιση $V \to \mathbb{R}^d$ που ορίζει μια *διαμόρφωση* (conformation) του γράφου. Κάθε διαμόρφωση $\boldsymbol{\rho} = \{\rho_1, \rho_2, \rho_3, ..., \rho_{|V|}\}$ επάγει ένα σύνολο αποστάσεων μεταξύ των κορυφών που αποτελούν άκρα ακμών $\boldsymbol{\lambda} = \{\lambda_{u,v} \mid (u, v) \in E\}$ για $\lambda_{u,v} = \|\rho_u - \rho_v\|$, όπου η συνάρτηση $\|\cdot\|$ υποδηλώνει την συνήθη ευκλείδια απόσταση, και θα τις ονομάζουμε *αποστάσεις ακμών*. Αυτές οι αποστάσεις καθορίζουν τα βάρη των ακμών για την συγκεκριμένη εμβύθιση. Εφόσον ο αριθμός όλων των διαμορφώσεων που ικανοποιούν τις επαγόμενες αποστάσεις ακμών είναι πεπερασμένος ως προς τις *Ευκλείδειες κινήσεις* (μετατοπίσεις και περιστροφές), τότε ο γράφος λέγεται *άκαμπτος*, ενώ σε αντίθετη περίπτωση ονομάζεται *εύκαμπτος*.

Οι συντεταγμένες των εμβυθίσεων ενός γράφου με δεδομένες αποστάσεις ακμών $\boldsymbol{\lambda}$ μπορούν να υπολογιστούν ως πραγματικές λύσεις αλγεβρικών εξισώσεων που μοντελοποιούν αυτές τις αποστάσεις

$$\lambda_{u,v}^2 = \sum_{i=1}^{d} (x_{u,i} - x_{v,i})^2 \tag{1}$$

όπου η μεταβλητή $x_{u,i}$ υποδηλώνει την i-οστη συντεταγμένη της κορυφής u. Ως εκ τούτου, η έννοια των άκαμπτων γράφων επεκτείνεται στο μιγαδικό επίπεδο με τις μιγαδικές ρίζες αυτών των συστημάτων. Σημειώνουμε ότι εφόσον μια πολλαπλότητα καθορίζεται από αλγεβρικές εξισώσεις, όπως στην περίπτωση της S^d, για να βρούμε τις εμβυθίσεις χρησιμοποιούμε τις αντίστοιχες εξισώσεις που μας δίνει η νόρμα, αλλά και τις εξισώσεις που καθορίζουν την πολλαπλότητα.

Στην περίπτωση των άκαμπτων γράφων, μια τροποποιημένη μορφή της Εξίσωσης 1 όπως στα [28, 64] κάνει εφικτή την χρήση εργαλείων από την θεωρία απαλοιφής. Η

τροποποίηση αυτή συνίσταται στην εισαγωγή καινούριων μεταβλητών

$$s_u = \sum_{i=1}^{d} x_{u,i}^2 \tag{2}$$

και η αντικατάστασή τους στην Εξίσωση 1. Ονομάζουμε τον συνδυασμό της τροποποιημένης Εξίσωσης 1 και της Εξίσωσης 2 για όλες τις κορυφές και ακμές του γράφου *σφαιρικές εξισώσεις* (sphere equations).

Η συγκεκριμένη αλγεβρική μοντελοποίηση δεν είναι η μοναδική που εφαρμόζεται στα πλαίσια της Θ.Α.Γ., καθώς συχνά χρησιμοποιούμε τους πίνακες Cayley-Menger από την Γεωμετρία Αποστάσεων [12]. Ο μηδενισμός και το πρόσημο των υπο-οριζουσών συγκεκριμένου μεγέθους ενός πίνακα Cayley-Menger εκφράζει την εμβυθισιμότητα μιας συλλογής αποστάσεων σε έναν ευκλείδειο χώρο. Εφόσον κάποιες αποστάσεις είναι γνωστές και άλλες εκφράζονται με μεταβλητές, δημιουργούνται αφινικές πολλαπλότητες που προέρχονται από αυτές τις μηδενικές ορίζουσες και οι ρίζες τους εκφράζουν τις διαφορετικές διαμορφώσεις των γράφων. Εκτός της αφινικής πολλαπλότητας, η επιβεβαίωση της ύπαρξης πραγματικών διαμορφώσεων με αυτήν την μέθοδο χρειάζεται και την ικανοποίηση γεωμετρικών ανισώσεων που προκύπτουν από τους ίδιους πίνακες.

Έχει αποδειχθεί ότι ο διαχωρισμός μεταξύ εύκαμπτων και άκαμπτων γράφων έχει σχέση με την συνδυαστική δομή ενός γράφου για σχεδόν όλες τις εμβυθίσεις [36]. Τους γράφους που είναι άκαμπτοι για κάθε τέτοια διαμόρφωση στον αντίστοιχο χώρο τους ονομάζουμε *γενικά άκαμπτους γράφους* (generically rigid graphs). Μια ειδική κλάση γενικά άκαμπτων γράφων είναι όσοι παύουν να είναι άκαμπτοι εφόσον αφαιρεθεί μία οποιαδήποτε ακμή. Αυτοί ονομάζονται *ελαχιστικώς γενικά άκαμπτοι γράφοι* (Ε.Α.Γ.- generically minimally rigid graphs) και είναι αυτοί που απασχολούν την παρούσα διατριβή. Σημειώνουμε ότι οι Ε.Α.Γ. στο επίπεδο είναι γνωστοί ως *γράφοι Laman* (Laman graphs), ενώ τους Ε.Α.Γ. στον χώρο τους ονομάζουμε *γράφους Geiringer* (Geiringer graphs), εναρμονιζόμενοι με τους συγγραφείς του [35]. Επίσης οι Ε.Α.Γ. γράφοι σε έναν ευκλείδειο χώρο $\mathbb{R}^d$ είναι Ε.Α.Γ. και στην d-διάστατη σφαίρα S^d [70] (αυτή η ιδιότητα δεν ισχύει γενικά για όλες τις πολλαπλότητες διάστασης d).

Ένα βασικό θεώρημα στην Θ.Α.Γ. είναι η συνθήκη του Maxwell, σύμφωνα με την οποία αν ένας γράφος $G = (V, E)$ είναι Ε.Α.Γ. στον $\mathbb{R}^d$ τότε ο συνολικός αριθμός των πλευρών του είναι $|E| = d \cdot |V| - \binom{d+1}{2}$, ενώ για κάθε υπογράφο $G' = (V', E') \subset G$ ισχύει η ανισότητα $|E'| \leq d \cdot |V'| - \binom{d+1}{2}$. Η συγκεκριμένη συνθήκη είναι και επαρκής για τον χαρακτηρισμό των γράφων Laman [48, 57], κάτι που δεν συμβαίνει σε μεγαλύτερες διαστάσεις για τις οποίες έχουν βρεθεί συγκεκριμένα αντιπαραδείγματα. Η συνθήκη του Maxwell εκφράζει τους συνολικούς βαθμούς ελευθερίας του συστήματος που πρέπει να κορεστούν από τις ακμές ώστε ο γράφος να είναι άκαμπτος: στον $\mathbb{R}^d$ κάθε κορυφή έχει d βαθμούς ελευθερίας (άρα συνολικά μια διαμόρφωση $|V|$ κορυφών έχει $d \cdot |V|$ βαθμούς ελευθερίας), από τους οποίους αφαιρούμε τους βαθμούς ελευθερίας των ευκλείδειων κινήσεων (d για τις μετατοπίσεις και $\binom{d}{2}$ για τις περιστροφές). Αλγεβρικά η συνθήκη του Maxwell υποδηλώνει ότι το αντίστοιχο σύστημα εξισώσεων είναι τετράγωνο, ενώ κανένα υποσύστημα δεν είναι ασυμβίβαστο. Άρα το αλγεβρικό σύστημα στους μιγαδικούς έχει πάντα τον ίδιο αριθμό λύσεων για κάθε

γενική επιλογή του $\boldsymbol{\lambda}$ [63]. Προφανώς ο αριθμός των μιγαδικών διαμορφώσεων είναι ένα άνω φράγμα για τον μέγιστο αριθμό των πραγματικών διαμορφώσεων ενός γράφου, ο οποίος εξαρτάται από την επιλογή συγκεκριμένων αποστάσεων ακμών.

Ένα από τα βασικά ερωτήματα στην Θ.Α.Γ. είναι η εύρεση πραγματώσιμων άνω φραγμάτων στον αριθμό των εμβυθίσεων των Ε.Α.Γ. με δεδομένο αριθμό κορυφών. Μέχρι τώρα τα γνωστά άνω φράγματα δεν βελτίωναν ασυμπτωτικά το $O\left(2^{d\cdot|V|}\right)$, το οποίο μπορεί κανείς να το υπολογίσει με άμεση εφαρμογή του θεωρήματος του Bézout στην Εξίσωση 1. Παρόλο που έχουν γίνει προσπάθειες να χρησιμοποιηθούν περισσότερο πολύπλοκα εργαλεία για να βελτιώσουν αυτό το τετριμμένο όριο (όπως τον βαθμό των αλγεβρικών συστημάτων χρησιμοποιώντας Γεωμετρία Αποστάσεων [13] ή εφαρμόζοντας το άνω φράγμα των μεικτών όγκων [64]). Από την άλλη πλευρά, τα αντίστοιχα κάτω φράγματα στον μέγιστο αριθμό των διαμορφώσεων είναι αρκετά μικρότερα. Έχει υπολογιστεί ότι υπάρχουν γράφοι με $\Omega\left(2.3003^{|V|}\right)$ διαμορφώσεις στον $\mathbb{R}^2$ [24] και $\Omega\left(2.5198^{|V|}\right)$ διαμορφώσεις στον $\mathbb{R}^3$ [25, 28], ενώ στους μιγαδικούς χώρους έχουν βρεθεί γράφοι με $\Omega(2.5079^{|V|})$ στον $\mathbb{C}^2$ [16, 35], $\Omega\left(2.5698^{|V|}\right)$ στην σφαίρα S^2 [31] και $\Omega\left(3.0683^{|V|}\right)$ στον $\mathbb{C}^3$ [35]. Σημειώνουμε ότι εκτός από την εύρεση γενικών φραγμάτων, έχουν χρησιμοποιηθεί υπάρχοντα φράγματα στις μιγαδικές λύσεις αλγεβρικών συστημάτων για τις περιπτώσεις συγκεκριμένων γράφων Laman και Geiringer. Αυτά χρησιμοποιήθηκαν για να δωθεί ένας στόχος για την εύρεση αποστάσεων που μεγιστοποιούν τον αριθμό των εμβυθίσεων στους πραγματικούς [28].

Η βασική επιδίωξη της παρούσας θέσης είναι να μειωθεί το κενό μεταξύ των άνω και των κάτω φραγμάτων, χρησιμοποιώντας εργαλεία από την αλγεβρική γεωμετρία, την θεωρία γράφων και αναπτύσσοντας τους κατάλληλους αλγορίθμους. Η συνεισφορά της διατριβής αφορά τους τομείς που παρουσιάζονται στις παρακάτω παραγράφους. Τα πορίσματα και οι μέθοδοι έχουν δημοσιευθεί σε επιστημονικά περιοδικά [4, 5] ή έχουν εγκριθεί προς δημοσίευση [7].

Ερευνούμε κατά πόσον το πολυ-ομογενές φράγμα Bézout (Π.Φ. Bézout- multihomogeneous Bézout bound) μπορεί να αντικαταστήσει το φράγμα των μεικτών όγκων ως ένα αποτελεσματικό άνω φράγμα των ριζών για τις σφαιρικές εξισώσεις. Γενικά, ισχύει η παρακάτω ανισότητα

πραγματικών λύσεων $\leq$ # μιγαδικών λύσεων $\leq$ μεικτός όγκος $\leq$ Π.Φ. Bézout $\leq$ Bézout

όσον αφορά τον αριθμό των λύσεων ενός αλγεβρικού συστήματος και τα αντίστοιχα άνω φράγματα [63], με την πολυπλοκότητα υπολογισμού των παραπάνω να έχει αντίστροφη φορα. Όπως ήδη αναφέρθηκε για τα άνω φράγματα, το φράγμα Bézout (που υπολογίζεται με έναν απλό πολλαπλασιασμό) είναι ελάχιστα αντιπροσωπευτικό. Από την άλλη ο μεικτός όγκος που λαμβάνει υπόψιν την δομή των εξισώσεων μέσω των πολυτόπων του Newton έχει μεγάλο υπολογιστικό κόστος (λεπτομέρειες για τον υπολογισμό των φραγμάτων βρίσκονται στο Παράρτημα Α- Appendix A).

Για αυτόν τον σκοπό παρουσιάζουμε 2 μεθόδους που εφαρμόζονται στην περίπτωση των Ε.Α.Γ. για τον υπολογισμό του Π.Φ. Bézout το οποίο επίσης λαμβάνει υπόψιν την δομή των εξισώσεων, αλλά με μικρότερη λεπτομέρεια σε σχέση με τον μεικτό όγκο. Η πρώτη μέθοδος είναι συνδυαστική και βασίζεται στην συσχέτιση του Π.Φ. Bézout με τον

αριθμό των διαφορετικών προσανατολισμών του αρχικού γράφου, με βάση περιορισμούς στον βαθμό των εξερχόμενων ακμών. Επιπλέον, έχουμε αναπτύξει έναν αναδρομικό αλγόριθμο για τον υπολογισμό όλων των πιθανών προσανατολισμών και τον υλοποιήσαμε σε γλώσσα `Python`. Η δεύτερη μέθοδος συσχετίζει έναν τετράγωνο πίνακα με το αλγεβρικό σύστημα με μέγεθός $\sim |E|$, του οποίου η permanent δίνει το επιθυμητό άνω φράγμα.

Παρουσιάζουμε την σύγκριση μεταξύ των 2 μεθόδων ως προς τον απαιτούμενο υπολογιστικό χρόνο σε μια πλειάδα περιπτώσεων. Για τον υπολογισμό της permanent χρησιμοποιούμε τις αντίστοιχες υλοποιήσεις της `maple` και της `Python`. Η υλοποίηση του αναδρομικού αλγορίθμου είναι σημαντικά πιο γρήγορη, γεγονός που ήταν αναμενόμενο, καθώς ο αλγόριθμος του Ryser που θεωρείται ο πιο αποτελεσματικός για τον υπολογισμό της permanent ενός τετράγωνου πίνακα μεγέθους $|E|$ έχει πολυπλοκότητα $|E|^2 \cdot 2^{|E|}$, ενώ όλοι οι πιθανοί προσανατολισμοί ενός γράφου είναι το πολύ $2^{|E|}$.

Τα πειραματικά μας δεδομένα δείχνουν ότι στην συντριπτική πλειονότητα των περιπτώσεων γράφων Laman και σε όλες των γράφων Geiringer με $|V| \leq 11$ ο μεικτός όγκος και το Π.Φ. Bézout των σφαιρικών εξισώσεων ταυτίζονται. Επιπλέον, όλοι οι γράφοι Geiringer με $|V| \leq 10$ που είναι επίπεδοι γραφοθεωρητικά έχουν ίσο Π.Φ. Bézout και αριθμό μιγαδικών διαμορφώσεων. Για τους επίπεδους γράφους Laman αυτή η ισότητα σπάνια ισχύει στις ενδιαφέρουσες περιπτώσεις των εμβυθίσεων στο επίπεδο, αλλά ισχύει για τις εμβυθίσεις τους στην σφαίρα S^2. Και στις 2 προαναφερθείσες κλάσεις το Π.Φ. Bézout για τους μη επίπεδους γράφους είναι αυστηρό άνω φράγμα.

Τα παραπάνω αποτελέσματα λειτουργούν ως κίνητρο για την μελέτη των συνθηκών που δείχνουν ότι το Π.Φ. Bézout είναι ακριβές. Για αυτόν τον σκοπό εφαρμόζουμε το 2ο θεώρημα του Bernstein, που αφορά την ακρίβεια του μεικτού όγκου [9]. Προσαρμόζουμε τα πολύτοπα του Newton στην περίπτωση των αλγεβρικών συστημάτων που έχουν πλήρη πολυ-ομογενή δομή. Συνεπακόλουθα, αναπτύσσουμε μια μέθοδο και έναν αλγόριθμο που πιστοποιεί τα κριτήρια που θέτει το θεώρημα του Bernstein διενεργώντας πολύ λιγότερους ελέγχους από όσους προβλέπονται.

Οι μέθοδοι υπολογισμού του Π.Φ. Bézout χρησιμοποιούνται για την εξαγωγή γενικών άνω φραγμάτων στα πλαίσια της παρούσας διατριβής. Αρχικά εφαρμόζουμε το φράγμα Brègman-Minc για τις permanent πινάκων, βελτιώνοντας για πρώτη φορά τα ασυμπτωτικά φράγματα Ε.Α.Γ. σε διάσταση $d \geq 5$ σε σχέση με το τετριμμένο Bézout φράγμα. Επιπλέον, αποδεικνύουμε ότι η άμεση χρήση φραγμάτων για τον προσανατολισμό επίπεδων γράφων [30] μειώνει το ασυμπτωτικό άνω φράγμα για τους επίπεδους Geiringer γράφους.

Στην συνέχεια, παρουσιάζουμε μια μέθοδο που φράσσει με αναδρομικό τρόπο τους προσανατολισμούς ενός γράφου. Αυτή η μέθοδος αφορά γραφικές στις οποίες μελετήσαμε προσανατολισμούς με σταθερό αριθμό εισερχόμενων ακμών για κάθε κορυφή. Δείχνουμε ότι ο αριθμός αυτών των προσανατολισμών ταυτίζεται με αυτούς που χρησιμοποιούμε για τον υπολογισμό του Π.Φ. Bézout των σφαιρικών εξισώσεων και εφαρμόζουμε μια τεχνική απαλοιφής που οδηγεί σε ένα άνω φράγμα για αυτούς. Το άνω φράγμα στον αριθμό των προσανατολισμών δίνει βελτιωμένα άνω φράγματα για όλες τις διαστάσεις σε σχέση και με το Bézout φράγμα, αλλά και με το Brègman-Minc. Συγκεκριμένα, για τις πιο ενδιαφέρουσες κλάσεις γράφων, αποδείξαμε ότι οι Laman

γράφοι έχουν το πολύ $O\left(3.7764^{|V|}\right)$ διαμορφώσεις, ενώ οι Geiringer γράφοι έχουν το πολύ $O\left(6.8399^{|V|}\right)$ διαμορφώσεις, ενώ τα προϋπάρχοντα φράγματα ήταν της τάξης του $O\left(4^{|V|}\right)$ και $O\left(8^{|V|}\right)$ αντίστοιχα.

Σε σχέση με τα κάτω όρια στον μέγιστο αριθμό πραγματικών διαμορφώσεων, ασχολούμαστε με τις περιπτώσεις των εμβυθίσεων στο επίπεδο, το χώρο και την σφαίρα. Για να το πετύχουμε αυτό εφαρμόζουμε μεθόδους αναζήτησης των κατάλληλων αποστάσεων πλευράς που μεγιστοποιούν αυτόν τον αριθμό. Σε κάθε γράφο ο στόχος ήταν ο αριθμός των μιγαδικών διαμορφώσεων, καθώς εικάζεται ότι για την πλειονότητα των Ε.Α.Γ. συμπίπτει με τον αριθμό πραγματικών διαμορφώσεων (αλλά όχι για όλες [41]). Για αυτόν τον λόγο χρησιμοποιούμε τόσο τις εξισώσεις σφαίρας, όσο και τις εξισώσεις κα τις ανισώσεις που δίνουν οι ορίζουσες των πίνακων Cayley-Menger από την γεωμετρία αποστάσεων. Εφαρμόζουμε κλασσικές μεθόδους αναζήτησης παραμέτρων για την αύξηση των πραγματικών ριζών ενός αλγεβρικού συστήματος (αναζήτηση κοντά σε παραμέτρους που απειρίζουν τον αριθμό των λύσεων, στοχαστικές μέθοδοι, μέθοδος κυλινδρικής αλγεβρικής ανάλυσης- CAD). Επιπλέον χρησιμοποιούμε τον αλγόριθμο του J.Legerský (ενός από τους συγγραφείς του [4] του οποίου αποτελέσματα παρουσιάζονται στην παρούσα διατριβή) που αυξάνει τον αριθμό των διαμορφώσεων στον $\mathbb{R}^3$ βασισμένος στην μέθοδο των *καμπυλών σύνδεσης* (coupler curves) που είχε ξαναχρησιμοποιηθεί στην Θ.Α.Γ. [13].

Ως εκ τούτου, παρουσιάζουμε μια πλήρη κατηγοριοποίηση των Ε.Α.Γ. ως προς τον μέγιστο αριθμό διαμορφώσεων κάθε γράφου με $|V| \leq 7$ στις περιπτώσεις των $\mathbb{R}^2$ και $\mathbb{R}^3$, ενώ στην περίπτωση της σφαίρας αυτή η κατηγοριοποίηση αφορά τους γράφους με $|V| \leq 6$. Σε όλες τις κατηγορίες βρίσκουμε κάτω όρια και για επιλεγμένους μεγαλύτερους γράφους. Σημειώνουμε ότι προηγουμένως δεν είχαν υπάρξει μελέτες που να αντιμετωπίζουν το συγκεκριμένο ερώτημα για την περίπτωση της σφαίρας.

Επιπλέον, διαλέγοντας συγκεκριμένους γράφους με βάση τον αριθμό των μιγαδικών διαμορφώσεων, καταφέρνουμε να αυξήσουμε τα ασυμπτωτικά κάτω όρια σε κάθε μία από τις εξεταζόμενες περιπτώσεις. Συγκεκριμένα, στην περίπτωση του επιπέδου δείχνουμε ότι υπάρχουν γράφοι με $\Omega(2.3780^{|V|})$ διαμορφώσεις στο επίπεδο, $\Omega(2.5198^{|V|})$ διαμορφώσεις στην σφαίρα και $\Omega(2.6553^{|V|})$ διαμορφώσεις στον χώρο.

Η διάρθρωση της διατριβής είναι η εξής:

Κεφάλαιο 1- Εισαγωγή (Introduction). Ορίζονται βασικές αρχές της Θ.Α.Γ. Επίσης, περιγράφονται τα ερευνητικά θέματα που απασχολούν την διατριβή, καθώς και προϋπάρχουσες προσεγγίσεις σε αυτά.

Κεφάλαιο 2- Βασικές έννοιες (Preliminaries). Γίνεται περιγραφή εργαλείων και εννοιών που θα χρησιμοποιηθούν στα επόμενα Κεφάλαια. Συγκεκριμένα, αρχικά περιγράφεται η μέθοδος Henneberg, που χρησιμοποιείται για την κατασκευή Ε.Α.Γ. Στην συνέχεια, παρουσιάζονται δύο μέθοδοι αλγεβρικής μοντελοποίησης για τις εμβυθίσεις των γράφων, οι σφαιρικές εξισώσεις και οι ορίζουσες των πινάκων Cayley-Menger.

Κεφάλαιο 3- Το Π.Α.Φ. Bézout για τους Ε.Α.Γ. (On the multihomogeneous Bézout bound of the embedding number). Παρουσιάζονται οι μέθοδοι για τον υπολογισμό

του Π.Α.Φ. Bézout των σφαιρικών εξισώσεων, καθώς και στοιχεία που συγκρίνουν τον υπολογιστικό χρόνο που απαιτείται για αυτές τις μεθόδους σε σχέση με το όριο τον υπολογισμό του μεικτού όγκου και του ακριβούς αριθμού των διαμορφώσεων. Στην συνέχεια, εξετάζονται πειραματικά δεδομένα ως προς την ακρίβεια του φράγματος και παρουσιάζεται μια μέθοδος που ελέγχει την ακρίβεια βασισμένη στο 2ο θεώρημα του Bernstein. Το περιεχόμενο αυτού του κεφαλαίου αποτελεί μέρος του [5].

Κεφάλαιο 4- Άνω φράγματα για τον αριθμό των διαμορφώσεων των Ε.Α.Γ. (Upper bounds on the embedding number of minimally rigid graphs). Αυτό το κεφάλαιο χωρίζεται σε δυο μέρη. Στο πρώτο, παρουσιάζονται εφαρμογές υπαρχόντων άνω φραγμάτων στις μεθόδους που παρουσιάστηκαν στο προηγούμενο Κεφάλαιο και αποτελούν μέρος του [5]. Στο δεύτερο, αναπτύσσουμε μια καινούρια μέθοδο που φράσσει τον αριθμό των πιθανών προσανατολισμών ενός γράφου και τελικά οδηγεί σε βελτιωμένα άνω φράγματα για όλες τις διαστάσεις εμβύθισης. Η μέθοδος αυτή και τα αποτελέσματά της έχουν εγκριθεί προς δημοσίευση [7].

Κεφάλαιο 5- Ο μέγιστος αριθμός εμβυθίσεων γράφων στο επίπεδο, τον χώρο και την σφαίρα (On the maximal number of real embeddings in $\mathbb{R}^2$, $\mathbb{R}^3$ and S^2). Σε αυτό το κεφάλαιο παρουσιάζονται τα αποτελέσματα και οι μέθοδοι που οδήγησαν στην αύξηση των κάτω φραγμάτων για τον μέγιστο αριθμό εμβυθίσεων. Τα αποτελέσματά αυτού του Κεφαλαίου ως προς τον $\mathbb{R}^3$ έχουν δημοσιευθεί στα πρακτικά του International Symposium on Symbolic and Algebraic Computation 2018 (ISSAC'18) [3]. Η επέκταση αυτών των αποτελεσμάτων με τα αντίστοιχα στο επίπεδο και την σφαίρα αποτελούν αντικείμενο του [4].

Κεφάλαιο 6- Συμπεράσματα και ανοιχτά ερωτήματα (Conclusion and open questions). Στο τελευταίο κεφάλαιο αναλύονται τα βασικά συμπεράσματα της παρούσας διατριβής, καθώς και τα ερευνητικά ερωτήματα που προκύπτον και μπορούν να διερευνηθούν στο μέλλον.

ACKNOWLEDGEMENTS

I would like to give my warmest thanks for this thesis to my advisor Ioannis Emiris. First of all I thank him because he gave me the opportunity to enroll in a high quality PhD European program, the ARCADES Network. I also thank him for the continuous guidance he offered to me all these years and his eagerness to transmit me his knowledge on various topics. I must say that I was always overwhelmed by his deep intuition in all our research problems. Finally, I want to thank him for his support in every issue that was not directly related to my PhD.

I would also like to thank all my colleagues in ΕρΓΑ Lab that were always willing to share their ideas and contributed to a great work atmosphere: Christos Conaxis who offered always a great aid for every administration issues and he also helped me to learn the basics on Computer Algebra, Clément Laroche (also an ARCADES member) who was always happy to talk about research and other issues in different occasions, Yannis Psarros who helped me understand some basics on the embedding problem which is the core of my thesis, Charalambos Tzamos who actually works with me in a new project on rigidity theory, and also Anna Karasoulou, Vangelis Anagnostopoulos, Manolis Christoforou, Tolis Halkis, Christina Katsamaki and Apostolos Florakis. Special thanks to Michalis Samaris, who made me aware of ARCADES PhD program (though not an ΕρΓΑ lab member) and was always willing to give me his view on graph theoretical issues of my research.

I would like to thank all the other PhD fellows in the ARCADES network for the time we spent together and the ideas we exchanged: Sotiris Chouliaras, Konstantinos Gavriil, Fanis Katsoulis, Alvaro Fuentes Suarez, Yairon Cid Ruiz, Fatmanur Yıldırım, Ahmed Blidia, Francesco Patrizi, Andrea Raffo, Michael Jimenez and especially Jan Legerský who was a great help during my stay in Austria and an excellent collaborator on the research project we worked together.

I also like to thank the other co-authors of my papers, Elias Tsigaridas, Joseph Schicho and Raimundas Vidunas for the common time we spent together working on various projects. Especially, I would also like to thank Joseph Schicho for his hospitality during my secondment in Linz University. In the same period, I enjoyed the conversations with Georg Grasegger, who also helped me with the computations of Table 3.1 (for the combinatorial algorithm) and explained to me the modifications of the algebraic systems in the absence of a triangle in $d = 3$ (which is generalized in Appendix B).

I would also like to thank my parents Kostas (που θα ήθελε να ήταν εδώ) and Athina for their continuous affection and support. Last but not least, I want to thank my family, Danai and Iasonas, for their endless patience and love all this time.

This thesis is part of the project ARCADES which has received funding from the European Union's Horizon 2020 research and innovation programme under the Marie Skłodowska-Curie grant agreement No 675789. It has been done at the Department of Informatics of the National and Kapodistrian University of Athens in collaboration with Athena Research and Innovation Centre.

CONTENTS

LIST OF FIGURES

LIST OF TABLES

1. INTRODUCTION

Rigidity theory is a mathematical area that lies in the intersection of graph theory, computational algebra and computational geometry. Although the foundations of rigidity theory can be traced in 19th century, there is nowadays a refreshment of scientific research on this subject motivated by applications in mollecular biology [11, 32, 50] , sensor network localization [73], robotics [47, 69, 72] and architecture [2, 29]. Besides these applications, there is active interest in rigidity theory as an independent mathematical subject. One of the major open problems in rigidity theory is to determine tight bounds on the maximal number of embeddings of rigid graphs in an euclidean space or a manifold up to a given number of vertices. In this thesis, we present methods that improve both the asymptotic upper bounds and the asymptotic lower bounds on this maximal number.

Rigidity theory examines the properties of graphs that may have rigid embeddings in a given space. In this thesis, we are interested in embeddings of simple undirected graphs in the euclidean space $\mathbb{R}^d$, or the d-dimensional sphere S^d. If the vertices or the edges of a graph G are not specified, then we denote by $V(G)$ the first and $E(G)$ the latter. Let us present some basic definitions of rigidity theory in this context using the usual euclidean norm. Analogous definitions can be applied for embeddings in other spaces or using other norms [17, 56, 70]. Let $G = (V, E)$ be a simple undirected graph (denoted also as $G(V, E)$ or simply G in the rest of the manuscript) and $\boldsymbol{\rho} = \{\rho_1, \rho_2, \dots \rho_{|V|}\} \in \mathbb{R}^{d\cdot|V|}$ be an embedding of G in $\mathbb{R}^d$, i.e. a map from the set of vertices V to $\mathbb{R}^d$. The pair of a simple undirected graph G and an embedding $\boldsymbol{\rho}$ is also known as *bar framework* (or simply framework) and is usually denoted with $G(\boldsymbol{\rho})$. Every such framework induces a set of edge lengths $\boldsymbol{\lambda} = \{\lambda_{u,v} \mid (u, v) \in E\}$ such that $\lambda_{u,v} = \|\rho_u - \rho_v\|$, where $\|\cdot\|$ denotes the usual euclidean norm.

This induced set of edge lengths can be used to define whether a framework is rigid or not. A framework $G(\boldsymbol{\rho})$ is called *rigid* if there is only a finite number of embeddings (the term *realizations* is used equivalently in this context) for graph G that satisfy the edge length constraints imposed by $\boldsymbol{\lambda}$ up to rigid motions (rotations and translations)[1]. Otherwise, if the number of realizations is infinite up to rigid motions, then $G(\boldsymbol{\rho})$ is called *flexible*. Equivalently, rigid frameworks do not admit continuous deformation preserving the edge lengths, while flexible frameworks can be continuously deformed (see Figure 1.1).

The embeddings of a graph $G(V, E)$ for a given set of edge lengths $\boldsymbol{\lambda}$ can be specified as the real solutions of algebraic equations that capture the edge length constraints. The simplest algebraic formulation is to consider the set of *squared distance equations*

$$\lambda_{u,v}^2 = \sum_{i=1}^{d} (x_{u,i} - x_{v,i})^2, \quad \forall (u, v) \in E \tag{1.1}$$

where $x_{u,i}$ represents the $i-$th coordinate of vertex u.

The complex solutions of these systems naturally extend the notion of graph embedding in

[1] Let us remark that each different realization defines a separate framework.

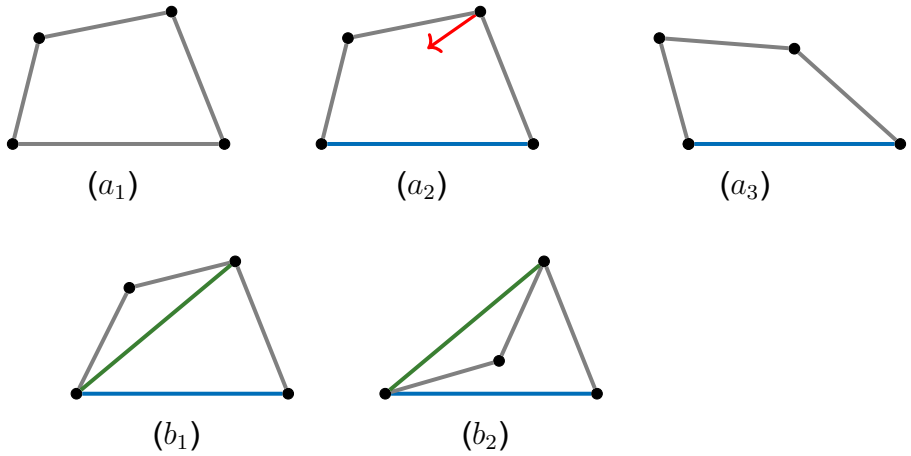

Figure 1.1: *An example of a flexible an a rigid graph embedding. The four-bar linkage (a_1, a_2, a_3) is a flexible framework on the plane: pinning down the two bottom vertices to factor out trivial motions (for more details see Section 2.2.1) and moving the up right vertex in the direction of the flex results to a continuous deformation of the framework deformed satisfying the same edge lengths. Throughout the deformation from the left framework (a_1) to the right one (a_3) there is an infinity of realizations up to rigid motions. On the other hand, if an edge is added, then there are only two realizations up to rigid motions and reflections (b_1 and b_2) and there is no way to continuously deform this framework.*

complex spaces, thus the possible configurations of $|V|$ points in $\mathbb{C}^d$ that satisfy the system of Equations 1.1 are called *complex embeddings*. Notice that in the case of complex embeddings the system of Equations 1.1 is not relevant with the usual complex norm. Clearly, a graph embedding is either rigid in both $\mathbb{R}^d$ and $\mathbb{C}^d$, or flexible for both cases. We remark that whenever we refer to complex embeddings in the case of the $d-$dimensional sphere S^d, it is the set of the complex solutions of squared distance equations combined with

$$\sum_{i=1}^{d+1} x_{u,i}^2 = 1, \qquad \forall u \in V \tag{1.2}$$

and the embedding space shall be denoted $S^d_{\mathbb{C}}$.

In fact, rigidity in $\mathbb{R}^d$ (or S^d) is also a *generic property* of the underlying graph without taking into account the specific embedding [1, 36]. In other words a graph is *generically rigid* if it is rigid for an open dense subset of embeddings $\boldsymbol{\rho} \in \mathbb{R}^{d\cdot|V|}$. An important class of generically rigid graphs are the *generically minimally rigid graphs*. A graph $G(V, E)$ is generically minimally rigid **iff** G is generically rigid while $G - e$ is flexible, for every $e \in E$. We remark that the classes of generically rigid graphs and generically minimally rigid coincide in $\mathbb{R}^d$ and S^d [70]. Additionally, a graph that is generically rigid (or generically minimally rigid) in a real space holds this property for the corresponding complex space.

A milestone theorem in rigidity theory relates a simple edge count with a necessary condition for minimal rigidity.

Theorem 1 (Maxwell [53]) *A simple undirected graph $G(V, E)$ is minimally rigid in $\mathbb{R}^d$ if $|E| = d \cdot |V| - \binom{d+1}{2}$ and the inequality $|E'| \leq d \cdot |V'| - \binom{d+1}{2}$ holds for every subgraph $G' = (V', E') \subset G$.*

Maxwell's condition corresponds intuitively to the number of vertex coordinates reduced by the number of degrees of freedom (dof) of rigid motions (d for the translations and $\binom{d}{2}$ for the rotations).

Maxwell's condition is also sufficient in the plane, as proved by G.Laman in the 70s [48], giving a full characterization for minimally rigid graphs in $\mathbb{R}^2$. These graphs are well-known as *Laman graphs* in the bibliography, while Maxwell's condition is called *Laman's condition*. What was recently found is that this result was originally discovered (but then forgotten) by H. Pollaczek-Geiringer [57, 58]. Following [35], minimally rigid graphs in $\mathbb{R}^3$ will be called *Geiringer graphs* in this thesis, to honour her legacy.

Unlike Laman graphs, there is no full combinatorial characterization of Geiringer graphs and this maybe constitutes the main open problem in rigidity theory. In fact, Maxwell's count fails as a sufficient condition in this case and higher dimensions (see Figure 1.2 for the famous *double banana* counter-example). The only subclass of Geiringer graphs that is fully characterized are the planar Geiringer graphs (Gauchy's theorem on strictly convex simplicial polyhedra [71]).

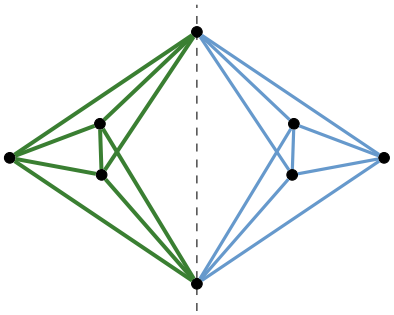

Figure 1.2: *The double-banana graph is composed by two identical rigid components (blue and green) that are glued to two common vertices. Although this structure satisfies Maxwell's condition in $\mathbb{R}^3$, it is not rigid: its two rigid components revolve in the space around the implied dashed axis that passes through the common vertices.*

Although minimally rigid graphs constitute the main focus of this thesis, we are also concerned with another important class of rigid graphs. A *globally rigid embedding* is an embedding that can have a unique realization up to isometries for the same edge lengths. Global rigidity can also be a generic property [42] and there is a combinatorial characterization for globally rigid graphs in $\mathbb{R}^2$ [18], but not in higher dimensions. In any dimension, it is possible to check if a generic framework is globally rigid using the rank of stress matrices of rigidity matroids [34]. It is obvious that if a graph $G(V, E)$ is generically globally rigid, then every graph that has the same vertex set and a superset of its edges is also globally rigid.

From an algebraic point of view, Maxwell's condition states that minimally rigid graphs can be related with square algebraic systems, such that no subsystem is over-constrained. In the case of the system of Equations 1.1, this can be achieved by fixing as many coordinates as the dof of rigid motions for the embedding space. The methods and the results of this thesis rely on the algebraic modelling of the minimally rigid graph embeddings with well-constrained systems of equations. The main focus is the number of embeddings of specific graphs up to rigid motions, which will be called simply *embedding number*, and the bounds on this number for graphs with a given number of vertices.

Given a minimally rigid graph $G(V, E)$ in $\mathbb{R}^d$ and a set of edge lengths $\boldsymbol{\lambda}$, $r_d(G, \boldsymbol{\lambda})$ denotes the embedding number in $\mathbb{R}^d$ for this specific edge labelling, while $r_d(G)$ denotes the maximal finite number of its embeddings for any generic $\boldsymbol{\lambda} \in \mathbb{R}_+^{|E|}$. In the case of $\mathbb{C}^d$, the embedding number is the same for every generic choice of $\boldsymbol{\lambda}$ [41, 63] and will be denoted $c_d(G)$. It is obvious that $c_d(G)$ serves as an upper bound for $r_d(G)$. Although these numbers coincide in many cases (see for example [13, 24, 28]), it has been proven that there are examples of a Laman graph such that $c_d(G) > r_d(G)$ [41] . We will also denote with $r_d(|V|)$ and $c_d(|V|)$ the maximal embedding number over all minimally rigid graphs in $\mathbb{R}^d$ with $|V|$ vertices in the real and complex case respectively. Finally, for the spherical embedding number we will use the notation $r_{S^d}(G, \boldsymbol{\lambda}), r_{S^d}(G), c_{S^d}(G), r_{S^d}(|V|), c_{S^d}(|V|)$ analogously with the euclidean case.

The main problem treated in the present thesis is to reduce the gap between upper and lower bounds of the embedding number. In the following paragraphs, we will describe the existing work on the field, our contribution and the organization of the text.

Related work A direct application of Bézout's bound in the system of squared distance equations 1.1 results to $O(2^{d\cdot|V|})$ as an asymptotic upper bound for $c_d(|V|)$ (and consequently for $r_d(|V|)$), taking into account Maxwell's condition for the cardinality of the system of equations. This bound will be called *Bézout bound* in the rest of this text.

In an effort to improve the asymptotic upper bound for Laman embeddings, mixed volume techniques have been applied [64]. The system of equations used in that case is a modified version of Equations 1, which is suitable for sparse elimination [2]. This approach did not manage to improve the (trivial) Bézout bound in the general case.

Another algebraic formulation that computes the embedding number relies on distance geometry, since the determinantal varieties of Cayley-Menger matrices can be used to specify graph embeddings. Applying a theorem on the degree of determinantal varieties[38], the authors in [13] delivered what used to be the best known upper bound on $c_d(|V|)$:

$$2 \cdot \prod_{j=0}^{|V|-d-2} \frac{\binom{|V|-1+j}{|V|-d-1-j}}{\binom{2j+1}{j}}. \tag{1.3}$$

[2]We also use this formulation and we call these systems *sphere equations* - see Section 2.2

which also does not improve asymptotically upon the trivial bound.

Besides asymptotic upper bounds, the mixed volume bound has been used for specific graphs, in order to give an estimate for the embedding number [28]. Although this is the tightest upper bound [63] in general, if the comparison ignores the precise variety where roots lie, its computation is #P-hard (by reduction from the permanent).

Remark that there exist also real algebraic bounds [10, 45] that are sharper than mixed volume and other complex bounds for polynomials which possess suitable structure. In the case of the embedding number, these are by far higher than the (more general) complex bounds.

The computation of exact numbers for $c_d(G)$ is more demanding than mixed volume computation. In the case of Laman graphs there exist combinatorial algorithms that count the embedding number in both $\mathbb{C}^2$ and $S^2_{\mathbb{C}}$ [16, 31], but it is almost infeasible to compute $c_d(G)$ for graphs with more than 18 vertices in a desktop computer. Computations for Geiringer embeddings have been even more difficult, since no combinatorial algorithms exist in this case. Gröbner base solvers have been used for these computations [35], but they may require more than 3 days for a single 11-vertex graph.

Finding the maximal number of real embeddings requires repetitive equation solving in an effort to approach the complex embedding number $c_d(G)$ with $r_d(G)$. This problem demands efficient sampling of the edge length constraints that are considered as parameters of the algebraic system. In rigidity theory, this sampling has been achieved using coupler curves [13] and stochastic methods [24], establishing tight bounds for $r_2(6)$ and $r_2(7)$ respectively. Let us note that the question of searching for parameters that maximize the real solutions of a given algebraic system is a well-known problem in real algebraic geometry. One of the most famous cases is the gradient descent method that was used to maximize the number of real Stewart-Gough Platform configurations [22].

Let us now compare the trivial asymptotic upper bound with the existing lower bounds. Asymptotic lower bounds on graph embeddings can be established by gluing frameworks in order to construct arbitrary big rigid graphs [13, 35]. In the bibliography lower bounds have been computed for the cases of Laman and Geiringer graphs. In the case of complex spaces it has been proven that there exist Laman graphs with $\Omega(2.5079^{|V|})$ and $\Omega(3.0683^{|V|})$ embeddings in $\mathbb{C}^2$ and $\mathbb{C}^3$ respectively [35], while in the case of spherical embeddings in $S^2_{\mathbb{C}}$ [31], while for Geiringer we have that $c_{S^2}(|V|) \in \Omega(2.5698^{|V|})$. As for real lower bound, the existing bound on the plane and the space have been $\Omega(2.3003^{|V|})$ [24] and $\Omega(2.5198^{|V|})$ [25, 28] respectively. A summary of these cases, comparing the existing asymptotic lower and upper, is given in Table 1.1.

Contribution As presented above the gap between the asymptotic upper bounds and the lower bounds is enormous. In the present thesis we develop methods to compute efficient graph-specific upper bounds on the embedding number and we subsequently reduce the asymptotic upper bound. We also present sampling procedures that increase the lower bounds on the real embedding number.

Table 1.1: *Power basis of the existing asymptotic upper and lower bounds for minimally rigid graphs in all embedding spaces treated.*

embedding space	$\mathbb{R}^2$	$\mathbb{C}^2$	$S^2_{\mathbb{C}}$	$\mathbb{R}^3$	$\mathbb{C}^3$
lower bound	2.3003	2.5079	2.5698	2.5198	3.0683
upper bound	4	4	4	8	8

Initially, we propose two methods that compute the multihomogeneous Bézout (m-Bézout) bound of algebraic systems modeling graph embeddings. These methods apply in both euclidean and spherical cases. The first one relates this bound with the number of outdegree-constrained graph orientation, based on a standard partition of variables. In this context, we also present a recursive combinatorial algorithm that computes these orientations. The second one uses the well-known connection between the computation of matrix permanents and m-Bézout bounds. For that reason, we demonstrate the construction of the $(0,1)$-matrix that captures the algebraic formulation we use. Then we compare computation runtimes between these two methods and also other algorithms that compute mixed volumes or the exact number of roots for the same algebraic systems.

Regarding the exactness of the bound, we present experimental results that compare m-Bézout with mixed volume bounds and the actual number of complex embeddings of all Laman and Geiringer graphs with $|V| \leq 9$ vertices, and some selected Laman graphs up to $|V| = 18$ and Geiringer graphs up to $|V| = 12$. These results show that the m-Bézout is exact for the large majority of spherical embeddings in the case of planar Laman graphs, while it is exact for all planar Geiringer graphs. Motivated by this observation, we adjust Bernstein's discriminant conditions on the exactness of mixed volume to the case of m-Bézout bounds using Newton Polytopes whose mixed volume equals to the m-Bézout. This method shows that an exponential number of conditions is always verified for the specific algebraic systems reducing the number of computations required. Despite this reduction, this number remains exponential, but based on experimental results we conjecture that it can be eventually linear.

In the sequel we make a first attempt to reduce the asymptotic upper bound using existing bounds on the methods described above. Direct application of the best upper bound for orientations [30] improve the asymptotic upper bound for the subclass of planar Geiringer graphs, while using the Brègman-Minc bound on the permanents of $(0,1)$-matrices [14, 54] we were able to decrease the asymptotic upper bound for all minimally rigid graphs in dimensions $d \geq 5$.

In order to achieve better bounds, we develop a method bounding recursively the outdegree - constrained orientations of a minimally rigid graph which is related with the m-Bézout bound [7]. For this reason, we introduce a graphical structure, *pseudographs*, and we relate the orientations of minimally rigid graphs with pseudographs. Finally, we prove that the bound of the recursive method on the orientations of pseudographs improves the

bound on the embedding number. More precisely, in the case of Laman graphs the new bound is in the order of $O(3.7764^{|V|})$, while in the case of Geiringer graphs it is $O(6.8399^{|V|})$.

Finally, we also manage to improve lower bounds on the maximal real embedding number in the case of $\mathbb{R}^2, \mathbb{R}^3$ and S^2 [4]. Our goal is to find the set of edge lengths $\boldsymbol{\lambda}$ for a graph G, such that the number of real embeddings for this specific set $r_d(G, \lambda)$ would match the number of complex embeddings $c_d(G)$, thus maximizing $r_d(G)$. Using sphere equations and the Cayley-Menger embeddability conditions, we applied some standard methods that sample parameters in order to increase real solutions of algebraic and semi-algebraic systems (sampling close to non-generic parameters, stochastic methods, cylindrical algebraic decomposition- CAD). Besides these methods, a new algorithm by J.Legerský (co-author of [4]) inspired by coupler curves was used to increase the maximal number of embeddings in the spatial case.

These methods lead to a full characterization of all minimally rigid graphs with $|V| \leq 7$ up to $r_d(G)$ in the cases of $\mathbb{R}^2$ and $\mathbb{R}^3$, while in the case of S^2 this characterization is achieved for $|V| \leq 6$. We also find maximal embedding numbers for selected bigger graphs, leading to new asymptotic lower bounds. More precisely, we prove that there are graphs with $\Omega(2.3780^{|V|})$ embeddings in the case of $\mathbb{R}^2$, $\Omega(2.5198^{|V|})$ embeddings in S^2 and $\Omega(2.6553^{|V|})$ in $\mathbb{R}^3$.

Organization The rest of the thesis is organized as follows. In Chapter 2 we give some preliminaries on the construction of minimally rigid graphs and the algebraic modelling that specifies the embeddings for a given set of edge lengths. More precisely, Henneberg steps are described in Section 2.1. These are used to construct all minimally rigid graphs in a given embedding space. Afterwards, in 2.2 we introduce two algebraic formulations used to count the embedding number. The first one is variation of the squared distance equations between adjacent vertices, that we call sphere equations. The latter uses semi-algebraic sets derived from Cayley-Menger determinants.

In Chapter 3, we study the m-Bézout bound of sphere equations. In Section 3.1 we present two methods for its computation and subsequently we compare the runtimes of these methods with existing computational ones that compute mixed volumes and the embedding number. In Section 3.2 we study the exactness of this bound. First we present experimental results indicating that the bound is tight for certain classes of minimally rigid graphs. Then we develop a method that checks whether the m-Bézout bound is exact, using Bernstein's second theorem on the exactness of mixed volume. The results of this Chapter are part of the joint work with I.Z. Emiris and J. Schicho and have been published in [5].

In Chapter 4, we present certain approaches that improve existing upper bounds, using the methods presented in the previous chapter. In Section 4.1, we apply existing bounds in our methods that directly improve the asymptotic upper bounds for certain classes of graphs. These results are also part of [5]. In Section 4.2, we develop a new method that bounds degree-constrained orientations leading to new upper bounds for minimally rigid graphs in any embedding space in $\mathbb{R}^d$ or S^d. This project is a joint work with I.Z. Emiris

and R. Vidunas and its results have been accepted for publication [7].

In Chapter 5, we present the methods that led to new lower bounds on the maximal embedding number in $\mathbb{R}^2, \mathbb{R}^3$ and S^d. These methods rely on efficient sampling of the parameter space that maximized the number of real solutions for the embedding number. This Chapter is part of the joint work with I.Z. Emiris, J.Legerský and E.Tsigaridis. A part of this chapter dealing with the spatial embeddings was published in the proceedings of ISSAC 2018 [3], while the totality of the results presented here constitute the subject of a journal publication [4]. The algorithms for the coupler curve visualization and sampling in the spatial case were created by J.Legerský. The results for the graphs with the maximal embedding number in $\mathbb{R}^2$ were also contributed independently by the same author.

Finally in Chapter 6, we give an overview of the results of the present thesis and open questions motivated by them.

2. PRELIMINARIES

In this chapter we present some basic concepts about the construction of rigid graphs and the algebraic formulation used to compute the embedding number.

2.1 Henneberg construction

In general, Maxwell's condition (Theorem 1) is not suitable to find the set (or a superset) of all minimally rigid graphs with a given number of vertices. On the other hand, a sequence of moves known as Henneberg steps can construct such sets of minimally rigid graphs in $\mathbb{R}^d$ starting from the complete graph on d vertices K_d [66] [1].

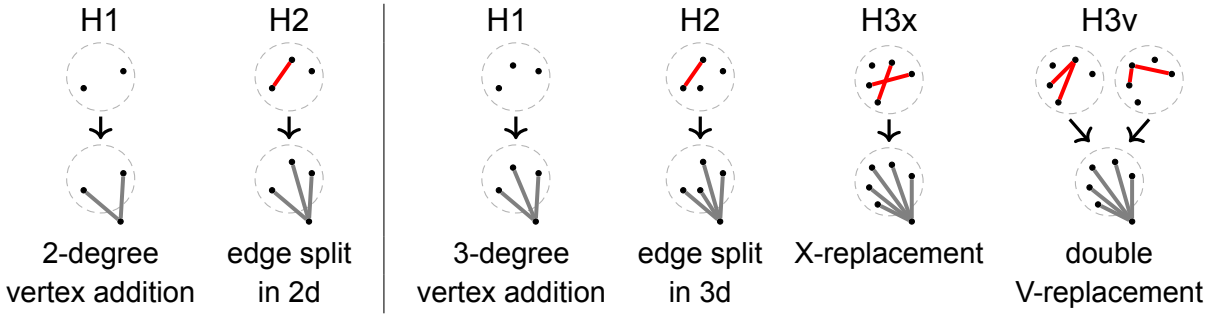

Figure 2.1: *Henneberg steps for Laman and Geiringer graphs.*

The first two moves are known as Henneberg 1 (H1) move or 0-extension and Henneberg 2 (H2) move or 1-extension or edge split. These operations add one vertex as follows (we consider a construction regarding rigidity in dimension d, see Figure 2.1 for $d = 2$ and $d = 3$):

- in an H1 move, the vertex added is connected with d existing vertices.
- in an H2 move, an edge is deleted in the existing graph and the added vertex is connected with the vertices of the deleted edge and $d - 1$ more existing vertices (thus the total degree of the added vertex is $d + 1$).

In all dimensions H1 and H2 steps preserve rigidity and minimal rigidity: if G^* is constructed by applying an H1 or an H2 move to a (minimally) rigid graph G, then G^* is also (minimally) rigid. Similarly, if G is generically flexible, then an H1 or H2 move also preserves this property.

In the case of $d = 2$ all minimally rigid graphs can be obtained by H1 and H2 operations, giving one more method to characterize Laman graphs. On the other hand, these two

[1] Recall from Chapter 1 that minimally rigid graphs in $\mathbb{R}^d$ have the same property in $\mathbb{C}^d, S^d, S^d_{\mathbb{C}}$.

Table 2.1: *Numbers of Laman and Geiringer graphs up to the last Henneberg move and graph planarity.*

Laman graphs

n	3	4	5	6	7	8	9	10	11
H1 planar	1	1	3	11	62	491	5,041	60,040	791,195
H1 non-planar	-	-	-	-	4	85	1,917	46,903	1,201,401
H2 planar	-	-	-	1	3	18	122	1,037	9,884
H2 non-planar	-	-	-	1	1	14	142	2,152	36,793

Geiringer graphs

n	4	5	6	7	8	9	10	11
H1 planar	1	1	1	4	12	45	221	1,215
H1 non-planar	-	-	2	16	299	9,718	527,250	41,907,790
H2 planar	-	-	1	1	2	5	12	34
H2 non-planar	-	-	-	5	61	1,719	85,401	6,267,144

moves are not sufficient to construct all minimally rigid graphs in $d \geq 3$, so extended Henneberg steps are required. These give a superset of minimally rigid graphs.

For Geiringer graphs, there is an additional step in which 2 edges are deleted and the new vertex is connected with the the vertices of the deleted edge and 1 more existing vertex. This is known as Henneberg 3 (H3) step (See Figure 2.1 for the 2 versions of this move in the space, i.e. H3x and H3v steps). Let us comment that the Geiringer graphs whose construction requires an H3 move in the last step have minimal degree 5 and no such graph exist for any graph with $n \leq 11$ vertices. It is conjectured that H1, H2 and H3 completely characterize rigid graphs in $\mathbb{R}^3$ [61, 66]. However, it has been proven that H3 move does not always preserve rigidity in dimension 4 [51].

We used Henneberg steps to construct sets of Laman and Geiringer graphs up to isomorphism (see Table 2.1), using canonical labeling as in [16, 35]. Since Henneberg moves add a vertex with a fixed degree, we can separate the sets of graphs with the same number of vertices up to their minimal degree. So if a graph in dimension 2 has minimal degree 2, then it can be constructed with an H1 move in the last step. If the minimal degree is 3 it certainly requires an H2 move in the last step of the Henneberg sequence. This division is useful because the H1 move trivially doubles the number of embeddings, since the new vertex lies in the intersection of d different $(d-1)$-spheres. This means that we can deduce the embedding number of a graph G in $\mathbb{R}^d$ with a d-valent vertex v, if we know the embedding number of the graph $G - \{v\}$, without computing the number of solutions of an algebraic system. On the other hand, computations have shown that the effect of other Henneberg steps on the embedding number varies significantly depending on a graph [35]. Thus, we will call minimally rigid graphs with a d-valent vertex *trivial*, while if the degree of the vertices is always bigger or equal than $d+1$, the graph shall be called *non-trivial*.

2.2 Algebraic Formulation

We introduce the algebraic formulations that serve to compute the embedding number and bounds on it. Initially, we present an algebraic formulation that is based on a variant of the squared distance equations 1.1. This formulation has been used several times in the context of studies on rigid graphs that exploit sparse elimination techniques [28, 64]. Subsequently, we present the Cayley-Menger embeddability conditions that are related with the vanishing or the sign of certain determinants of a distance matrix.

2.2.1 Sphere equations

The basis of the first formulation are the squared distance equations. In order to compute the embedding number using such system we need to remove rigid motions by fixing $\binom{d+1}{2}$ coordinates yielding a $0-$dimensional system. In the case of dimension 2, we may fix both coordinates of one vertex and one coordinate of a second vertex. If these vertices are adjacent to one edge, then the length constraint imposes only one solution for the remaining coordinate of the second vertex up to rotations. In general, if the graph contains a complete subgraph with d vertices $v_1, v_2, \dots v_d$, then we can choose the coordinates of this K_d graph in a way that they satisfy the edge lengths of this subgraph. These shall be the *fixed vertices*, while K_d will be also called fixed. The number of (real) solutions of the system with the fixed vertices will give the (real) embedding number of the graph for a specific edge labelling. So, in the case of Laman graphs, we need to fix an edge, while in 3 dimensions a triangle should be fixed. Note that for the first set of graphs there is always a K_2 (edge). As for the 3-dimensional case, Geiringer graphs with no triangles (K_3) are very rare (the first one is the 10-vertex complete bipartite graph $K_{6,4}$) [2].

We will transform the squared distance equations to fit some requirements of sparse elimination, using an algebraic system with two sets of equations. First we define the set of *magnitude equations* that introduce new variables representing the distance of each vertex from the origin. Substituting the new variables to the squared distance equations, we get the *edge equations*, which represent the edge length constraints between the adjacent vertices of an edge. The algebraic system derived from the combination of these two sets shall be called *sphere equations*.

Definition 1 *Let $G(V, E)$ be a simple undirected graph. We denote by $\boldsymbol{\lambda} = \{\lambda_{u,v} \mid (u, v) \in E\}$ the set of the (given) edge lengths and by $X_u = \{x_{u,1}, x_{u,2}, \dots x_{u,d}\}$ the variables assigned to the coordinates of each vertex. The following system of equations gives the embeddings of G:*

$$\begin{aligned} \|X_u\|^2 &= s_u, \qquad \forall\, u \in V \backslash V(K_d)\,, \\ s_u + s_v - 2\langle X_u, X_v\rangle &= \lambda_{u,v}^2, \qquad \forall\, (u, v) \in E \backslash E(K_d)\,, \end{aligned} \tag{2.1}$$

[2] The technical details of the sphere equations in the absence of K_d will be discussed in Appendix B. For simplicity, in the rest of this manuscript we assume the existence of a K_d, unless stated otherwise.

where $\langle X_u, X_v \rangle$ *is the Euclidean inner product. We will denote the set of variables* $\widetilde{X}_u = X_u \bigcup \{s_u\}$ *in the euclidean case using* s_u *as the* $(d+1)$*-th variable* $x_{u,d+1}$*. If a vertex is fixed, its variables are substituted with constant values. This formulation can be obviously used in the case of embeddings on the unit* d*-dimensional sphere* S^d *using* $|X_u| = d+1$ *coordinates and setting* $s_u = 1$*.*

This algebraic system has $m = d \cdot |V| - d^2$ edge equations and $|V| - d$ magnitude equations if there is at least one subgraph K_d of G. Notice that the edges of the fixed K_d serve to specify the fixed vertices and are not included in this set of equations, so $m < |E|$. We will denote the set of the complex solutions for this algebraic system $\boldsymbol{S}(G, \boldsymbol{\lambda}, K_d(\boldsymbol{\rho})) \subset \mathbb{C}^{d \cdot |V|}$ for a given embedding $\boldsymbol{\rho}$ of a complete graph K_d satisfying the edge length constraints and the set of real solutions $\boldsymbol{S}_{\mathbb{R}}(G, \boldsymbol{\lambda}, K_d(\boldsymbol{\rho})) = \boldsymbol{S}(G, \boldsymbol{\lambda}, K_d(\boldsymbol{\rho})) \cap \mathbb{R}^{d \cdot |V|}$ for the same embedding of K_d. Clearly $c_d(G) = |\boldsymbol{S}(G, \boldsymbol{\lambda}, K_d(\boldsymbol{\rho}))|$ for any generic set of lenghts λ, while $r_d(G, \boldsymbol{\lambda}) = |\boldsymbol{S}_{\mathbb{R}}(G, \boldsymbol{\lambda}, K_d(\boldsymbol{\rho}))|$. Notice that both $c_d(G)$ and $r_d(G, \lambda)$ are independent of the choice for a fixed K_d.

2.2.2 Cayley-Menger determinants

A Cayley-Menger (CM) matrix is a matrix of squared distances between n points in an Euclidean space extended by a row and column of ones:

$$CM = \begin{pmatrix} 0 & 1 & 1 & \cdots & 1 \\ 1 & 0 & \lambda_{1,2}^2 & \cdots & \lambda_{1,n}^2 \\ 1 & \lambda_{1,2}^2 & 0 & \ddots & \cdots \\ \cdots & \cdots & \ddots & \ddots & \cdots \\ 1 & \lambda_{1,n}^2 & \lambda_{2,n}^2 & \cdots & 0 \end{pmatrix},$$

where $\lambda_{i,j}$ is the distance between point i and j.

One of the main theorems in distance geometry gives the following embeddability conditions for a CM matrix [12]:

Theorem 2 *The squared distances of a CM matrix can be embedded in* $\mathbb{R}^d$ *iff*

- *rank*$(CM) = d+2$
- $(-1)^{\kappa} \det(CM') \geq 0$*, for every submatrix* CM' *with size* $\kappa + 1 \leq d+2$ *that includes the extending row/column.*

In the case of graph embeddings, we can use a matrix with known entries and variables: each known entry corresponds to a squared edge length, while the variables correspond to lengths between non-edges. This results to a system of determinantal equations and inequalities. Any solution of the semi-algebraic system is an embedding of the graph in

$\mathbb{R}^d$ up to isometries, indicating that each one of these solutions correspond to 2 solutions in the case of sphere equations since reflections are factored out in this formulation.

Considering only the solutions of the determinantal variety, we get the complex embeddings of the graph. The set of inequalities is related with certain geometrical constraints on the edge lengths, such as positivity and triangular inequalities in dimension 2. In dimension 3, *tetrangular inequalities* (which are a generalization of triangular inequalities on the area of the triangles of a tetrahedron) should be also satisfied, while in bigger dimensions there are additional constraints (in this thesis only dimensions 2 and 3 are taken into consideration with this algebraic formulation) [20].

The systems of equations of determinantal varieties are over-constrained. For example, there are 35 equations in 10 variables for 7-vertex Laman graphs, while for 7-vertex Geiringer graphs, there are 21 equations in 6 variables. Despite this fact, it is possible to find 0-dimensional square subsystems of these systems of equations [24, 28].

Notice that the zero set of the whole determinantal variety corresponds to the missing edge lengths of the complete graph. This means that the solutions of the subsystem are restricted to a subset of the missing edge lengths. If the graph extended by the edges corresponding to the variables of the subsystem is globally rigid, then the subsystem gives an upper bound on the number of embeddings of the whole graph [40], since globally rigid graphs have unique realizations (see Chapter 1).

In the cases treated in Chapter 5, square subsystems can be easily detected, if no restriction is imposed on the number of variables. Unfortunately, these subsystems are not always 0-dimensional and cannot serve to find the embedding number of a graph or a useful upper bound. Nevertheless, our experimental results lead to the conclusion that there can be subsystems derived from a graph $G(V, E)$ with $|V|-(d+1)$ equations satisfying the 0-dimensionality condition. For the most important cases, we show that for dimensions 2 and 3 there is always an extension of a minimally rigid graph with $|V| - (d + 1)$ edges resulting to a globally rigid graph.

Lemma 1 *For every minimally rigid graph $G(V, E)$ in dimensions $d = 2$ and $d = 3$, there is at least one extended graph $J = G \cup \{e_1, e_2, .., e_\xi\}$, with $\xi = |V| - (d + 1)$ and $e_i \notin E$, which is globally rigid in $\mathbb{R}^d$.*

Proof: The only 4-vertex minimally rigid graph in dimension 2 (respectively 5-vertex in dimension 3) is obtained by applying an H1 step to the triangle (resp. tetrahedron in dimension 3). If we extend this graph with the only non-existing edge, we obtain a complete graph, so the lemma holds. Let the lemma hold for every graph that has less or equal vertices with $G_{|V|} = (V, E)$. H2 steps are known to preserve global rigidity in any dimension [18]. So we need to prove the induction for H1 steps in both dimensions and H3 steps in dimension 3.

Let a Laman graph $G_{|V|+1}$ be constructed by an H1 move applied to $G_{|V|}$ with $|V|$ vertices, whose extended globally rigid graph is $J_{|V|}$. Without loss of generality, this move

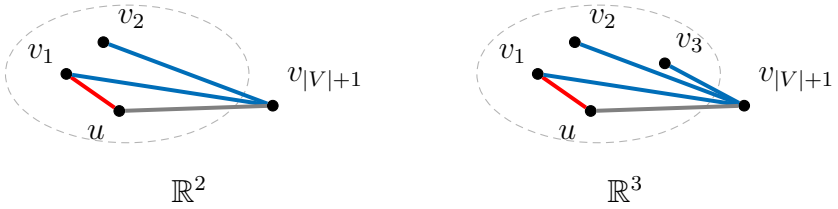

Figure 2.2: *$J_{|V|+1}$ is constructed by an H1 step applied to $J_{|V|}$ (blue edges), extended with the edge $(u, v_{|V|+1})$. This is equivalent with applying an H2 step and adding the deleted edge $(u, v_{|V|+1})$.*

connects a new vertex $v_{|V|+1}$ with vertices v_1, v_2. Let u be a neighbour of v_1 in $G_{|V|+1}$ such that $v_2 \neq u$. The edge (u, v_1) exists also in $G_{|V|}$ and $J_{|V|}$. If we set $J'_{|V|+1} = (J_{|V|} \cup \{(v_1, v_{|V|+1}), (v_2, v_{|V|+1}), (u, v_{|V|+1})\}) - \{(v_1, u)\}$, then $J'_{|V|+1}$ is globally rigid, because it is constructed from $J_{|V|}$ by an H2 step. Hence, $J_{|V|+1} = J'_{|V|+1} \cup \{(u, v_1)\}$ is also globally rigid, proving the statement in the case of H1 steps in dimension 2. The same result holds in arbitrary dimension (see Figure 2.2 for $d = 3$).

Both H3x and H3v steps consist of an H2 step followed by a second edge deletion in the existing graph and a new connection with $v_{|V|+1}$ (see Figure 2.1). So, if we apply an $H3$ move in $J_{|V|}$ and subsequently add the second deleted edge, then $J_{|V|+1}$ is globally rigid. □

Even though, there are always globally rigid extentions with $|V| - (d + 1)$ supplementary edges, it is not always possible to find a CM subvariety corresponding to them. Such subvarieties can be detected for all Laman and Geiringer graphs with $|V| \leq 7$ vertices, but there exist bigger graphs for which this property does not hold.

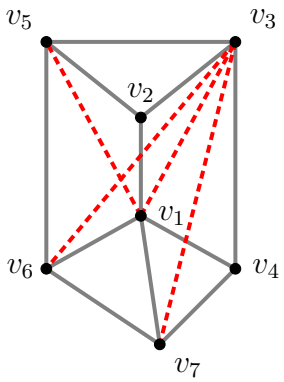

Figure 2.3: *The embeddings of the Laman graph L_{48H2} (grey edges) can be represented by submatrices of $CM_{L_{48H2}}$ that involve only variables corresponding to the 4 red dashed edges. The extended graph is globally rigid. This construction can be used to find also the spherical embeddings.*

We now give some representative examples of optimal CM subsystems in the cases of

Laman and Geiringer that are used to find lower bounds in Chapter 5. For instance, L_{48H2} is a 7-vertex Laman graph (see Figure 2.3), which has $c_2(L_{48H2}) = r_2(L_{48H2}) = 48$ and $c_{S^2}(L_{48H2}) = r_{S^2}(L_{48H2}) = 64$ (See Section 5.2). There are 11 subsystems of this CM variety in 4 variables, which all have exactly the same number of solutions. In the following CM matrix, we present one of these choices involving the variables x_1, x_2, x_6 and x_7.

$$CM_{L_{48H2}} = \begin{pmatrix} 0 & 1 & 1 & 1 & 1 & 1 & 1 & 1 \\ 1 & 0 & \lambda^2_{v_1,v_2} & x_1 & \lambda^2_{v_1,v_4} & x_2 & \lambda^2_{v_1,v_6} & \lambda^2_{v_1,v_7} \\ 1 & \lambda^2_{v_1,v_2} & 0 & \lambda^2_{v_2,v_3} & x_3 & \lambda^2_{v_2,v_5} & x_4 & x_5 \\ 1 & x_1 & \lambda^2_{v_2,v_3} & 0 & \lambda^2_{v_3,v_4} & \lambda^2_{v_3,v_5} & x_6 & x_7 \\ 1 & \lambda^2_{v_1,v_4} & x_3 & \lambda^2_{v_3,v_4} & 0 & x_8 & x_9 & \lambda^2_{v_4,v_7} \\ 1 & x_2 & \lambda^2_{v_2,v_5} & \lambda^2_{v_3,v_5} & x_8 & 0 & \lambda^2_{v_5,v_6} & x_{10} \\ 1 & \lambda^2_{v_1,v_6} & x_4 & x_6 & x_9 & \lambda^2_{v_5,v_6} & 0 & \lambda_{v_6,v_7} \\ 1 & \lambda^2_{v_1,v_7} & x_5 & x_7 & \lambda^2_{v_4,v_7} & x_{10} & \lambda_{v_6,v_7} & 0 \end{pmatrix}$$

In order to compute $r_2(L_{48H2})$, the positive real solutions of the determinantal variety should also satisfy the triangular inequalities.

The same extended graph is used to compute the spherical embeddings of L_{48H2}. An additional constraint is needed in that case, which represents the distance from the origin, as a new column and row with ones. The determinantal subsystem is derived from the rank condition of 3-dimensional embeddings. Elementary matrix operations can lead to a formulation that considers the cosines of the angles between two points as matrix entries, denoted as η_{v_i,v_j}.

$$CM_{S^2(L_{48H2})} = \begin{pmatrix} 0 & 1 & 1 & 1 & 1 & 1 & 1 & 1 & 1 \\ 1 & 0 & \lambda^2_{v_1,v_2} & x_1 & \lambda^2_{v_1,v_4} & x_2 & \lambda^2_{v_1,v_6} & \lambda^2_{v_1,v_7} & 1 \\ 1 & \lambda^2_{v_1,v_2} & 0 & \lambda^2_{v_2,v_3} & x_3 & \lambda^2_{v_2,v_5} & x_4 & x_5 & 1 \\ 1 & x_1 & \lambda^2_{v_2,v_3} & 0 & \lambda^2_{v_3,v_4} & \lambda^2_{v_3,v_5} & x_6 & x_7 & 1 \\ 1 & \lambda^2_{v_1,v_4} & x_3 & \lambda^2_{v_3,v_4} & 0 & x_8 & x_9 & \lambda^2_{v_4,v_7} & 1 \\ 1 & x_2 & \lambda^2_{v_2,v_5} & \lambda^2_{v_3,v_5} & x_8 & 0 & \lambda^2_{v_5,v_6} & x_{10} & 1 \\ 1 & \lambda^2_{v_1,v_6} & x_4 & x_6 & x_9 & \lambda^2_{v_5,v_6} & 0 & \lambda_{v_6,v_7} & 1 \\ 1 & \lambda^2_{v_1,v_7} & x_5 & x_7 & \lambda^2_{v_4,v_7} & x_{10} & \lambda_{v_6,v_7} & 0 & 1 \\ 1 & 1 & 1 & 1 & 1 & 1 & 1 & 1 & 0 \end{pmatrix}$$

$$\sim \begin{pmatrix} 0 & 1 & 1 & 1 & 1 & 1 & 1 & 1 & 2 \\ 1 & 0 & \eta_{v_1,v_2} & y_1 & \eta_{v_1,v_4} & y_2 & \eta_{v_1,v_6} & \eta_{v_1,v_7} & 1 \\ 1 & \eta_{v_1,v_2} & 0 & \eta_{v_2,v_3} & y_3 & \eta_{v_2,v_5} & y_4 & y_5 & 1 \\ 1 & y_1 & \eta_{v_2,v_3} & 0 & \eta_{v_3,v_4} & \eta_{v_3,v_5} & y_6 & y_7 & 1 \\ 1 & \eta_{v_1,v_4} & y_3 & \eta_{v_3,v_4} & 0 & y_8 & y_9 & \eta_{v_4,v_7} & 1 \\ 1 & y_2 & \eta_{v_2,v_5} & \eta_{v_3,v_5} & y_8 & 0 & \eta_{v_5,v_6} & y_{10} & 1 \\ 1 & \eta_{v_1,v_6} & y_4 & y_6 & y_9 & \eta_{v_5,v_6} & 0 & \eta_{v_6,v_7} & 1 \\ 1 & \eta_{v_1,v_7} & y_5 & y_7 & \eta_{v_4,v_7} & y_{10} & \eta_{v_6,v_7} & 0 & 1 \\ -2 & 1 & 1 & 1 & 1 & 1 & 1 & 1 & 0 \end{pmatrix}$$

The semi-algebraic conditions of the latter formulation, requires that any solution of the determinantal subsystem lies in the interval $[-1, 1]$ and that the triangular inequalities on

the sphere are satisfied. The second is equivalent to the positivity of $2\eta_{v_i,v_j}\eta_{v_i,v_k}\eta_{v_j,v_k} - \eta^2_{v_i,v_j} - \eta^2_{v_i,v_k} - \eta^2_{v_j,v_k} + 1$ for 3 point of vertex embeddings v_i, v_j, v_k on the sphere, where η_{v_i,v_j} is the cosine of the angle between points i and j and can be obtained as the determinant of a 5x5 submatrix containing both columns and rows with ones.

Our example in the 3-dimensional case is the graph G_{48} (see Figure 2.4). This graph has the maximal number of embeddings among all 7-vertex Geiringer graphs ($c_3(G_{48}) = r_3(G_{48}) = 48$ - see Section 5.2). There are 5 different square systems in 3 variables that completely define the embeddings. We can choose one of them involving only x_1, x_2, x_3:

$$CM_{G_{48}} = \begin{pmatrix}
0 & 1 & 1 & 1 & 1 & 1 & 1 & 1 \\
1 & 0 & \lambda^2_{v_1,v_2} & \lambda^2_{v_1,v_3} & \lambda^2_{v_1,v_4} & \lambda^2_{v_1,v_5} & \lambda^2_{v_1,v_6} & x_1 \\
1 & \lambda^2_{v_1,v_2} & 0 & \lambda^2_{v_2,v_3} & x_2 & x_3 & \lambda^2_{v_2,v_6} & \lambda^2_{v_2,v_7} \\
1 & \lambda^2_{v_1,v_3} & \lambda^2_{v_2,v_3} & 0 & \lambda^2_{v_3,v_4} & x_4 & x_5 & \lambda^2_{v_3,v_7} \\
1 & \lambda^2_{v_1,v_4} & x_2 & \lambda^2_{v_3,v_4} & 0 & \lambda^2_{v_4,v_5} & x_6 & \lambda^2_{v_4,v_7} \\
1 & \lambda^2_{v_1,v_5} & x_3 & x_4 & \lambda^2_{v_4,v_5} & 0 & \lambda^2_{v_5,v_6} & \lambda^2_{v_5,v_7} \\
1 & \lambda^2_{v_1,v_6} & \lambda^2_{v_2,v_6} & x_5 & x_6 & \lambda^2_{v_5,v_6} & 0 & \lambda^2_{v_6,v_7} \\
1 & x_1 & \lambda^2_{v_2,v_7} & \lambda^2_{v_3,v_7} & \lambda^2_{v_4,v_7} & \lambda^2_{v_5,v_7} & \lambda^2_{v_6,v_5} & 0
\end{pmatrix}$$

The set of real embeddings in that case is given by the solutions of the subsystem that satisfy positivity, triangular and tetrangular inequalities.

Extending this graph with the edge (v_1, v_7) suffices for global rigidity. This edge corresponds to the variable x_1 and it is possible to get a single equation by applying resultants in the 3x3 system of determinantal equations (see Figure 2.4).

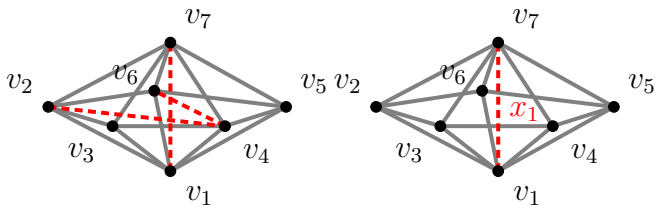

Figure 2.4: *The graph G_{48} (grey edges). There are submatrices of $CM_{G_{48}}$ that involve only variables corresponding to the 3 red dashed edges of the left graph. The graph G_{48} extended by the edge v_1v_7 (that corresponds to the variable x_1) is globally rigid.*

Since a single edge is needed to find the whole embedding, we can use only the inequalities involving only this variable (5 triangular and 5 tetrangular inequalities instead of 35 that involve all variables).

3. ON THE MULTIHOMOGENEOUS BÉZOUT BOUND OF THE EMBEDDING NUMBER

In this chapter we are concerned with the m-Bézout bound of the sphere equations (see Definition 1). In Section 3.1 we propose two methods for computing the m-Bézout bound. The first one is a combinatorial method relating outdegree constrained graph orientations with this bound. The latter uses a standard formulation via matrix permanents. We also compare the runtimes of these methods with the runtimes of algorithms that compute mixed volumes and the embedding number.

In Section 3.2, we examine the exactness of m-Bézout bounds. Initially, we present experimental results that compare these bounds with embedding numbers and mixed volumes. Then, we present a general method to decide if the m-Bézout bound of a minimally rigid graph is tight or not without directly computing the embeddings.

All the results of this chapter have been published in [5].

3.1 Computing m-Bézout bounds

In this section, we concentrate on the m-Bézout bound of the sphere equations of a graph $G(V, E)$ up to a fixed complete subgraph K_d. Let us remind that K_d may not be a subgraph of a minimally rigid graph for $d \geq 3$. We will give details on the computation of the bound in the absence of K_d in Appendix B. For the rest of this chapter, unless further specified, K_d will denote a given complete subgraph and not all possible choices.

In order to compute the m-Bézout bound we will choose a natural partition such that each subset of variables $\widetilde{X}_u$ contains these ones which correspond to the coordinates and the magnitude of a single vertex u. We will separate the magnitude equations from the edge equations, since the first ones there is only one set of variables with degree 2, while in every edge equation the degree of the u-th set of variables is always 1, resulting to the following expansion:

$$\prod_{u \in V'} 2 \cdot Y_u \prod_{(u,v) \in E'} (Y_u + Y_v) = 2^{|V|-d} \cdot \prod_{u \in V'} Y_u \prod_{(u,v) \in E'} (Y_u + Y_v),$$

where $V' = V \setminus V(K_d)$, $E' = E \setminus E(K_d)$ and Y_u are symbolic parameters representing $\widetilde{X}_u$. We remark that if $v \in V(K_d)$ and $(u, v) \in E'$, then $Y_v = 0$, since vertex u is fixed and no variables are assigned for it.

This means that we only need to find the coefficient of the monomial $\prod_{u \in V'} Y_u^d$ in the polynomial of the product (see Theorem 15 in Appendix A for details on the m-Bézout):

$$\prod_{(u,v) \in E'} (Y_u + Y_v) \tag{3.1}$$

Let us denote this coefficient by $\mathcal{B}(G, K_d)$, which is related only to the combinatorial structure of edge equations. The m-Bézout bound for the number of embeddings of a graph in $\mathbb{C}^d$ up to a fixed K_d is $mBe(G, K_d) = 2^{|V|-d} \cdot \mathcal{B}(G, K_d)$. Notice that this bound is the same for spherical embeddings in $S^d_{\mathbb{C}}$.

We remark that although $c_d(G)$ is invariant under different choices of fixed K_d, the m-Bézout bound of a graph G may vary up to this choice. Thus, one needs to compute m-Bézout bounds up to all fixed complete subgraphs in order to find the minimal one. The same observation holds for the BKK bound of sphere equations.

We will use graph orientations and matrix permanents to compute the bound based on the expansion of Equation 3.1. Let us mention that matrix permanents have been already used to bound the number of Eulerian orientations (which are graph orientations with equal indegree and outdegree for every vertex) in [60], but to the best of our knowledge there are no published results on the connection between matrix permanents and outdegree constrained graph orientations in the general case.

3.1.1 A combinatorial algorithm to compute m-Bézout bounds

This subsection focuses on a method relating m-Bézout bounds for minimally rigid graphs with graph orientations. Our method is inspired by two different approaches that characterize Laman graphs. First, Recski's theorem states that if a graph is Laman then any multigraph obtained by doubling an edge should be the union of two spanning trees [61]. Additionally, pebble games give a relation between the existence of an orientation and the number of constraints in a graph and its subgraphs [49]. The following theorem gives a combinatorial method to compute the m-Bézout bound, proving that $mBe(G, K_d)$ is exactly the number of certain outdegree-constrained orientations. These orientations shall be called *valid orientations*.

In the following theorem E' is the same as in Equation 3.1.

Theorem 3 *Let $G(V, E)$ be a minimally rigid graph in $\mathbb{C}^d$ that contains at least one complete subgraph with d vertices. Let $\{v_1, \dots v_d\}$ be the vertex set of such subgraph which is the fixed K_d. By removing the edges of K_d from G, graph $G' = (V, E')$ is defined. Then $\mathcal{B}(G, K_d)$ defined above is the number of outdegree-constrained orientations denote the of G', such that*

- *the outdegree of $v_1, \dots, v_d$ is 0.*
- *the outdegree of every vertex in $V \backslash \{v_1, \dots, v_d\}$ is d.*

Proof: By expanding the product $\prod_{(u,v)\in E'} (Y_u + Y_v)$, the monomial $\prod_{u\in V'} Y_u^d$ can be obtained when each Y_u from a given edge contributes exactly d times in that product. This means that every time we shall choose one of the two sets of variables that correspond to the

adjacent vertices of the edge represented in the parenthesis. This choice yields an orientation in the directed graph and vice versa. Thus, the number of different orientations in all edges gives us how many times this monomial will appear in the expansion, completing the proof. □

Algorithm 1: Count graph orientations

```
1  Function(orient)
   Input: |V| (# of vertices), E (graph edges without E(K_d)),
   outdeg (desired outdegree list. If vertex u ∈ V(K_d) then outdeg[u] = 0, otherwise outdeg[u] = d).
   Output: # of outdegree-constrained orientations
2  deg = vertex degrees of graph G(V, E)
   /* Ending condition for the recursion                                   */
3  if |E| = 0 then
4      return (1)
   /* No valid orientations in this case                                   */
5  if ∃u, outdeg[u] > deg[u] or outdeg[u] < 0 then
6      return (0)
   /* Examine the conditions yielding unique orientations                 */
7  for u ≤ |V| do
8      if outdeg[u] = 0                    // u admits only new indirerected edge orientations
9      then
10         for all edges (u, v) ∈ E do
11             outdeg[v] = outdeg[v] − 1
12             E'=E\{(u, v)}
13             newdeg =vertex degree of graph G'(V, E')
14             return (orient(|V|, Enew, outdeg, newdeg))
15     else if outdeg[u] = deg[u]          // u admits only new outdirerected edge orientations
16     then
17         for all edges (u, v) ∈ E do
18             outdeg[u] = outdeg[u] − 1
19             E'=E\{(u, v)}
20             newdeg =vertex degrees of graph G'(V, E')
21             return (orient(|V|, E', outdeg, newdeg))
   /* No more unique orientations exists: set both orientations for 1st edge */
22 (u, v) = E[1]
23 outdeg1[u] = outdeg[u] − 1
24 outdeg2[v] = outdeg[v] − 1
25 E'=E\{(u, v)}
26 newdeg =vertex degree of graph G'(V, E')
27 orient1=orient(|V|, E', outdeg1, newdeg)
28 orient2=orient(|V|, E', outdeg2, newdeg)
29 return (orient1+orient2)
```

This theorem gives another way to prove that an H1 move doubles the m-Bézout bound of minimally rigid graphs. Hence, minimally rigid graphs constructed only by H1 moves have at most $2^{|V|-d}$ embeddings (actually this bound is tight, see Section 2.1).

Corollary 1 *An H1 move always doubles the m-Bézout bound up to the same fixed K_d. Moreover, if a graph can be constructed only with H1 moves, then the m-Bézout bound for this graph is exactly $2^{|V|-d}$.*

Proof: Let $\mathcal{B}(G, K_d)$ be the number of outdegree-constrained orientations for a graph $G(V, E)$ up to a given K_d. This means that the m-Bézout bound is

$$mBe(G, K_d) = 2^{|V|-d} \cdot \mathcal{B}(G, K_d).$$

Now, let G^* be a graph obtained by an H1-move on the graph G. Since H1 adds a degree-d vertex to G, this means that there is only one way to reach outdegree d for the new vertex of G^*. So the outdegree-constrained orientations of G^* up to the same K_d are exactly $\mathcal{B}(G, K_d)$ and

$$mBe(G^*, K_d) = 2^{|V|+1-d} \cdot \mathcal{B}(G, K_d) = 2 \cdot mBe(G, K_d).$$

The second statement of this corollary can be proven using the previous equality: starting from K_d, only one orientation satisfies the requirements of Theorem 3 for each H1 move. So, the m-Bézout bound of a minimally graph constructed only by H1 moves is $2^{|V|-d}$. □

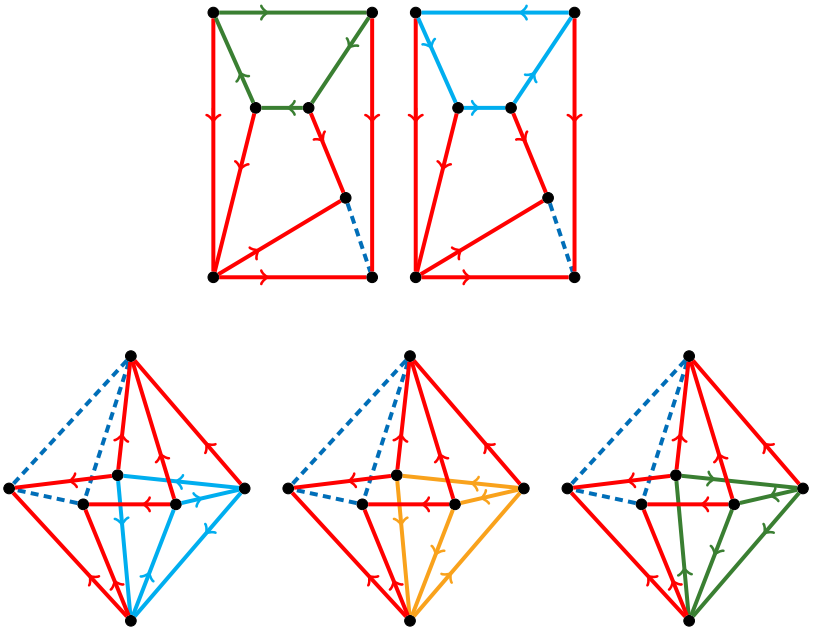

Figure 3.1: *The orientations of graphs L_{56} and G_{48}. Notice that there is only one way to direct the red edges up to the choice of K_d (dashed blue).*

Let us demonstrate our method examining one Laman and one Geiringer graph.

Example 1 *Here are two examples of this counting method in the case of L_{56} graph in dimension 2 and G_{48} in dimension 3, which are both 7-vertex graphs (see Figure 3.1). Graph*

L_{56} has 56 complex embeddings in the plane and 64 embeddings on the sphere, while G_{48} has 48 embeddings in $\mathbb{C}^3$ (these numbers coincide also with the maximum number of real embeddings, see [35, 31] and Section 5.2). The mixed volumes of the algebraic systems are 64 and 48 respectively.

The dashed lines indicate the fixed edges of K_d. The edge direction for any edge that includes a fixed vertex is always oriented outwards the non-fixed vertex. This yields a unique orientation *up to the fixed K_d, which is coloured in red for both graphs. The rest of the graph admits $\mathcal{B}(L_{56}, K_2) = 2$ orientations for L_{56}, while the number of different orientations for G_{48} is $\mathcal{B}(G_{48}, K_3) = 3$. So the m-Bézout bound is $2^{7-2} \cdot 2 = 64$ for L_{56} and $2^{7-3} \cdot 3 = 48$ for G_{48}.*

We have implemented a software tool in Python to count the number of orientations for an arbitrary graph given the desired outdegrees. The basic part of this code (see Algorithm 1) is to decide recursively which choices of direction are allowed in every step and is available in zenodo [6].

3.1.2 Computing m-Bézout bounds using the permanent

The permanent of an $m \times m$ matrix $A = (a_{i,j})$ is defined as follows:

$$\text{per}(A) = \sum_{\sigma \in \mathcal{S}_m} \prod_{i=1}^{m} a_{i,\sigma(i)}, \tag{3.2}$$

where $\mathcal{S}_m$ denotes the group of all permutations of m integers.

One of the most efficient ways to compute the permanent is by using Ryser's formula [67]:

$$\text{per}(A) = \sum_{M \subseteq \{1,2,\ldots,m\}} (-1)^{m-|M|} \prod_{i=1}^{m} \sum_{j \in M} a_{i,j}. \tag{3.3}$$

There is a very relevant relation between per(A) and the m-Bézout bound, see [26]:

Theorem 4 *Given a system of algebraic equations and a partition of the variables in k subsets, as in Theorem 15, we define the square matrix A with $m = \sum_{j=1}^{n} m_j$ rows, where each set of variables corresponds to a block of m_j rows. Let $a_{i,j}$ be the degree of the i-th equation in the j-th set of variables. The columns of A correspond to the equations, where the subvector of the i-th column associated to the j-th set of variables has m_j entries, all equal to $a_{i,j}$. Then, the m-Bézout bound of the given system is equal to*

$$\frac{1}{m_1!\, m_2! \cdots m_n!} \cdot \text{per}(A). \tag{3.4}$$

We will refer to A matrix as the *m-Bézout matrix* of a polynomial system. This implies that in the case of minimally rigid graphs, we obtain a square m-Bézout matrix A with

columns associated to the equations of non-fixed edges, and $|V|-d$ blocks of d rows each, corresponding to the non-fixed vertices. An entry $a_{i,j}$ is one if the vertex corresponding to i is adjacent to the edge corresponding to the equation indexing j, otherwise it is zero. This is an instance of a $(0,1)$-permanent. Therefore Theorem 4 gives the coefficient

$$\mathcal{B}(G,K_d)=\left(\frac{1}{d!}\right)^{|V|-d}\cdot \text{per}(A),$$

in bounding the system's roots, since all $m_i=d$, while $n=|V|-d$.

Including the effect of magnitude equations the corollary below follows.

Corollary 2 *The m-Bézout bound of the sphere equations for an $|V|$-vertex rigid graph in d dimensions up to a given K_d is exactly*

$$mBe(G,K_d)=\left(\frac{2}{d!}\right)^{|V|-d}\cdot \text{per}(A), \tag{3.5}$$

assuming that matrix A is the m-Bézout matrix up to K_d defined as above.

The permanent formulation for the computation of the m-Bézout bound gives us another way to prove Corollary 1.

Corollary 3 *Let G be a minimally rigid graph in $\mathbb{C}^d$ and A_G be its $(m\times m)$ m-Bézout matrix up to a fixed K_d. Then, for every graph G^* obtained by an H1 operation on G, the permanent of its m-Bézout matrix A_{G^*} up to the same K_d is per$(A_{G^*})=d!\cdot$ per(A_G).*

Proof: Without loss of generality, we consider that the last d rows of matrix A_{G^*} represent the new vertex, while the last d columns of this matrix represent the edges adjacent to this vertex, since matrix permanent is invariant under row or column permutations. The rest of the matrix is the same as A_G. This yields the following structure:

$$A_{G^*}=\begin{pmatrix} A_G & A' \\ \mathbf{0} & \mathbf{1}\end{pmatrix}$$

where **0** is a $(d\times m)$ zero submatrix, **1** is a $(d\times d)$ submatrix with ones and A' the $(m\times d)$ submatrix of the new edge columns without the new rows. It is clear from the definition of the permanent (See Equation 3.2), that column permutations that do not include a zero entry are counted as 1 in this sum, while if they include a zero entry the product is zero. The only column permutations that do not include a zero entry for the d last rows are those that are related to the d last edges, so there are $d!$ nonzero column permutations for this block of rows.

This means that the permutations for the other m rows exclude the last three columns, so they are exactly per(A_G) permutations in this case. Thus, per$(A_{G^*})=d!\cdot$ per(A_G). □

Since $mBe(G^*, K_d) = \left(\frac{2}{d!}\right)^{|V|+1-d} \cdot \text{per}(A_{G^*})$, it follows that

$$mBe(G^*, K_d) = 2 \cdot mBe(G, K_d),$$

as in Corollary 1.

Let us give an example of this counting method for a minimally rigid graph.

Example 2 *We use the L_{136} graph to provide an example for this formulation (see Figure 3.2- other examples can be found in [6]). L_{136} is the 8-vertex Laman graph with the maximal embedding number $c_2(G) = 136$ among all Laman graphs with the same number of vertices [16]. On S^2, it has 192 complex embeddings, which is also maximum (but not unique), since there is another graph sharing the same $c_{S^2}(G)$.*

The m-Bézout matrix $A_{L_{136}}$ for the fixed edge (v_1, v_2) is the following:

	(v_1,v_4)	(v_1,v_8)	(v_2,v_3)	(v_2,v_5)	(v_2,v_7)	(v_3,v_4)	(v_3,v_5)	(v_4,v_6)	(v_4,v_8)	(v_5,v_6)	(v_6,v_7)	(v_7,v_8)
x_3	0	0	1	0	0	1	1	0	0	0	0	0
y_3	0	0	1	0	0	1	1	0	0	0	0	0
x_4	1	0	0	0	0	1	0	1	1	0	0	0
y_4	1	0	0	0	0	1	0	1	1	0	0	0
x_5	0	0	0	1	0	0	1	0	0	1	0	0
y_5	0	0	0	1	0	0	1	0	0	1	0	0
x_6	0	0	0	0	0	0	0	1	0	1	1	0
y_6	0	0	0	0	0	0	0	1	0	1	1	0
x_7	0	0	0	0	1	0	0	0	0	0	1	1
y_7	0	0	0	0	1	0	0	0	0	0	1	1
x_8	0	1	0	0	0	0	0	0	1	0	0	1
y_8	0	1	0	0	0	0	0	0	1	0	0	1

and its permanent is per$(A_{L_{136}}) = 192$, which gives the m-Bézout bound since $d = 2$.

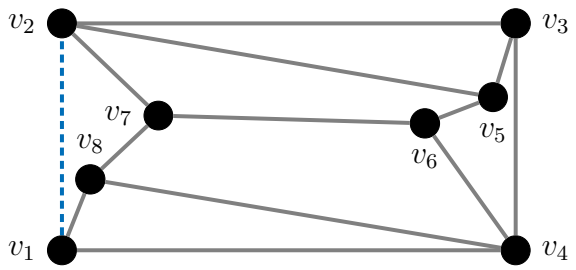

Figure 3.2: *The L_{136} graph. The dashed edge is the fixed one.*

3.1.3 Runtimes

The computation of the m-Bézout bounds using our combinatorial algorithm up to a fixed K_d is much faster than the computation of mixed volume and complex embeddings. In order to compute the mixed volume we used `phcpy` in `SageMath` [68] and we computed complex solutions of the sphere equations using `phcpy` and and `MonodromySolver` [23]. Let us notice that, `MonodromySolver` seems to be faster than mixed volume software we used in the case of Geiringer graphs. We also compared our runtimes with the combinatorial algorithm that counts the exact number of complex embeddings in $\mathbb{C}^2$ [16].

We will try to give some indicative cases for which we compared the runtimes. For example, computing the mixed volume of the spherical embeddings up to one fixed edge for the maximal 12-vertex Laman graph for a given fixed K_2 takes around 390ms, while our algorithm for the m-Bézout bound required 13ms. If we wanted to compute mixed volumes up to all fixed K_2 we needed 8.6s, while the m-Bézout computation took 270ms. The runtime for the combinatorial algorithm that computes the number of complex embeddings is 6.363s for the same graph.

For larger graphs i.e. 18-vertex graphs, the combinatorial algorithm may take ~ 17h to compute the number of complex embeddings in $\mathbb{C}^2$. We tested a 18-vertex graph that did not require more than 0.12s to compute one m-Bézout bound and 4s to compute m-Bézout bounds up to all choices of fixed edges.

In dimension 3 our model was the icosahedron graph, which has 12 vertices. The computation of the mixed volume took more than 6 days in this case, while our algorithm needed 60ms to give exactly the same result (54,272). `MonodromySolver` could track all $54,272$ solutions in ~ 1.3 hour, while Gröbner basis computations failed multiple times to terminate.

Computing the permanent required more time compared to our algorithm. For the icosahedron the fastest computation could be done using `Maple`'s implementation in `LinearAlgebra` package. It took ~ 0.96s to compute the permanent up to a given fixed triangle with this one. On the other hand the implementations in `Python` and `Sage` took much more time for the same graph (~ 8m and ~ 10m respectively).

This seems reasonable since if the total number of edge equations is m, then the combinatorial algorithm has to check at most 2^m cases, while according to [26] the complexity to compute the permanent using Ryser's formula is in the order of $m^2 \cdot 2^m$.

3.2 On the exactness of m-Bézout bounds

In this section we present experimental results and a general method that study the exactness of the m-Bézout bound. Our computations use already published results on the embedding number [35] in order to compare the m-Bézout bound with it. We also use computations from [4] (we remind that Chapter 5 is dedicated to the results of this publication) on the mixed volumes of sphere equations systems. All the other computations are

Table 3.1: *Runtimes of different algorithms on graphs with maximal $c_d(G)$ up to $|V| = 11$ and up to $|V| = 10$ for Laman and Geiringer graphs, respectively. We compute $c_2(G)$ by [16] and $c_3(G)$ by `phcpy` [8] (fails to find all solutions for $|V| > 11$). Also runtimes for computing $c_2(G)$, $c_3(G)$ by `MonodromySolver`. We compute mixed volume (MV) by `phcpy`, m-Bézout (mBe) by `Maple`'s permanent and our `Python` code [6]. Computation of the m-Bézout and MV is up to a fixed K_d (edges or triangles).*

	Laman graphs				
$\|V\|$	combin. $c_2(G)$	`Monodromy Solver`	`phcpy` MV	`Maple`'s perm.	mBe `Python`
6	0.0096s	0.2334s	0.0024s	0.0003s	0.0009s
7	0.0153s	0.566s	0.006s	0.00045s	0.0012s
8	0.0276s	1.373s	0.0122s	0.00065	0.002s
9	0.066s	4.934s	0.0217s	0.0018s	0.0032s
10	0.176s	12.78s	0.043s	0.0053s	0.0045s
11	0.558s	46.523s	0.17s	0.0077s	0.0074s
12	6.36s	2m47s	0.39s	0.049s	0.013s
18	17h 5m	-	1h 34m	24s	0.115s

	Geiringer graphs				
$\|V\|$	`phcpy` solver	`Monodromy Solver`	`phcpy` MV	`Maple`'s perm.	mBe `Python`
6	0.652s	0.141s	0.00945s	0.0002s	0.0097s
7	3.01s	0.584s	0.041s	0.001s	0.00165s
8	20.1s	2.297s	0.425s	0.0025s	0.00266s
9	2m 33s	14.97s	3.42s	0.0075s	0.006s
10	16m 1s	1m23s	1m 12s	0.08s	0.0105s
11	2h 14m	9m22s	27m31s	0.49s	0.024s
12	-	1h22m	> 6 days	0.96s	0.06s

part of this project (m-Bézout, spherical embeddings and some cases of graphs for which there was no information on their embedding number). These results show that there are some classes that the m-Bézout is a tight bound.

We also develop a method based on Bernstein's second theorem on the exactness of the mixed volume bound [9]. Our main goal is to reduce the number of checks on the Minkowski sum of Newton Polytopes that are required by this theorem. We consider that this method may be a first step to establish the existence of classes of graphs with tight m-Bézout bounds.

3.2.1 Experimental results

We compared m-Bézout bounds with the number of embeddings and mixed volumes using existing results [35, 28] for the embeddings in $\mathbb{C}^2$ and $\mathbb{C}^3$. We also computed the complex solutions of the equations that count embeddings on S^2 for all Laman graphs up to 8 vertices and a selection of graphs with up to 12 vertices that have a large number of embeddings. We remind that in general the m-Bézout bound is not unique up to all choices of a fixed K_d. It is natural to consider the minimal m-Bézout bound as the optimal upper bound of the embeddings for a given graph. Let us notice that we checked if the m-Bézout is minimized when the fixed K_d has a maximal sum of vertex degrees or when the vertex with the maximum degree belongs to the fixed K_d. There are counter-examples for both of these hypotheses.

Mixed volume and m-Bézout bound. In all cases we checked in $\mathbb{C}^3$ and S^2, the m-Bézout bound up to a fixed K_d is exactly the same as the mixed volume up to the same fixed vertices. There are some cases in $\mathbb{C}^2$ for which the m-Bézout bound is bigger than the mixed volume for certain choices of K_2. We shall notice that these cases do not correspond to the minimal m-Bézout bound for the given graph (thus the minimum m-Bézout and the minimum mixed volume are the same for these graphs).

Spatial embeddings and the m-Bézout bound. There are many Geiringer graphs for which the bound of the sphere equations is larger than the actual number of complex embeddings. Nevertheless, we observed that for all planar graphs (in the graph-theoretical sense) up to $|V| = 11$ the number of complex embeddings is exactly the same as the mixed volume bound and therefore the m-Bézout bound, while in the non-planar case the bounds are generally not tight. What is also interesting is that the m-Bézout bound is invariant for all choices of fixed triangles for all planar Geiringer graphs.

Embeddings of Laman graphs and the m-Bézout bound. For Laman graphs, the m-Bézout bound diverges from the number of actual embeddings in $\mathbb{C}^2$ more than in the case of Geiringer graphs. That happens both for planar and non-planar graphs. On the other hand the number of spherical embeddings of planar Laman graphs coincides with the

Table 3.2: *Mixed volumes, complex embedding numbers, and m-Bézout bounds for embeddings of Laman graphs in $\mathbb{C}^2$ and S^2. These graphs have the maximal number of embeddings in $\mathbb{C}^2$. The 12-vertex maximal Laman graph is the first non-planar in this category.*

n	$\mathbf{MV}_{2d}$	$c_2(G)$	$\mathbf{MV}_{S^2}$	$c_{S^2}(G)$	mBézout
6	32	24	32	32	32
7	64	56	64	64	64
8	192	136	192	192	192
9	512	344	512	512	512
10	1536	880	1536	1536	1536
11	4096	2288	4096	4096	4096
12	15630	6180	15630	*8704*	15630

minimum m-Bézout bound for a vast majority of cases (all planar graphs up to 6 vertices, 64/65 7-vertex planar graphs and 496/509 8-vertex planar graphs). Notice that the m-Bézout bounds for different choices of the fixed edge are, in general, different for planar Laman graphs.

3.2.2 Using Bernstein's second theorem

Our computations indicate that the m-Bézout bound is tight for almost all planar Laman graphs in S^2 and all planar Geiringer graphs. Therefore, we apply Bernstein's second theorem to establish a method that determines whether this bound is exact (see Appendix A for details on the BKK bound and Bernstein's second theorem- Theorems 16 and 17 respectively). We believe that a generalization of this method may show whether the experimental results provably hold for certain classes of graphs. In this subsection for reasons of simplicity, in all examples we will use the variables x_i, y_i, s_i and x_i, y_i, z_i for $\mathbb{C}^2$ and S^2 respectively (instead of the notation $x_{i,1}, \cdots x_{i,d}, s_i$ presented in Definition 1). Also $\boldsymbol{m}$ denotes the total number of variables.

The first step in this Section is to use Newton polytopes whose mixed volume equals to the m-Bézout bound (see for example [63]) since they are simpler than the Newton polytopes of the sphere equations.

Definition 2 *We set $\widehat{\boldsymbol{e}}_i = (0, 0, \ldots, \underset{\text{i-th position}}{1}, \ldots, 0)$ and let T_d^u be the simplex defined as the convex hull of the set*

$$\{\mathbf{0}, \widehat{\boldsymbol{e}}_{d\cdot(u-1)+1}, \widehat{\boldsymbol{e}}_{d\cdot(u-1)+2}, \ldots, \widehat{\boldsymbol{e}}_{d\cdot(u-1)+d}\},$$

where $\mathbf{0} = (0, 0, \ldots, 0)$ is the origin. Let $\widetilde{X}_u$ be the u-th set of variables under a partition of all variables, with set cardinality $d_u = |\widetilde{X}_u|$. Then $T_{d_u}^u$ is the simplex that corresponds to the

variables of this set. The m-Bézout Polytope *of a polynomial, with respect to a partition of the variables, is the Minkowski sum of the $T^u_{d_u}$ for all u, such that each simplex is scaled by the degree of the polynomial in $\widetilde{X}_u$.*

For a multihomogeneous system, simplices $T^u_{d_u}$ belong to complementary subspaces. Then, each m-Bézout Polytope is the Newton polytope of the respective equation. For general systems, our procedure amounts to finding the smallest polytopes that contain the system's Newton polytopes and can be written as Minkowski sum of simplices lying in the complementary subspaces specified by the variable partition.

In the case of rigid graphs in $\mathbb{C}^d$, every set of variables has $d+1$ elements. Thus, the m-Bézout Polytope of the magnitude equations for a vertex u is $2 \cdot T^u_{d+1}$, while the m-Bézout Polytope of the equation for edge (u, v) is $T^u_{d+1} + T^v_{d+1}$. This implies that the Minkowski sum of the m-Bézout Polytopes for the sphere equations of a minimally rigid graph $G(V, E)$ is exactly

$$\mathcal{P}_G = \sum_{u \in V'} (\deg(u) + 2) \cdot T^u_{d+1},$$

where $\deg(u)$ is the degree of vertex u in the graph and V' the set of non-fixed vertices.

In general, it is hard to compute the Minkowski sum of polytopes in high dimension. But in the case of the m-Bézout Polytopes the following theorem describes the facet normals of $\mathcal{P}_G$.

Theorem 5 *Let $G(V, E)$ be a minimally rigid graph in $\mathbb{C}^d$ and $\mathcal{P}_G$ be the Minkowski sum defined above. The set of the inner normal vectors of the facets of $\mathcal{P}_G$ are exactly*

- *all unit vectors $\widehat{e}_i$, and*
- *the $|V| - d$ vectors of the form*

$$\widehat{\boldsymbol{\delta}}_u = \sum_{j=1}^{d+1} -\widehat{\boldsymbol{e}}_{(d+1)\cdot(u-1)+j} = (0, 0, \ldots, -1, -1, \ldots, -1, \ldots, 0),$$

  where there are $d+1$ nonzero entries corresponding to the variables that belong to the u-th variable set.

Proof: Since each T^u_{d+1} belongs to a complementary subspace, $\mathcal{P}_G$ can be seen as the product of polytopes $\prod_{u \in V'} (\deg(u) + 2) \cdot \Delta_{d+1}$, where Δ_{d+1} is the unit $(d+1)$-simplex [1]. The inner normal vectors of the facets of Δ_{d+1} in $\mathbb{R}^{d+1}$ are the unit vectors $\widehat{\boldsymbol{e}}_i$ and $\widehat{\boldsymbol{\delta}} = \sum_{j=1}^{d+1} -\widehat{\boldsymbol{e}}_j$

[1] The idea of using the product of polytopes is derived by a proof for the mixed volumes corresponding to the weighted m-Bézout bound in [55]

in $\mathbb{R}^{d+1}$. The theorem follows since the normal fan of a product of polytopes is the direct product of the normal fans of each polytope [74]. □

This theorem yields a method to find the H-representation of $\mathcal{P}_G$, in other words the polytope is described as the intersection of linear halfspaces and the respective equations are given by the theorem. In all cases where $MV = mBe$, the polytopes $\mathcal{P}_G$ can be used instead of the Newton Polytopes of the equations.

The verification of Bernstein's second theorem requires a certificate for the existence of roots of face systems (see Definition 10) for every face of $\mathcal{P}_G$, where faces range from vertices of dimension 0 to facets of codimension 1. We propose a method that confirms or rejects Bernstein's condition checking a much smaller number of systems based on the form of facet normals. For this, we shall distinguish three cases below.

The normal of a lower dimensional face can be expressed as the vector sum of facet normals, whose cardinality actually equals the face codimension. This means that we need to verify normals distinguished in the following three cases:

1. vector sums of one or more "coordinate" normals $\widehat{\boldsymbol{e}}_i$'s,
2. vector sums of one or more "non-coordinate" normals $\widehat{\boldsymbol{\delta}}_u$'s,
3. "mixed" vector sums containing both $\widehat{\boldsymbol{e}}_i$'s and $\widehat{\boldsymbol{\delta}}_u$'s.

Notice that since there are $(d+2)\cdot(|V|-d)$ different normals, in order to check all resulting face systems, $2^{(d+2)\cdot(|V|-d)}$ computations are required. We now examine each of these three cases separately, in order to exclude a very significant fraction of these computations.

First case (coordinate normals). Let $F = (f_i)_{1\leq i\leq m}$ be the system of the sphere equations, let the initial forms be $f_i^{\widehat{e}}$ for some normal $\widehat{\boldsymbol{e}}$, and let $F^{\widehat{e}}$ be the resulting face system. We will deal with the coordinate normals case starting with an example.

Example 3 *We present the equations of face system $F^{\widehat{\boldsymbol{e}}_1}$ in $\mathbb{C}^2$. Normal e_1 corresponds to variable x_1. This means that the inner products with the exponent vectors of the monomials in the magnitude equation $f_1 = x_1^2 + y_1^2 - s_1$ are $2, 0, 0$. Thus, $f_1^{\widehat{\boldsymbol{e}}_1} = y_1^2 - s_1$, excluding the monomial x_1^2. In the case of the edge equation $f_{(1,2)} = s_1 + s_2 - 2(x_1x_2 + y_1y_2) + \lambda_{1,2}^2$, for a generic edge length $\lambda_{1,2}$, the inner products are $0, 0, 1, 0, 0$. It follows that $f_{(1,2)}^{\widehat{\boldsymbol{e}}_1} = s_1 + s_2 - 2y_1y_2 + \lambda_{1,2}^2$. If the degree of x_1 in an equation f_i is zero, then $f_i^{\widehat{\boldsymbol{e}}_1} = f_i$, since the inner product of all the exponent vectors with e_i is zero.*

This example shows that since all x_1 monomials are removed, $F^{\widehat{\boldsymbol{e}}_1}$ is an over-constrained system that has the same number of equations as F, but a smaller number of variables. The same holds obviously for every $F^{\widehat{\boldsymbol{e}}_i}$, while for $\widehat{\boldsymbol{e}} = \sum_{i\in I} \widehat{\boldsymbol{e}}_i$ (where I is an index set)

the initial forms in $F^{\widehat{e}}$ are obtained after removing all monomials that include one or more of the variables corresponding to the $\widehat{e}_i$'s of the sum. In other words, the initial forms in system $F^{\widehat{e}}$ can be obtained by evaluating to zero all the variables indexed by the set I.

Lemma 2 *Let $\widehat{e}$ be a sum of $\widehat{e}_i$ normals as described above. Now, F does not verify Bernstein's condition in the coordinate normals case (and has an inexact BKK bound) due to system $F^{\widehat{e}}$ having a toric root r', only if F has a root r with zero coordinate for at least one of the variables in I, such that the projection of r to the coordinates $j \notin I$ equals r'.*

We can now exclude the case of sums of coordinate normals from our examination, since it shall not generically occur, because the next lemma shows that r has no zero coordinate.

Lemma 3 *The set of solutions of the sphere equations for a rigid graph generically lies in $(\mathbb{C}^*)^{d \cdot n}$.*

Proof: We indicate by $\boldsymbol{S}(G, \boldsymbol{\lambda}, K_d(\boldsymbol{\rho}))$ the set of complex embeddings for a rigid graph G up to an edge labeling $\boldsymbol{\lambda}$ and the embedding of d fixed vertices $\boldsymbol{\rho} = (\rho_1, \rho_2, \ldots \rho_d)$. This set of embeddings is finite by definition. If there is a zero coordinate in the solution set, there exists a vector $\rho' \in \mathbb{C}^d$, such that no zero coordinates belong to the zero set $S^*(G, \boldsymbol{\lambda}, K_d(\boldsymbol{\rho} + \rho'))$, where $\boldsymbol{\rho} + \rho' = (\rho_1 + \rho', \rho_2 + \rho', \ldots \rho_d + \rho')$. Since we want to verify Bernstein's condition for a generic number of complex embeddings of G, we can always use the second set of embeddings. □

This lemma excludes a total of $2^{(d+1)\cdot(|V|-d)}$ cases when verifying Bernstein's second theorem for a given algebraic system.

Second case (non-coordinate normals). In the second case, the inner product of exponent vectors with $\widehat{\boldsymbol{\delta}}_u$ is minimized for all variables $\widetilde{X}_u$ with maximum degree. Let us give again an example to explain this statement.

Example 4 *It is an example in $\mathbb{C}^2$ for face system $F^{\widehat{\boldsymbol{\delta}}_1}$. The inner products for the magnitude equation $f_1 = x_1^2 + y_1^2 - s_1$ and the edge equation $f_{(1,2)} = s_1 + s_2 - 2 \cdot (x_1 x_2 + y_1 y_2) + \lambda_{1,2}^2$, $\lambda_{1,2}$ being a generic edge length, are $-2, -2, -1$ and $-1, 0, -1, -1, 0$ respectively. So, $f_1^{\widehat{\boldsymbol{\delta}}_1} = x_1^2 + y_1^2$ and $f_{(1,2)}^{\widehat{\boldsymbol{\delta}}_1} = s_1 - 2 \cdot (x_1 x_2 + y_1 y_2)$. If the degree of a polynomial f_i in the set of variables $\widetilde{X}_u$ is zero, then $f_i^{\widehat{\boldsymbol{\delta}}_u} = f_i$.*

The number of equations of $F^{\widehat{\boldsymbol{\delta}}_u}$ equals the number of variables. Following Bernstein's proof on the discriminant conditions, we introduce a new system by applying a suitable variable transformation from the initial variable vector **x** to a new variable vector **t** with same indexing. This transformation uses an $\boldsymbol{m} \times \boldsymbol{m}$ full rank matrix B such that every

monomial $\mathbf{x}^{\alpha}$ is mapped to $\mathbf{t}^{B\cdot\alpha}$ (see [9, 19] for more details). Furthermore, $|\det B| = 1$ so that the transformation preserves the mixed volume of F [19].

In our case, we construct matrix B with the following properties:

$$\begin{aligned} B\cdot\widehat{\boldsymbol{\delta}}_u^T &= e_{(d+1)\cdot(u-1)+1}, \\ B\cdot\widehat{\boldsymbol{e}}_{(d+1)\cdot(u-1)+j}^T &= \widehat{\boldsymbol{e}}_{(d+1)\cdot(u-1)+j},\ \forall j\in\{2,\ldots,d+1\}, \\ \det(B) &= \pm 1. \end{aligned}$$

The intuition behind these choices is given in Lemma 4 and its proof. This yields the following map from variables **x** to new variables **t**:

$$x_{u,1}\mapsto\frac{1}{t_{u,1}},\ x_{u,2}\mapsto\frac{t_{u,2}}{t_{u,1}},\ \cdots,\ s_u\mapsto\frac{t_{u,d+1}}{t_{u,1}}. \tag{3.6}$$

We will refer to the set of $x_{u,1}$'s as the *$\widehat{\boldsymbol{\delta}}$-variables* of F, since the image of their exponent vectors is the set of $\widehat{\boldsymbol{\delta}}_u$'s, while the exponent vectors for the other variables remain same. This transformation maps system $F(\mathbf{x})$ to a new system $\widehat{F}(\mathbf{t})$ of Laurent polynomials in the new variables. In the case of $\mathbb{C}^2$, the sphere equations are mapped as follows:

$$\begin{aligned} \widehat{f}_u &= \frac{1}{t_{u,1}^2}+\frac{t_{u,2}^2}{t_{u,1}^2}-\frac{t_{u,3}}{t_{u,1}},\ \text{(magnitude equations)} \\ \widehat{f}_{(u,v)} &= \frac{t_{u,3}}{t_{u,1}}+\frac{t_{v,3}}{t_{v,1}}-2\cdot\left(\frac{1}{t_{u,1}t_{v,1}}+\frac{t_{u,2}t_{v,2}}{t_{u,1}t_{v,1}}\right)+\lambda_{u,v}^2\ \text{(edge equations)}\ . \end{aligned}$$

The degree $\alpha(\widehat{f},t_{u,1})$ of a polynomial $\widehat{f}$ with respect to the variable $t_{u,1}$ will be either zero or negative. Let us now multiply every polynomial in $\widehat{F}(\mathbf{t})$ with each one of the monomials $t_{u,1}^{-\alpha(\widehat{f},t_{u,1})}$. These monomials are defined as the least common multiple of the denominators in the Laurent polynomials $\widehat{f}$, yielding the following system $\widetilde{F}(\mathbf{t})$:

$$\begin{aligned} \widetilde{f}_u &= 1+t_{u,2}^2-t_{u,1}t_{u,3},\ \text{(magnitude equations)} \\ \widetilde{f}_{(u,v)} &= t_{v,1}t_{u,3}+t_{u,1}t_{v,3}-2\cdot(1+t_{u,2}t_{v,2})+\lambda_{u,v}^2\cdot t_{u,1}t_{v,1}.\ \text{(edge equations)} \end{aligned}$$

This transformation yields the necessary conditions to verify if the face systems of the non-coordinate normals have solutions in $(\mathbb{C}^*)^{\boldsymbol{m}}$. We will refer to $t_{u,1}$'s as the set of $\widehat{\boldsymbol{\delta}}$-variables of $\widetilde{F}(\mathbf{t})$, while the rest should be the e-variables. Note that the transformation gives a well-constrained system, while zero evaluations of the $\widehat{\boldsymbol{\delta}}$-variables shall result to an over-constrained system, that should have no solutions if the bound is exact.

Lemma 4 *There exists a sum $\widehat{\boldsymbol{\delta}}$ of different $\widehat{\boldsymbol{\delta}}_u$ normals, such that face system $F^{\widehat{\boldsymbol{\delta}}}$ has a solution in $(\mathbb{C}^*)^{\boldsymbol{m}}$ if the algebraic system $\widetilde{F}(\mathbf{t})$, which is defined above, has a zero solution for $t_{u,1}$ for one or more vertices u.*

Proof: Matrix B is constructed to change the variables $x_{u,1}$ to variables $t_{u,1}$, for vertices u. From the definitions of $\widehat{F}(\mathbf{t})$ and $\widetilde{F}(\mathbf{t})$, it follows that given a monomial $\mathbf{t}^{\boldsymbol{\beta}}$ in a polynomial $\widehat{f}$ of $\widehat{F}(\mathbf{t})$, the inner product $\langle \boldsymbol{\beta}, B \cdot \widehat{\boldsymbol{\delta}}_u^T \rangle$ is not minimized among other monomials in $\widehat{f}$ if and only if the degree of $t_{u,1}$ in the respective monomial of the transformed polynomial $\widetilde{f}$ is positive. Thus, the existence of toric solutions for the face system $F^{\widehat{\boldsymbol{\delta}}_u}$ is equivalent to existence of toric solutions for the zero evaluation $\widetilde{F}(\mathbf{t}, t_{u,1} = 0)$.

So, if $\widetilde{F}(\mathbf{t}, t_{u,1} = 0)$ has a solution in $\mathbb{C}^{\boldsymbol{m}}$ such that $\widetilde{F}(\mathbf{t}, t_{u,1} = t_{v_1,1} = \cdots = t_{v_k,1} = 0)$ has a solution in $(\mathbb{C}^*)^{\boldsymbol{m}}$, then $F^{\widehat{\boldsymbol{\delta}}_u + \widehat{\boldsymbol{\delta}}_{v_1} + \cdots + \widehat{\boldsymbol{\delta}}_{v_k}}$ has a solution in $(\mathbb{C}^*)^{\boldsymbol{m}}$. □

The computational gain in this case is that, without the lemma, one would have checked every different combination of the $\widehat{\boldsymbol{\delta}}_u$'s, namely a total of $2^{|V|-d}$ checks. Now, it suffices to check only one zero evaluation for each of them, hence only $|V| - d$ checks.

Third case (mixed normals). The third case, that includes the sums of vectors $\widehat{\boldsymbol{\delta}}_u$ and $\widehat{\boldsymbol{e}}_i$ can be also treated with the transformation $\widetilde{F}(\mathbf{t})$ introduced above. Since the minimization of the inner product is invariant for d of the $d+1$ variables per vertex, the non-existence of zero solutions in $\widetilde{F}(\mathbf{t})$ implies that no F^w has solutions in $(\mathbb{C}^*)^{\boldsymbol{m}}$ for all vectors w that are sums of vectors $\widehat{\boldsymbol{\delta}}_u$ with those vectors $\widehat{\boldsymbol{e}}_i$ for which the equality $B \cdot \widehat{\boldsymbol{e}}_i^T = \widehat{\boldsymbol{e}}_i$ holds. In order to proceed we need the following lemma. This shows that using d of the $d+1$ $\widehat{\boldsymbol{e}}_i$'s of a vertex suffices to verify if a face system of a mixed normal has solutions in $\mathbb{C}^{\boldsymbol{m}}$.

Lemma 5 *Let us define a sum of normals*

$$-\widehat{\boldsymbol{\delta}}_u = \sum_{j=1}^{d+1} \widehat{\boldsymbol{e}}_{(d+1)\cdot(u-1)+j} \in \mathbb{R}^{d+1}.$$

For every $w \in \mathbb{R}^{\boldsymbol{m}}$, such that w is a sum of $-\widehat{\boldsymbol{\delta}}_u$ and other normals outside the set $\{\widehat{\boldsymbol{\delta}}_u, \widehat{\boldsymbol{e}}_{(d+1)\cdot(u-1)+1}, \ldots, \widehat{\boldsymbol{e}}_{(d+1)\cdot(u-1)+d+1}\}$ (hence in a subspace complementary to that of $-\widehat{\boldsymbol{\delta}}_u$), the face system F^w cannot have a solution in $(\mathbb{C}^*)^{\boldsymbol{m}}$.

Note that $-\widehat{\boldsymbol{\delta}}_u$ is the sum of $d+1$ normals in complementary subspaces.

Proof: We will treat the case of dimension $d = 2$ for simplicity of notation; the proof generalizes to arbitrary d. Without loss of generality, we consider $u = 1$. Then $w \in \mathbb{R}^3 \times \mathbb{R}^{\boldsymbol{m}-3}$ with $w = (-\widehat{\boldsymbol{\delta}}_1, v)$ and $v \in \mathbb{R}^{\boldsymbol{m}-3}$. The inner products of $-\widehat{\boldsymbol{\delta}}_1$ with the exponent vectors of the magnitude equation in $\mathbb{R}^2$ for the first coordinate are $2, 2, 1$, so $f_1^{-\widehat{\boldsymbol{\delta}}_1} = -s$. It is obvious that no w which is a sum of $-\widehat{\boldsymbol{\delta}}_1$ and normals not belonging to the set $\{\widehat{\boldsymbol{\delta}}_1, \widehat{\boldsymbol{e}}_1, \widehat{\boldsymbol{e}}_2, \widehat{\boldsymbol{e}}_3\}$ defines a face system with no solutions in $(\mathbb{C}^*)^{\boldsymbol{m}}$. Similarly, the inner products of $-\widehat{\boldsymbol{\delta}}_1$ with the exponent vectors of the magnitude equation $f_1 = x_1^2 + y_1^2 + z_1^2 - 1$ on S^2 are $2, 2, 2, 0$, yielding $f_1^{-\widehat{\boldsymbol{\delta}}_1} = -1$ which has no solutions in $\mathbb{C}^{\boldsymbol{m}}$. □

Lemma 5 reveals that in order to verify the conditions of Bernstein's theorem, we can use the transformations $\widetilde{F}(\mathbf{t})$ for all choices of d variables from every set $\widetilde{X}_u$, since there is no need to check the cases that include the sum of all $\widehat{e}_i$ normals of a single vertex. This result, combined with Lemmas 3 & 4 leads to the following corollary.

Corollary 4 *There is a vector $w \in \mathbb{R}^m$ such that the face system of the sphere equations F^w has a toric root if and only if there is a choice of $\widehat{\boldsymbol{\delta}}$-variables such that the transformed algebraic system $\widetilde{F}(\boldsymbol{t})$ has a zero solution in $\mathbb{C}^m$ for at least one $\widehat{\boldsymbol{\delta}}$-variable.*

Since the first d coordinate variables $x_{u,j}$ are symmetric (while s_u variables are not), we can exploit these symmetries excluding some choices. So, without loss of generality, we may keep $x_{1,1}$ as a $\widehat{\boldsymbol{\delta}}$-variable from variable set X_1, and check all possible choices for $\widehat{\boldsymbol{\delta}}$-variables from all other variable sets $\widetilde{X}_u$, such that $u \neq 1$ and u is not among the fixed vertices.

Summary of three cases. In general, if one selects to take into consideration all possible sums of facet normals, then $2^{(d+2)\cdot(|V|-d)}$ cases should be checked. We have shown that the category of face systems defined by a sum of coordinate normals cannot have toric solutions, discarding $2^{(d+1)\cdot(|V|-d)}$ cases. In the two other cases, the investigation of toric solutions can be combined using the $\widetilde{F}(\mathbf{t})$ transformation. If a face system has toric solutions, then in the non-coordinate normals case some $\widehat{\boldsymbol{\delta}}$-variables may have zero solutions, while in the mixed normals case both $\widehat{\boldsymbol{\delta}}$-variables and $\widehat{e}$-variables may have zero solutions. A naive approach to verify these two cases would result to $2^{(d+1)\cdot(|V|-d)}\cdot(2^{(|V|-d)}-1)$ checks, but using Corollary 4 one needs to verify the zero evaluations of $\widehat{\boldsymbol{\delta}}$-variables for all choices of $\widehat{\boldsymbol{\delta}}$-variables. The latter, can be further reduced from $d^{|V|-d}$ to $d^{|V|-d-1}$, due to the fact that the coordinate variables are symmetric. Summarizing, when checking Bernstein's condition, for any of the $d^{|V|-d-1}$ choices of $\widehat{\boldsymbol{\delta}}$-variable transformation that construct $\widetilde{F}(\mathbf{t})$, it suffices that $|V|-d$ zero evaluations should be applied for each of the $\widehat{\boldsymbol{\delta}}$-variables.

Theorem 6 *Bernstein's condition can be verified in the case of the sphere equations after checking a total of at most $(|V|-d)\cdot d^{|V|-d-1}$ face systems.*

This discussion yields an effective algorithmic procedure (see Algorithm 2) to verify whether the m-Bézout bound is exact. Function `ConstructDeltaPoly` takes as input the system of the sphere equations F and a list of $\widehat{\boldsymbol{\delta}}$-variables to construct the polynomials $\widetilde{F}(\mathbf{t})$. The central role is played by function `IsmBezoutOfGraphExact`, which verifies if the polynomials $\widetilde{F}$ have zero solutions for the $\widehat{\boldsymbol{\delta}}$-variables.

Let us present two examples, further treated in the code found in [6].

Example 5 *The first (and the simplest non-trivial) example we have treated is an application of our method to the equations that give the embeddings of Desargues graph (double*

Algorithm 2: m-Bézout exactness for minimally rigid graphs

1 `Function(`*ConstructDeltaPoly*`)`

Input: F (sphere equations), V' (non-fixed vertices), L (variable indices mapped to $\widehat{\boldsymbol{\delta}}$-variables from each partition set)

Output: $\widetilde{F}$

`/* Transformation to` $\widehat{F}(\mathbf{t})$ `*/`

2 $changevars = \left(\bigcup_{u \in V'} \{x_{u,L(u)} \mapsto \frac{1}{t_{u,L(u)}}\} \right) \bigcup \left(\bigcup_{\substack{u \in V' \\ l \in \{1,\cdots,d+1\} \setminus \{L(u)\}}} \{x_{u,l} \mapsto \frac{t_{u,l}}{t_{u,L(u)}}\} \right)$

3 $\widehat{F}(\mathbf{t}) = F(changevars)$

4 $\widetilde{F}(\mathbf{t}) = \{\}$

5 **for** $\widehat{f} \in \widehat{F}(\mathbf{t})$ **do**

`/*` $\alpha(\widehat{f}, t_{u,L(u)}) =$ `(non-positive) degree of` $\widehat{f}$ `in variable` $t_{u,L(u)}$ `*/`

6 $\widetilde{f} = \prod_{u \in V'} t_{u,L(u)}^{-\alpha(\widehat{f}, t_{u,L(u)})} \cdot \widehat{f}$

7 $\widetilde{F}(\mathbf{t}) = \widetilde{F}(\mathbf{t}) \bigcup \{\widetilde{f}\}$

8 **return** $(\widetilde{F}(\mathbf{t}))$

9 `Function(`*IsmBezoutOfGraphExact*`)`

Input: F (sphere equations), V' (non-fixed vertices), Conjecture (If **True**, only one choice of $\widetilde{F}$, else all choices of $\widetilde{F}$)

Output: **True** (m-Bézout$= c_d(G)$) or **False** (m-Bézout$> c_d(G)$)

`/* Verification of Bernstein's condition */`

10 **if** *Conjecture=**True*** **then**

`/* Transformation to` $\widetilde{F}(\mathbf{t})$ `*/`

11 $L = [1, 1, \ldots, 1]$ `// L length = number of` $u \in V'$

12 $\widetilde{F}$=ConstructDeltaPoly(F,V',L)

`/* Check for zero solutions of` $\widehat{\boldsymbol{\delta}}$`-variables (main computation) */`

13 **for** $u \in V'$ **do**

`/* Check if zero evaluation has solutions using ideal of transformed face system */`

14 **if** $\widetilde{F}(\mathbf{t}, \{t_{u,l_u} = 0\})$ *has a solution* **then**

15 **return** (**False**)

16 **else if** *Conjecture=**False*** **then**

17 **for** *all choices of 1 out of* d *variables in every* $\widetilde{X}_u$, $u \neq 1$ **do**

18 $L = [1, (l_u, u \in V' \setminus \{1\})]$ `// always same choice for` X_1

19 $\widetilde{F}$=ConstructDeltaPoly(F,V',L)

`/* Check for zero solutions of` $\widehat{\boldsymbol{\delta}}$`-variables (main computation). */`

20 **for** $u \in V'$ **do**

21 **if** $\widetilde{F}(\mathbf{t}, \{t_{u,l_u} = 0\})$ *has a solution* **then**

22 **return** (**False**)

23 **return** (**True**)

prism) in $\mathbb{C}^2$ and S^2 (see Figure 3.3). The embedding number for this graph in $\mathbb{R}^2$ is 24 [13] and on S^2 it is 32 (see Chapter 5). They both coincide with the generic number of complex solutions of the associated algebraic system. The m-Bézout bound for these systems is 32, hence it is inexact in the $\mathbb{C}^2$ case. This shall be explained by the fact that the sphere equations in $\mathbb{C}^2$ have face systems of non-coordinate normals with toric roots.

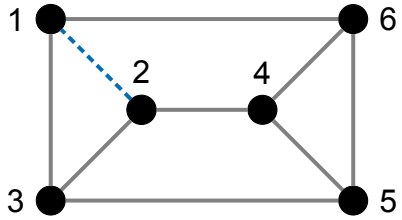

Figure 3.3: *Desargues graph (double prism).*

The system of the sphere equations (with vertices 1 and 2 fixed) is a 12×12 well-constrained system, but we can easily eliminate the linear equations obtaining an 8 by 8 well-constrained system. Subsequently, we can also fix vertex 3 up to reflection about the edge $(1, 2)$, obtaining finally a system of 6 polynomials in the variables $\{x_4, y_4, x_5, y_5, x_6, y_6\}$.

If we apply the transformation of variables mentioned above, we can construct a system of polynomials in variables $\{t_{4,1}, t_{4,2}, t_{5,1}, t_{5,2}, t_{6,1}, t_{6,2}\}$, such that evaluating $t_{4,1}, t_{5,1}$ or $t_{6,1}$ to zero corresponds to the face systems of $\widehat{\boldsymbol{\delta}}_4, \widehat{\boldsymbol{\delta}}_5$ or $\widehat{\boldsymbol{\delta}}_6$ respectively. This is one possible choice of $\widehat{\boldsymbol{\delta}}$-variables to construct $\widetilde{F}(\mathbf{t})$. Solving these 3 different systems for every $\widehat{\boldsymbol{\delta}}_u$ with Gröbner basis in `Maple` we find the existence of solutions in $\mathbb{C}^2$, indicating that the number of complex solutions is strictly smaller than the m-Bézout bound.

In order to get nonzero solutions in $\mathbb{C}^2$, we need to evaluate to zero all $t_{4,1}, t_{5,1}, t_{6,1}$ variables, implying that the normal direction for which Bernstein's second theorem shows mixed volume to be inexact is $(-1, -1, -1, -1, -1, -1)$. This is a normal of a 3-dimensional face, where the face dimension is obtained as 6-3. The normal equals the sum of 3 facet normals.

In the spherical case, no solutions exist, not only for the first choice of $\widetilde{F}(\mathbf{t})$, but also for all the other possible ones (see Algorithm 2), suggesting that the bound is tight, so the number of spherical embeddings is 32 and equals the m-Bézout bound.

Example 6 *The Jackson-Owen graph has the form of a cube with an additional edge adjacent to two antisymmetric vertices (see Figure 3.4). This graph is the smallest known case that has fewer real than complex embeddings, in $\mathbb{R}^2$ and $\mathbb{C}^2$ respectively [41]. The m-Bézout bound up to the fixed edge shown in the figure is 192, while the number of embeddings in $\mathbb{C}^2$ is 90. This shall be explained by a face system of mixed normals that has toric roots.*

The system of the sphere equations is 18×18, reduced to 13×13 after linear elimination. The set of variables is $\{x_3, y_3, x_4, y_4, x_5, y_5, x_6, y_6, x_7, y_7, x_8, y_8, s_8\}$.

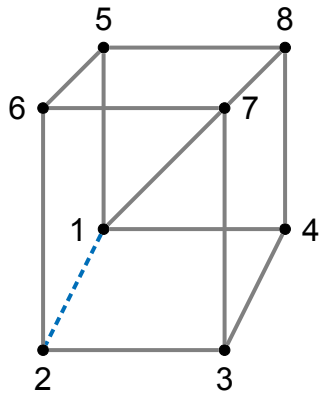

Figure 3.4: *The Jackson-Owen graph*

We apply the transformation of variables, resulting to a new system of polynomials in variables $\{t_{3,1}, t_{3,2}, t_{4,1}, t_{4,2}, t_{5,1}, t_{5,2}, t_{6,1}, t_{6,2}, t_{7,1}, t_{7,2}, t_{8,1}, t_{8,2}, t_{8,3}\}$*. As in the case of Desargues' graph, the evaluation of* $t_{3,1}, t_{4,1}, t_{5,1}, t_{6,1}, t_{7,1}, t_{8,1}$ *to zero corresponds to the face systems of* $\widehat{\boldsymbol{\delta}}_3, \widehat{\boldsymbol{\delta}}_4, \widehat{\boldsymbol{\delta}}_5, \widehat{\boldsymbol{\delta}}_6, \widehat{\boldsymbol{\delta}}_7, \widehat{\boldsymbol{\delta}}_8$ *respectively.*

We found a solution following zero evaluation of all $\widehat{\boldsymbol{\delta}}$*-variables of* $\widetilde{F}(\mathbf{t})$ *and* $t_{8,3}$*. The normal direction is* $(-1,-1,-1,-1,-1,-1,-1,-1,-1,-1,-1,-1,0) \in \mathbb{R}^{13}$*. This is an example for the mixed normals case, the normal being a sum of one* $\widehat{e}_i$ *and all 6* $\widehat{\boldsymbol{\delta}}_u$*'s.*

Another way to apply our method is the computation of a suitable resultant matrix for a given over-constrained system, which follows from evaluating some variable to zero. It is obvious that if the system has any solutions, the rank of the resultant matrix with sufficiently generic entries is strictly smaller than its size, otherwise it has full rank, assuming we have a determinantal resultant matrix. We have used `multires` module for `Maple` [15] to examine the existence of solutions, repeating the previous results. However, these tools seem to be slower than other techniques which directly compute the embedding number.

In all our experimental computations, the existence of zero solutions of only one choice of $\widetilde{F}(\mathbf{t})$ (and not all $d^{|V|-d-1}$) suffices to verify Bernstein's conditions. Therefore, we state the following conjecture:

Conjecture 1 *The conditions of Bernstein's second theorem for the system of the sphere equations* F *are satisfied if and only if the system* $\widetilde{F}(\mathbf{t})$ *has solutions for every zero evaluation of the* $\widehat{\boldsymbol{\delta}}$*-variables.*

If Conjecture 1 holds, then one only needs to check $|V|-d$ face systems that correspond to the zero evaluations of $\widetilde{F}(\mathbf{t})$ for each one of the $\widehat{\boldsymbol{\delta}}$-variables, instead of the $(|V|-d)\cdot d^{|V|-d-1}$ face systems indicated in Theorem 6. Algorithm 2 includes the option to consider the

Conjecture 1 to be either True or False. The first option takes into consideration only one choice of $\widehat{\delta}$-variables, while in the second one all different choices of $\widehat{\delta}$-variables are checked, as in Theorem 6.

Bounds on the maximal number of graph embeddings.

4. UPPER BOUNDS ON THE EMBEDDING NUMBER OF MINIMALLY RIGID GRAPHS

In this Chapter we present methods that improve the upper bound of the embedding number for minimally rigid graphs. Unless specified alternatively, we consider the case of minimally rigid graphs in $\mathbb{C}^d$ that have at least one complete subgraph K_d for the computation of the bounds. The asymptotic order of these bounds applies in the absence of such subgraph as well.

In Section 4.1 we use existing bounds that improve the upper bounds for $d \geq 5$ and planar Geiringer graphs. Subsequently, in Section 4.2 we develop a method that bounds the number of outdegree constrained orientations and leads to better bounds in all dimensions. We summarize the asymptotic upper bounds of this Chapter in Table 4.1, juxtaposing the classic Bézout bound to the results of our methods.

The results of Section 4.1 have been published in [5], while the results of Section 4.2 have been accepted for publication [7].

Table 4.1: *Power basis of asymptotic upper bounds for minimally rigid graphs in $\mathbb{C}^d$: the first line contains the bounds derived in Section 4.1 applying Brègman-Minc bound (B-M), while the second those presented in Section 4.2 (pseu.), and Béz. corresponds to the trivial Bézout bound.*

d	2	3	4	5	6	7	8	9
B-M	4.8990	8.9442	16.733	31.749	60.795	117.17	226.89	441
pseu.	3.7764	6.8399	12.686	23.899	45.533	87.469	168.90	327.45
Béz.	4	8	16	32	64	128	256	512

4.1 Application of existing bounds on permanents and orientations

In this Section we make use of both methods presented in Chapter 3 for the m-Bézout computation. Applying directly bounds on $(0,1)-$matrix permanents (the Brègman-Minc bound) and planar graph orientations, we improve upon the Bézout bound of the embedding number for certain classes of minimally rigid graphs.

First, we make use of the following proposition on the asymptotic bounds for the orientations of planar graphs in order to improve the asymptotic upper bound of planar Geiringer graphs, which are the only fully characterized class of minimally rigid graphs in 3d space, and hence of special interest.

Proposition 1 (Felsner and Zickfeld [30]) *The number of outdegree constrained orientations of a planar graph is bounded from above by*

$$2^{|V|-4} \cdot \prod_{u \in \mathcal{I}} \left(2^{-deg(u)+1} \cdot \binom{deg(u)}{outdeg(u)} \right) \tag{4.1}$$

where $\mathcal{I}$ is an independent set of the graph, $deg(u)$ and $outdeg(u)$ are respectively the degree and the outdegree of a vertex u. Furthermore, in the case of $outdeg(u) = 3$ this bound asymptoticaly behaves as $3.5565^{|V|}$.

Given the relation between m-Bézout bounds and graph orientations (see Theorem 3), this proposition leads to the following improvement upon the asymptotic upper bound for the number of embeddings of the subclass of planar Geiringer graphs.

Theorem 7 *Planar Geiringer graphs have at most $O\left(7.1131^{|V|}\right)$ embeddings.*

Notice that planar Geiringer graphs are edge graphs of simplicial polyhedra [33], so there are always triangle subgraphs for them.

We also employ the permanent to obtain asymptotic improvement upon Bézout's asymptotic bound for $d \geq 5$ by using the following bound.

Proposition 2 (Brègman [14], Minc [54]) *For a $(0,1)$-permanent A of dimension m, it holds:*

$$per(A) \leq \prod_{j=1}^{m} (\nu_j!)^{1/\nu_j}\,, \tag{4.2}$$

where ν_j is the sum of the entries in the j-th column (or the j-th row).

This leads to the following result.

Theorem 8 *For $d \geq 5$ the Bézout bound is strictly larger than the m-Bézout bound given by Equation (3.5) for any fixed K_d.*

Given a fixed dimension d, the asymptotic upper bound derived from the Brègman-Minc inequality is

$$O\left(\left(2 \cdot \frac{\sqrt{(2d)!}}{d!} \right)^{|V|} \right).$$

Proof: In this proof $Be_d(|V|)$ and $mBe_d(|V|)$ denote the Bézout and the maximal m-Bézout bound of minimally rigid graphs in $\mathbb{C}^d$ with $|V|$ vertices respectively. Since the number of edge equations for minimally rigid graphs with $|V|$ vertices is $|V| \cdot d - d^2$, the Bézout bound is

$$Be_d(|V|) = 2^{|V| \cdot d - d^2}.$$

The sum of columns for the permanent that computes the m-Bézout bound is $\nu_j = d$ for the edges that include one fixed vertex and one non-fixed vertex and $\nu_j = 2d$ for these that include two non-fixed vertices. We denote these sets of edges $E_{f.}$ and $E_{n.f.}$ respectively. Applying the Brègman-Minc bound and Equation (3.5) we get

$$mBe_d(|V|) \leq \left(\frac{2}{d!}\right)^{|V|-d} \cdot \prod_{i=1}^{E_{f.}} (d!)^{1/d} \prod^{E_{n.f.}} (2d!)^{1/2d} \leq \left(2 \cdot \frac{\sqrt{(2d)!}}{d!}\right)^{|V|-d}. \tag{4.3}$$

Combining these bounds we get a sufficient condition for $Be_d(|V|) > mBe_d(|V|)$:

$$2^{|V|\cdot d - d^2} > \left(2 \cdot \frac{\sqrt{(2d)!}}{d!}\right)^{|V|-d} \Leftrightarrow 2^{2d-2} \cdot (d!)^2 > (2d)!$$

Robbins' bound on Stirling's approximation [59] yields the following:

$$\sqrt{2\pi} \cdot d^{d+1/2} \cdot e^{-d} \cdot e^{R_-} < d! < \sqrt{2\pi} \cdot d^{d+1/2} \cdot e^{-d} \cdot e^{R_+},$$

where $R_+ = \frac{1}{12d}$ and $R_- = \frac{1}{12d+1}$. We now derive the following inequalities:

$$\begin{aligned} 2^{2d-2} \cdot (d!)^2 &> 2^{2d-2} \cdot 2\pi \cdot d^{2d+1} \cdot e^{-2d} \cdot e^{2R_-} \\ &> \sqrt{2\pi} \cdot 2^{2d+1/2} \cdot d^{2d+1/2} \cdot e^{-2d} \cdot e^{R_+/2} \qquad > 2d! \end{aligned}$$

that lead to a sufficient condition for $Be_d(|V|) > mBe_d(|V|)$ to hold:

$$\sqrt{d} > \frac{4}{\sqrt{\pi}} \cdot e^{R_+/2 - 2R_-}, \tag{4.4}$$

which is true for every integer $d \geq 5$.

Additionally, inequality (4.3) leads directly to the asymptotic bound

$$mBe_d(|V|) \in O\left(\left(2 \cdot \frac{\sqrt{(2d)!}}{d!}\right)^{|V|}\right) \tag{4.5}$$

for any given d. □

Obviously the asymptotic bound works also in the absence of K_d, since in the worst case there will be $d-2$ additional non fixed edges, so the exponent in Inequality 4.3 would be $|V|-2$ and the asymptotic order would be the same (See Appendix B).

4.2 A new method to reduce the upper bounds of the embedding number

In this section we develop a method to improve the upper bound on the embedding number of minimally rigid graphs. We introduce a graph structure that inherits some of the

properties of minimally rigid graphs, which we call *pseudographs*. Then, we apply an iterative method that eliminates a vertex or a path in each step, while maintaining some basic properties of the pseudograph. This is used initially to bound the number of orientations for connected pseudographs with fixed outdegree equal to 2, since these orientations are related with the m-Bézout bound of sphere equations for Laman graphs improving the existing upper bounds. In the sequel, we generalize this method for minimally rigid graphs in bigger dimensions. Finally, we derive general asymptotic formulas for our method.

4.2.1 Pseudographs and orientations with fixed outdegree 2.

We define the following graphical structure generalizing that of a graph.

Definition 3 *A* pseudograph $\mathcal{L}(V, E, H)$ *is a collection, where* V *is a set of vertices,* E *is a set of edges called* normal edges*, each incident to two vertices in* E*, and* H *is a set of edges called* hanging edges*, each with a single endpoint in* U *and directed out of the vertex*[1]*. Moreover, the graph* $G(V, E)$ *is called* normal subgraph*. If the normal subgraph is connected, then* $\mathcal{L}$ *is a* connected pseudograph*.*

Let the *total degree* p of a vertex v denote the total number of (normal and hanging) edges incident to v. Let h denote the *hanging degree* of v, which is the number of hanging edges incident to v, while the number of normal edges incident to v is its *normal degree* and equals $p - h$. The *extended degree* of v is the pair (p, h).

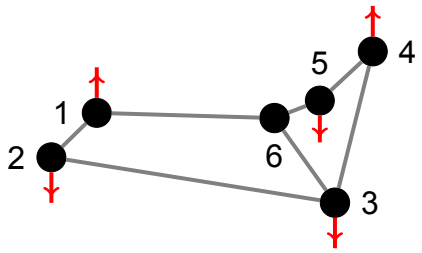

Figure 4.1: *A pseudograph with 6 vertices. The extended degrees are the following:* $(3, 1)$ *for vertices* $1, 2, 4, 5$*,* $(3, 0)$ *for vertex* 6*, and* $(4, 1)$ *for vertex* 3*.*

We shall consider orientations of a pseudograph $\mathcal{L}$ defined by specifying a direction on every normal edge, while by definition hanging edges are directed out of their unique vertex. Pseudograph orientations refer to the orientations of pseudographs. We count pseudograph orientations with fixed outdegree 2 for all vertices: we call these orientations *valid*. Clearly, if a vertex has a hanging edge, one more edge should be directed out of it, while if it has hanging degree 2, all its normal edges should be in-directed. A pseudograph

[1] Hanging edges are reminiscent of "directed loops" in hypergraphs [65]; "half-edges" also have a single endpoint.

containing a vertex with extended degree (p, h), such that $p < 2$ or $h > 2$, has no valid orientations.

We now prove the following necessary condition for the existence of a valid orientation of a pseudograph (which resembles Maxwell's count).

Proposition 3 *Let $\mathcal{L}(V, E, H)$ be a pseudograph with a valid orientation. Then $|H|+|E| = 2|V|$.*

Proof: $|H| + |E|$ is the sum of outdegrees over all edges; $2|V|$ equals the sum of outdegrees over vertices. □

4.2.2 Iterative elimination

Now we present the basic graphical operations used to reduce the size of a connected pseudograph. We specify an iterative elimination process comprised of a sequence of steps, with the requirement that the pseudograph stays connected. We shall distinguish two types of steps, depending on the extended degree of the vertex, or of the vertex path to be eliminated. The process terminates when the current pseudograph's normal subgraph is a tree; see details in Proposition 6.

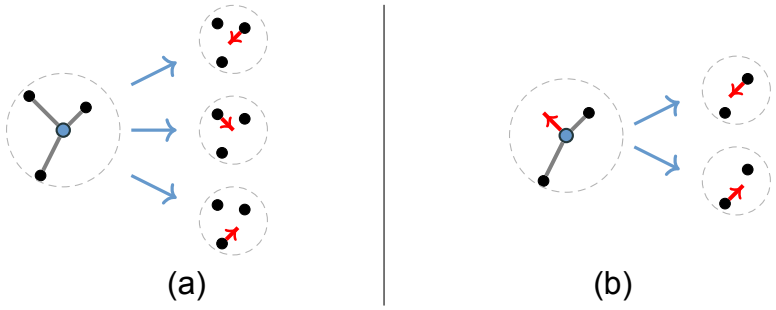

Figure 4.2: *Elimination of a vertex with extended degree (a) $(3, 0)$, encountered in vertex elimination, or (b) $(3, 1)$, encountered in path elimination. In (a) there are 3 choices for eliminating edges, resulting in 3 different pseudographs; in (b) there are 2 choices.*

Let us detail the two types of elimination steps.

The first type eliminates a single vertex v with extended degree other than $(3, 1)$. Let $\mathcal{L}(U, F, H)$ be a pseudograph: We choose to eliminate two edges incident to v (Figure 4.2a), thus maintaining the total edge count of Proposition 3. If v is incident to $h \leq 2$ hanging edges, these must be eliminated. Since the outdegree of v equals 2 in a valid orientation of $\mathcal{L}$, there are $2 - h \leq 2$ normal edges incident to v that get eliminated. All edges that are not eliminated become hanging in the new pseudograph, and correspond to edges directed towards v for a valid orientation of the initial pseudograph.

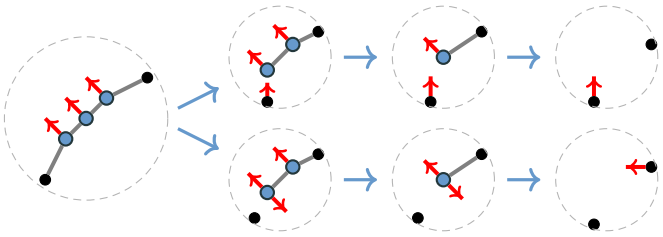

Figure 4.3: *Two choices after eliminating a $(3,1)$-path of length $\ell = 3$ respecting the edge count; $\ell - 1$ hanging edges get eliminated.*

The second type eliminates a path of $\ell \geq 2$ consecutive vertices, all of extended degree $(3,1)$ (Figure 4.3); we avoid single $(3,1)$ vertex elimination because that would yield a looser bound. Edges are eliminated similarly as before, namely we eliminate the ℓ hanging edges (one per vertex) and another ℓ normal edges incident to path vertices, thus eliminating 2ℓ edges. After eliminating the path, there are two choices for the normal edge that remains; in either case, it becomes hanging (Figure 4.2).

Now, we introduce two parameters for controlling the elimination process, namely the cost and the hanging edge equilibrium.

In every elimination step, there are several ways to choose the edges that remain in the new pseudograph. The number of choices corresponds to different pseudographs with valid orientations; their number is defined to be the *cost* of the step.

Remark 1 *The product of the costs of all steps in the elimination process bounds the number of valid orientations of the initial pseudograph. In other words, the cost expresses the quotient of the valid orientations of the original graph over the maximum number of valid orientations of the resulting graphs.*

In the proposition that follows, we show that, for vertex elimination, the cost is determined by the extended degree of the eliminated vertex, while for path elimination, the cost always equals 2.

Another important quantity in the elimination is the *hanging edge equilibrium*, defined as the difference between hanging edges in the resulting pseudograph and the original one.

Proposition 4 *Let v be a vertex with extended degree (p,h), then the cost and the hanging edge equilibrium of the elimination step are given by*

$$\binom{p-h}{2-h}, \text{ and } p-h-2$$

respectively. In the case of path elimination, for a path of length ℓ, the cost is 2 and the hanging edge equilibrium is $1-\ell$.

Proof: Recall that at vertex elimination, two edges are eliminated and, when there are hanging edges, these are eliminated first. So $2-h$ edges are left to be eliminated among the $p-h$ normal edges of the vertex, which yields the cost of this step. Since $2-h$ edges were eliminated, the number of the new hanging edges is $p-h-(2-h)$, while the initial number of hanging edges was h. Their difference yields $p-h-2$.

Let us view path elimination as a sequence of vertex eliminations. Then, eliminating the first vertex has cost 2. Each following vertex now has degree $(2,1)$ or $(3,2)$, hence its elimination cost is 1. Therefore the overall cost is 2 because it equals the product of all costs. As for the hanging edge equilibrium, the path contains ℓ hanging edges and, after the elimination step, one remains. □

If the iterative process continued up to the exhaustion of vertices and, moreover, all cases were as in Figure 4.2(a), there would be $O(3^{|V|})$ orientations which, by Theorem 3, yields a bound of $O(6^{|V|})$ on Laman embeddings. However, our process is defined to terminate earlier; see Proposition 6.

4.2.3 Bounding the number of valid orientations

In this subsection, by applying the process described above, we bound the number of valid orientations of connected pseudographs. In the sequel, n denotes the number of vertices of a connected pseudograph and k the total number of its hanging edges.

We first prove that there is always an elimination process that keeps the pseudograph connected. For this, we recall the definition of a block-cut tree [37, Chapter 4]. Recall that a cut-vertex is such that its removal increases the number of connected components in the graph and a biconnected component is a maximal subgraph with no cut vertices [2].

Definition 4 (Harary [37]) *Let $G(V,E)$ be any graph. Let also $bc(G)$ be the graph such that:*

- *This graph has a vertex for each biconnected component, and for each cut-vertex of G.*
- *There is an edge in $bc(G)$ for each pair of a biconnected component in G and a cut-vertex that belongs to that block.*

If G is connected, then $bc(G)$ is a tree and is called block-cut tree of G.

Following Definitions 3 and 4, block-cut trees can be used in the case of normal subgraph $G(V,E)$ of a connected pseudograph $\mathcal{L}(V,E,H)$ (Figure 4.4).

We can now prove the following statement, which allows us to use the bound in Expression (4.7).

[2] In [37, Ch. 3] these subgraphs are called blocks; "biconnected component" is used equivalently, e.g. [43, Ch. 8].

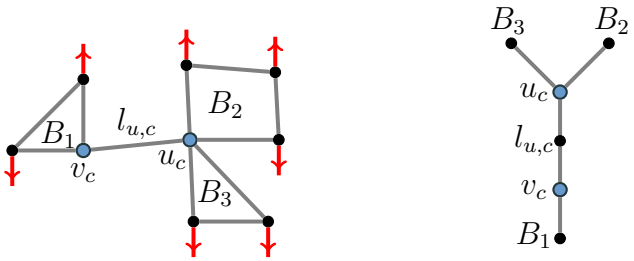

Figure 4.4: *A pseudograph $\mathcal{L}(V, E, H)$ and the block-cut tree of its normal subgraph $G(V, E)$.*

Proposition 5 *Given a connected pseudograph $\mathcal{L}(V, E, H)$, there is always an elimination process where, in each step, we either eliminate a vertex with extended degree other than $(3, 1)$, or we eliminate a $(3, 1)$-path with length at least 2, so that the resulting pseudograph remains connected.*

Proof: If there is a non-cut vertex with degree other than $(3, 1)$, then it can be eliminated and the proposition holds.

We now show that, if all vertices in $\mathcal{L}$ with degree other than $(3, 1)$ are cut-vertices, then there are at least two adjacent $(3, 1)$-vertices that can be eliminated keeping the pseudograph connected (an example is shown in Figure 4.4). Since $\mathcal{L}$ is connected, its normal subgraph G is connected as well, and there exist non-cut vertices in G; their extended degree must equal $(3, 1)$.

From the definition of block-cut trees, the leaves of $bc(G)$ represent biconnected components in G. In these components, all vertices but one are non-cut vertices, and their normal degree is 2, since their extended degree is $(3, 1)$. If such biconnected component had only one non-cut vertex, then this vertex would have normal degree 1. This means that there are at least two such vertices in a biconnected component of $\mathcal{L}$ and, since their normal degree equals 2, there exists a path containing $\ell \geq 2$ such vertices, denoted $(v_1, \ldots, v_\ell)$. This path can be eliminated and the resulting pseudograph remains connected; more precisely, we may eliminate successively each v_i, thus making vertex v_{i+1} have normal degree 1.

This completes the proof. □

Concerning the termination condition of our process, we establish the following for a connected pseudograph whose normal subgraph is a tree.

Proposition 6 *Let $\mathcal{L}(V, E, H)$ be a connected pseudograph such that $G(V, E)$ is a tree. Then*

1. *The number of valid orientations for $\mathcal{L}$ is either 1 or 0;*
2. *If $\mathcal{L}$ has a valid orientation, then $k = n + 1$;*

where $n = |V|$ *and* $k = |H|$.

Proof: Since $G(V, E)$ is a tree, we can always eliminate a vertex of normal degree 1 from our pseudograph. This means that $p - h = 1$, so using the formulas of Proposition 4 it is obvious that, if there is a valid orientation, then this is unique. If it does have a valid orientation, then from the total edge count in Proposition 3, we deduce $|E| + k = 2 \cdot n$. Since G is a tree, we substitute $|E| = n - 1$ in this formula, concluding the proof. □

Let $P(n, k)$ denote the maximal number of valid orientations for all connected pseudographs with n vertices and k hanging edges. Let us recall the Brègman-Minc bound and the connection between permanents, constrained orientations, and the bound of Laman graphs as discussed in Chapter 3 and in [5], where it was established that:

$$P(n, k) \leq (2!)^{k/2} \, (4!)^{(2n-k)/4} \cdot (2)^{-n} \approx 2.4495^n \cdot 0.6389^k. \tag{4.6}$$

We therefore seek upper bound estimates of the form

$$P(n, k) \leq \zeta^n \, \varepsilon^k \tag{4.7}$$

for real $\zeta, \varepsilon > 0$ and $k, n \geq 1$.

Proposition 6 implies $P(n, n + 1) = 1$ for every $n \geq 1$; this is the base case in Theorem 9. Proposition 5 precludes that multiple connected components be formed, thus leading to the theorem's inductive proof. Additionally, Propositions 3 and 6 establish that $k \leq n + 1$ for any connected pseudograph with at least one valid orientation. Indeed, $k > n + 1$ implies the normal subgraph has $< n - 1$ edges so cannot be connected.

We modify the form of the bound in Inequality (4.7) to $P(n, k) \leq \zeta^n \, \varepsilon^{k-1}$, with $\zeta, \varepsilon > 1$. The modification is justified in the proof below.

Theorem 9 *The number of valid orientations for a connected pseudograph is bounded above by*

$$P(n, k) \leq \zeta^n \cdot \varepsilon^{k-1},$$

where $\zeta = 24^{1/5}$ *and* $\varepsilon = 18^{-1/5}$.

Proof: We prove the statement by induction on n, k. The statement is true for the base cases $n = 1$, $k = 2$, which a pseudograph consisting of exactly one $(2, 2)$ vertex, and also for trees with $k = n + 1$, since $P(n, n + 1) = 1$ (Proposition 6), because $\zeta\varepsilon > 1$. In these cases the pseudograph has 1 or 0 orientations, representing a termination condition. If the exponent of ε were k, the statement would fail for small trees.

From Propositions 3 and 6, if a connected pseudograph has $k > n$ hanging edges, either it is a tree, or it has no valid orientations. So we assume pseudograph $\mathcal{L}$, with $n > 1$ vertices, has $k \leq n$ hanging edges. Suppose it has a vertex v of extended degree (p, h), such that:

1. $(p,h) \neq (3,1)$, and
2. elimination of v and its incident edges keeps the pseudograph connected.

Since the number of valid orientations of $\mathcal{L}$ is bounded by the cost of the elimination process (Remark 1) and the hanging edge equilibrium is $p-h-2$, the number of valid orientations after eliminating this vertex is bounded by

$$\binom{p-h}{2-h} P(n-1, k+p-h-2).$$

By the induction assumption, this is bounded by $C(p,h)\,\zeta^n \varepsilon^{k-1}$, where

$$C(p,h) = \binom{p-h}{2-h} \zeta^{-1} \varepsilon^{p-h-2}.$$

We now prove that $C(p,h) \leq 1$, for $p \geq 2 \geq h \geq 0$, and $(p,h) \neq (3,1)$. Direct substitution gives

$$C(p,h) = \binom{p-h}{2-h} \left(2^{h-p-1}\ 3^{2h-2p+3}\right)^{1/5}.$$

Note that:

- $C(2,0) = 24^{-1/5} < 1$, $C(3,0) = (9/16)^{1/5} < 1$, $C(4,0) = 1$, and the $C(p,0)$ for $p > 4$ are decreasing with p as follows:

$$\frac{C(p+1,0)}{C(p,0)} = \left(1 + \frac{2}{p-1}\right)\varepsilon < 1, \quad \text{for } p \geq 4. \tag{4.8}$$

- $C(2,1) = (3/4)^{1/5} < 1$, $C(4,1) = (9/16)^{1/5} < 1$, and the $C(p,1)$ for $p > 4$ are decreasing with p as follows:

$$\frac{C(p+1,1)}{C(p,1)} = \left(1 + \frac{1}{p-1}\right)\varepsilon < 1, \quad \text{for } p \geq 4. \tag{4.9}$$

- $C(3,2) = (3/4)^{1/5} < 1$, and the $C(p,2)$ for $p > 3$ are strictly decreasing with p, as the binomial factor equals the constant 1.

$C(2,2)$ is immaterial since $(2,2)$ is a base case corresponding to a pseudograph with a single vertex and $k > n$.

An induction step is proven under the assumptions *(i)–(ii)*. Incidentally, $C(3,1) = (4/3)^{1/5} > 1$, which is why we avoid eliminating this type of vertices in a vertex elimination step.

If assumptions *(i)–(ii)* fail, we can eliminate a path of $(3,1)$-vertices keeping the pseudograph connected by Proposition 5.

Let $\ell \geq 2$ denote the number of vertices in the eliminated path. Then, the number of orientations of $\mathcal{L}$ is bounded by

$$2P(n-\ell, k-\ell+1),$$

which, by induction, is bounded by

$$2\,\zeta^{n-\ell}\varepsilon^{k-\ell} = \left(\frac{3}{4}\right)^{(\ell-2)/5} \zeta^n \varepsilon^{k-1} \leq \zeta^n \varepsilon^{k-1}.$$

The bound is proven. □

4.2.4 A new upper bound on the embedding number of Laman graphs

This subsection combines the above discussion so as to establish a new upper bound on the number of embeddings for Laman graphs.

Let $G(V,E)$ be a Laman graph and a fixed edge $e=(v_1,v_2)\in E$. Let also $\mathcal{L}_{G,e}(V',E',H)$ be a collection such that $V'=V\backslash\{v_1,v_2\}$, $E'=\{e'\in E : v_1,v_2\notin e'\}$ and H is the set of all edges incident to one fixed vertex and one non fixed-vertex. Then $\mathcal{L}_{G,e}$ is a pseudograph that may contain one or multiple connected components; in Figure 4.5, this construction leads to a pseudograph with two connected components. Remark that the number of vertices n of $\mathcal{L}_{G,e}$ is related to the number of vertices of G by $n=|V|-2$.

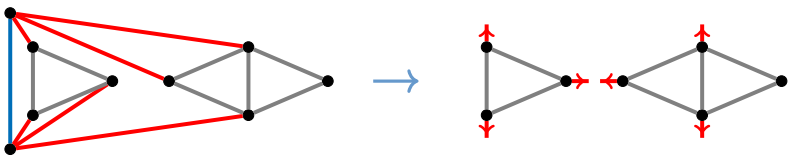

Figure 4.5: *After removing a fixed edge (vertical dashed blue) from a Laman graph, one gets a pseudograph with 2 connected components.*

A different choice of a fixed edge may result in different pseudographs, for a given Laman graph, while different Laman graphs may result in the same pseudograph, see Figure 4.6. This happens because any pseudograph representation lacks the information on connections with specific vertices of the fixed edge.

From the construction of $\mathcal{L}_{G,e}$ it follows that, when it is connected, its number of valid orientations equals that of its constrained orientations defined in Theorem 3. This bound is always positive, since it corresponds to well-constrained algebraic systems. If $\mathcal{L}_{G,e}$ has $\mu>1$ connected components $\mathcal{L}_1,\ldots,\mathcal{L}_\mu$, then the total number of valid orientations of $\mathcal{L}_{G,e}$ equals the product of valid orientations per connected component $\mathcal{L}_i$. This leads to the following corollary, which distinguishes components with one vertex in order to exploit Maxwell's count.

Corollary 5 *Let $G(V,E)$ be a Laman graph and $\mathcal{L}_{G,e}$ constructed as described above. Let μ' be the number of connected components of $\mathcal{L}_{G,e}$ with more than one vertex, and*

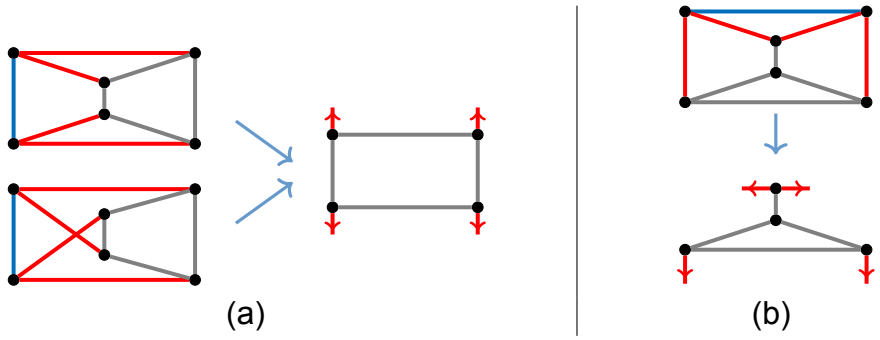

Figure 4.6: *(a) Two Laman graphs, Desargues' and $K_{3,3}$, both resulting in the same pseudograph for some fixed edge. (b) Choosing a different fixed edge for Desargues' graph results in a different pseudograph.*

n the number of its vertices. Then, the number of constrained orientations, defined in Theorem 3, is bounded above by

$$24^{n/5} \cdot 18^{-(k'-\mu')/5},$$

where k' is the total number of hanging edges in the components of $\mathcal{L}_{G,e}$ with more than one vertex.

Proof: Recall that $n = |V| - 2$. Let $n_1, n_2 \dots n_{\mu'}$ and $k_1, k_2 \dots k_{\mu'}$ be respectively the numbers of vertices and of hanging edges per connected component with strictly more than one vertex. The bound follows from Theorem 9, since $n \geq \sum_{i=1}^{\mu'} n_i$ and $k' = \sum_{i=1}^{\mu'} k_i$. □

Lemma 6 *Let $G(V, E)$ be a Laman graph, and $\mathcal{L}_{G,e}$, k' and μ' as above. Then $k' \geq 3\mu'$.*

Proof: Let $\mathcal{L}_i(V_i, E_i, H_i)$ be a connected component of $\mathcal{L}_{G,e}$ with k_i hanging edges. The normal subgraph $G_i(V_i, E_i)$ is a subgraph of a Laman graph. If $|V_i| \geq 2$, by Maxwell's count we have $|E_i| \leq 2 \cdot |V_i| - 3$ therefore $k_i \geq 3$. □

Now we are ready to prove the new upper bound for Laman graphs.

Theorem 10 *Let $G(V, E)$ be a Laman graph. Then the number of its embeddings in $\mathbb{C}^2$ (and S^2) is bounded from above by*

$$18^{-2/5} \cdot \left(4 \cdot (3/4)^{1/5}\right)^{|V|-2} = O\left(3.7764^{|V|}\right).$$

Proof: Applying $k' \geq 3\mu'$ from Lemma 6 in Corollary 5, the number of valid orientations is bounded by $24^{n/5} \cdot 18^{-2/5}$, for $n \geq 2$, since either the number of connected components with more than one orientation is $\mu' \geq 1$, or there is a single valid orientation. By doubling this bound and applying Theorem 3, the upper bound follows. For $n = 1$, Lemma 6 does not apply; there is trivially one orientation and the bound is 2. □

4.2.5 Geiringer graphs and higher dimensions

This subsection extends the method of the previous section to orientations of connected pseudographs with fixed outdegree $d \geq 3$, and subsequently establishes new upper bounds on the embedding number of minimally rigid graphs in $\mathbb{C}^d$ (and S^d), for $d \geq 3$.

Let $P_d(n,k)$ denote the maximal number of orientations with fixed outdegree d for connected pseudographs with n vertices and k hanging edges. As before, we seek bounds of the form

$$P_d(n,k) \leq \zeta_d^n \cdot \varepsilon_d^{k-1}$$

for each d. For a fixed outdegree $d \geq 3$, the elimination steps consist of:

- Eliminating single vertices of extended degree (p,h), with $p \geq d \geq h \geq 0$, and $(p,h) \neq (d+1, d-1)$; then the number of valid orientations is bounded by $\binom{p-h}{d-h} \cdot P_d(n-1, k+p-h-d)$.
- Eliminating paths of length $\ell \geq 2$ with $(d+1, d-1)$-vertices; then the number of valid orientations is bounded by $2 \cdot P_d(n-\ell, k-(d-1)\ell+1)$.

If we replace $(3,1)$-paths in Proposition 5 by $(d+1, d-1)$-paths, we have an analogous result, since $(d+1, d-1)$-vertices have normal degree 2. This implies that there is always an elimination process preserving connectivity. Moreover, the necessary count in Proposition 3 is generalized to $|E|+|H| = d \cdot |V|$ for every pseudograph $\mathcal{L}(V,E,H)$ with at least one orientation with fixed outdegree d; such orientations extend the notion of validity beyond $d = 2$.

An immediate consequence is that, if a connected pseudograph has a tree as normal subgraph and also has an orientation with fixed outdegree d, then it holds that $(d-1) \cdot n = k-1$ which is our base case, generalizing Proposition 6.

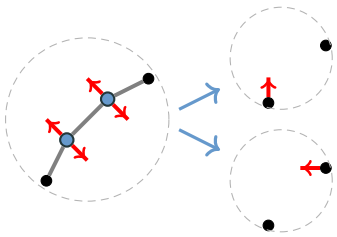

Figure 4.7: *Elimination of a $(4,2)$-path (with length $\ell = 2$) in the case of orientations with fixed outdegree 3. This elimination is analogous to that in Figure 4.3.*

In the following theorem we establish an upper bound on P_d. If $d = 2$, then ζ_2, ε_2 are evaluated as in Theorem 9. Here, elimination of single vertices of extended degree (d,d) and $(d+1, d-1)$ are excluded from our analysis. The first case because it is one of the base cases, as a pseudograph with exactly one vertex, and the latter because only path elimination with length $\ell \geq 2$ is considered for these vertices.

Theorem 11 *The maximal number of orientations with fixed outdegree d for a connected pseudograph is bounded from above by*

$$P_d(n,k) \le \zeta_d^n \cdot \varepsilon_d^{k-1}$$

for the following choices of ζ_d and ε_d:

$$\zeta_d = \max_{p \ge d} \left(2^{p-d} \binom{p}{d}^{2d-3} \right)^{\frac{1}{2p-3}}, \tag{4.10}$$

and

$$\varepsilon_d = \left(2 \binom{p}{d}^{-2} \right)^{\frac{1}{2p-3}} \tag{4.11}$$

for the value of p that maximizes ζ_d.

Proof: The single vertex elimination step and the path elimination step result in the following inequalities:

$$\zeta_d \, \varepsilon_d^{d+h-p} \ge \binom{p-h}{d-h} \tag{4.12}$$

for all $(p,h) \notin \{(d+1,d-1),(d,d)\}$ with $p \ge d \ge h$, and

$$\zeta_d^{\ell} \, \varepsilon_d^{d\ell-\ell-1} \ge 2 \tag{4.13}$$

for all $\ell \ge 2$. In the second case the equalities are achieved with $\zeta_d = 2^{d-1}$, $\varepsilon_d = 1/2$ for all ℓ. The same (ζ_d, ε_d)-point gives equality in (4.12) for $(p,d) \in \{(d,d-1),(d+1,d)\}$.

By taking the logarithm, (4.12) and (4.13) become linear in the $(\ln \zeta_d, \ln \varepsilon_d)$-plane. The corresponding lines have negative slope and contain point $((d-1)\ln 2, -\ln 2)$; the one defined by (4.13) for $\ell = 2$ is closest to the vertical. So the corresponding inequalities are dominated for $\zeta_d \le 2^{d-1}$ by (4.13) with $\ell = 2$.

Our key observation is that (4.12) for a relevant pair (p,h) is satisfied if:

1. The same inequality is satisfied for the shifted $p \to p+1$, $h \to h-1$, giving
$$\zeta_d \, \varepsilon_d^{d+h-p-2} \ge \binom{p-h+2}{d-h+2}.$$
2. Inequality (4.13) is satisfied for $\ell = 2$.

This implies that it is enough to consider (4.12) with $h = 0$. Considering *(ii)* with $\ell = 2$ and a particular case of (4.12) with $h = 0$, the two inequalities can be raised to non-negative powers and combined so as to eliminate ε_d, with the conclusion that

$$\zeta_d^{2p-3} \ge 2^{p-d} \binom{p}{d}^{2d-3}.$$

A permissible equality is achieved together with Equality (4.11). The maximization in Equality (4.10) through $p \geq d$ follows.

It remains to prove the key observation. Inequalities *(i)–(ii)* can be raised to positive powers and combined, with the conclusion that

$$\zeta_d \, \varepsilon_d^{d+h-p} \geq \binom{p-h+2}{d-h+1}^{\frac{2p-2h-3}{2p-2h+1}} 2^{\frac{2}{2p-2h+1}}.$$

Positivity fails for $(p,h) \in \{(d,d),(d,d-1),(d+1,d)\}$, but these cases are covered already.

Comparison with Inequality (4.12) shows that we need $U(p-h,d-h) \leq 1$, where

$$U(\chi,\psi) = \frac{1}{4}\binom{\chi}{\psi}^4 \left(\frac{(\chi-\psi+1)(\psi+1)}{(\chi+1)(\chi+2)}\right)^{2\chi-3}.$$

The inequality has to be shown for integer $\chi \geq \psi \geq 0$ such that $(\chi,\psi) \notin \{(2,1),(0,0),(1,0),(1,1)\}$, which correspond respectively to vertices $(d+1,d-1),(d,d),(d+1,d),(d,d-1)$. For fixed ψ, the maximum is achieved at $\chi = 2\psi$, since $U(\chi,\psi)$ increases. This follows from

$$\frac{U(\chi+1,\psi)}{U(\chi,\psi)} = \frac{(\psi+1)^2}{(\chi-\psi+1)(\chi-\psi+2)}\left(1-\frac{1}{(\chi+2)^2}\right)\left(1-\frac{\chi-2\psi+1}{(\chi+3)(\chi-\psi+1)}\right)^{2\chi}.$$

This ratio is <1 for $\chi \geq 2\psi$, and (by calculus on the product of the first and middle terms) it is >1 for $\chi < 2\psi$.

For this pair of values, we have

$$U(2\psi,\psi) = 2\prod_{\kappa=1}^{\psi}\left(1-\frac{1}{\kappa\,(2\kappa+1)}\right)^{4\kappa-3}.$$

Evidently, the χ-maximum $U(2\psi,\psi)$ is a decreasing function of ψ, and $U(4,2) = 3^9/25000 < 1$. For $\psi < 2$, we observe that $U(\chi,1) \leq U(3,1) = 3^7/4000 < 1$ and $U(\chi,0) < U(1,0) = 3/4 < 1$ for $\chi > 2$. □

We now describe a construction similar to Section 4.2.4, connecting Theorem 3 to the orientations of pseudographs with fixed outdegree d and $n > 1$. Let $G(V,E)$ be a minimally rigid graph in $\mathbb{C}^d$ and let K_d be one of its subgraphs. Removing K_d, as in the case of $d = 2$, we have a pseudograph, denoted $\mathcal{L}_{G,K_d}(V',E',H)$.

Applying Maxwell's condition to the edge count for the normal subgraphs of the pseudographs, we obtain $k_i \geq \binom{d+1}{2}$ for every connected component of $\mathcal{L}_{G,K_d}$ with at least d vertices.

If $n_i \leq d-1$ we examine 2 different cases: (a) $n_i = 1$ or 2 implying that the connected component has trivially one orientation, since the normal subgraph is either a single vertex, or a tree with 2 vertices. The number of hanging edges is $k_i = 2d-1$, in order to respect the total edge count. (b) $n_i = 3$, which implies $d \geq 4$, then there should be ≤ 3 normal

edges and $\geq d-2$ hanging edges, so $k_i \geq 3d-3$. By induction, for the i-th vertex, at least $i-1$ hanging edges shall be added.

Hence, if $\mathcal{L}_{G,K_d}$ has μ' connected components with more than 2 vertices and a total of k' hanging edges, then $k' \geq 3d-3$ for $d \geq 3$.

An immediate consequence is the following theorem that generalizes Theorem 10 by applying Theorem 3.

Theorem 12 *Let $G(V,E)$ be a minimally rigid graph in $\mathbb{C}^d$ (and S^d) that contains a K_d. Then the number of its embeddings is bounded from above by $\varepsilon_d^{3d-2} \cdot (2 \cdot \zeta_d)^{|V|-d} = O((2 \cdot \zeta_d)^{|V|})$. In the case of Geiringer graphs that contain a triangle this is*

$$\left(2 \cdot 10^2\right)^{-5/9} \left(8 \cdot (5/8)^{1/3}\right)^{|V|-3} = O\left(6.8399^{|V|}\right).$$

The asymptotic bound works also for minimally rigid graphs in $\mathbb{C}^d$ that do not contain a K_d. In that case, we may remove a maximal clique with $d' \geq 2$ vertices in order to obtain a pseudograph. Then, the exponent of ζ_d will never exceed $|V|-2$ (see Appendix B for details).

To demonstrate the improvement achieved by our this new bound on the embedding number of rigid graphs, namely $O\left((2\zeta_d)^{|V|}\right)$, we refer the reader to Table 4.1 which compares the values of $2\zeta_d$ to the power basis of Bézout bound and the bound derived in Section 4.1.

5. ON THE MAXIMAL NUMBER OF REAL EMBEDDINGS IN $\mathbb{R}^2$, $\mathbb{R}^3$ AND S^2

In this chapter we deal with the problem of finding edge length parameters that maximize the real embeddings of Laman and Geiringer graphs. We use both algebraic formulations presented in Section 2.2 and we use the complex embedding number as an upper bound.

In Section 5.1 we present the sampling methods we use in order to increase the number of real embeddings. Besides standard sampling methods, an algorithm inspired by coupler curves has been developed by J.Legerský in order to search efficiently huge parametric spaces combining local and global sampling in the case of Geiringer graphs.

The main results of our methods are presented in Section 5.2. These include a full characterization of graphs with a small number of vertices up to their real embedding number. More precisely we give the maximal numbers of real embeddings of all 6-vertex and 7-vertex Laman graphs in S^2 and $\mathbb{R}^2$ respectively, as well as the maximal numbers of real embeddings of all 7-vertex Geiringer graphs. We also specify parameters for selected bigger graphs. These computations improve the existing lower bound on the maximal number of real embeddings from $2.3003^{|V|}$ to $2.3811^{|V|}$ for $d = 2$ and from $2.51984^{|V|}$ to $2.6390^{|V|}$ for $d = 3$, while they establish $2.51984^{|V|}$ as a lower bound for the number of embeddings in S^2.

The part of this Chapter related to Geiringer graphs appear in the conference proceedings of ISSAC'18 [3]. The totality of the results have been published in [4].

5.1 Increasing the number of real embeddings

Our main goal throughout our experiments was to find the parameters that can maximize the number of real embeddings of minimally rigid graphs. One open problem in rigidity theory is whether the maximal number of real embeddings of a given graph can be the same as the number of complex embeddings. Although there exists an 8-vertex Laman graph for which it has been proven that $r_2(G) < c_2(G)$ [41], in most cases we consider the number of complex embeddings as the upper bound we try to reach (see also Chapter 1). In our research, we concentrate on the cases of graphs with the biggest number of complex embeddings, among all other minimally rigid graphs with the same number of vertices.

Additionally to some standard sampling methods, we develop a new method that can increase efficiently the number of real embeddings for certain Geiringer graphs. Our method is inspired by coupler curves approach and uses G_{48} (the 7-vertex Geiringer graph with the maximal number of embeddings) as a model. Taking advantage of our implementation based on this technique, we increase lower bounds on $r_3(G)$ for many graphs and establish new asymptotic lower bounds on the maximal number of embeddings of Geiringer graphs.

5.1.1 Standard sampling methods

Finding initial configurations We applied different heuristics to find initial configurations for our parameter sampling. First of all, we tried to compute the number of real embeddings of totally random configurations. This resulted in finding maximal numbers of real embeddings for graphs with $c_d(G) = 2^{|V|-d}$. For example, it took less than 20 minutes to detect parameters that attain the maximum for all 8-vertex non-trivial [1] Geiringer graphs with $r_3(G) = 32$.

We also used almost degenerate locus as starting points. In order to increase $r_2(G)$ of Laman graphs with maximal numbers of complex embeddings w.r.t. a given number of vertices, we chose lengths very close to the unit length. Similarly, in the case of Geiringer graphs, we perturbed degenerate conformations. For example, in order to find an initial point for G_{48}, we separated the edges into three sets with edge lengths being the same in each of them: the *ring edges* of the 5-cycle, the *top edges* that connect v_7 with the ring and the *bottom edges* that connect v_1 with the ring (see Figure 5.1). We subsequently found edge lengths that maximized the intervals imposed by triangular and tetrangular inequalities up to scaling and we perturbed the resulting lengths.

Finally, we also used as starting points conformations of smaller graphs with maximal numbers of embeddings. For instance, gluing v_7 and v_8 in G_{160} results in G_{48}. Perturbing a set of edge lengths $\boldsymbol{\lambda}$ of G_{48} such that $r_3(G_{48}, \boldsymbol{\lambda}) = 48$, we could get a starting point for the sampling of G_{160} that would result in a big number of real embeddings.

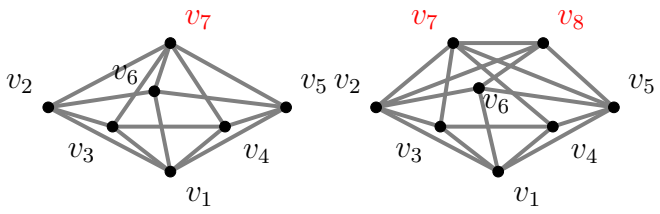

Figure 5.1: *Coinciding vertices v_7 and v_8 of G_{160} results in G_{48}.*

Stochastic methods We have used stochastic methods for different graphs in order to increase the number of embeddings. Our method uses a variant of the tools suggested in [24]. We penalize the loss of real roots and the increase of the imaginary part of complex solutions to decide if the resulted labeling constitutes a new starting point. This method could increase the number of embeddings, but rarely attained the maximum.

[1] In the sense that their minimal vertex degree is > 3, thus no H1 move is used in the final step of their construction and their embedding number cannot trivially deduced from a smaller graph. See Section 2.1 for details.

Parametric searching with CAD method The methods described in the previous paragraph are local methods. In order to search globally one parameter, we used `Maple`'s subpackage `RootFinding` [Parametric] in Maple18. This package is an implementation of Cylindrical Algebraic Decomposition principles for semi-algebraic sets. The input consists of the equations and the inequalities of the system and the list of variables separating them from parameters. The output is a cell decomposition of the space of parameters according to the number of solutions of the semi-algebraic conditions.

In our problem, we were able to take advantage of this implementation using Cayley-Menger determinants of 7-vertex graphs and searching for only one parameter (See Section 2.2.2). Sphere equations failed to give any result, while computational constraints did not let us search two or more parameters simultaneously.

This sampling was also used to increase the number of spherical and planar embeddings of Laman graphs with 7 vertices and the number of real embeddings of G_{48}. In some situations it was even possible to attend the maximal number of embeddings for a given graph.

5.1.2 Coupler curve

The previous methods fail to attain tight bounds for Geiringer graphs with maximal number of embeddings efficiently. For example, using CAD, we could find 28 real embeddings for G_{48}, but it seems impossible to increase this number by local searching in all parameters or global sampling only one of them. Thus, we developed a new method that samples only subset of edge lengths in every iteration. This procedure is motivated by visualization of coupler curves.

Let $G(V,E)$ be a minimally rigid graph with a triangle and an edge (u,u'). If $G' = (V, E \setminus (u,u'))$ is obtained from G by removing the edge (u,u'), then the set of embeddings satisfying the constraints given by generic edge lengths and fixing the triangle is 1-dimensional. The projection of this curve to the coordinates of the vertex u' is a so called *coupler curve*. The authors in [13] used this idea for proving that the Desargues (3-prism) graph has 24 real embeddings in $\mathbb{R}^2$. Namely, they found edge lengths such there are 24 intersections of the coupler curve with a circle representing the removed edge. This approach can be clearly extended into $\mathbb{R}^3$ — the number of embeddings of G is the same as the number of intersection of the coupler curve of u' with the sphere centered at u with a radius $\lambda_{u,u'}$. Now, we define specifically a coupler curve in $\mathbb{R}^3$.

Definition 5 *Let G' be a graph with edge lengths $\boldsymbol{\lambda} = (\lambda_e)_{e\in E_{G'}}$ with a triangle subgraph K_3 with vertex-set $\{v_1,v_2,v_3\}$ and a specific embedding $K_3(\boldsymbol{\rho})$ satisfying edge length constraints. If the set $S_{\mathbb{R}}(G',\boldsymbol{\lambda},K_3(\boldsymbol{\rho}))$ is one dimensional and $u' \in V_{G'}$, then the set*

$$\mathcal{C}_{u',\boldsymbol{\lambda}} = \{(x_{u'},y_{u'},z_{u'})\colon ((x_v,y_v,z_v))_{v\in V_{G^*}} \in \boldsymbol{S}_{\mathbb{R}}(G',\boldsymbol{\lambda},K_3(\boldsymbol{\rho}))\}$$

is called a coupler curve of u' w.r.t. the fixed triangle $K_3(\boldsymbol{\rho})$.

Assuming that a coupler curve is fixed, i.e., we have fixed lengths $\boldsymbol{\lambda}$ of the graph G', we can change the edge length $\lambda_{u,u'}$ so that the number of intersections of the coupler curve $\mathcal{C}_{u',\boldsymbol{\lambda}}$ with the sphere with the center at u and radius $\lambda_{u,u'}$, namely, the number of real embeddings of G, is maximal.

The following lemma shows that we can change three more edge lengths within one parameter family without changing the coupler curve. This one parameter family corresponds to shifting the center of the sphere along a line.

Lemma 7 *Let $G(V,E)$ be a minimally rigid graph and u,v,w,q,u' be vertices of G such that $(q,v),(v,w) \in E$ and the neighbours of u in G are v,w,q and u'. Let G' be the graph given by $(V',E') = (V, E \setminus \{(u,u')\})$ with generic edge lengths $\boldsymbol{\lambda} = (\lambda_e)_{e\in E'}$. Let $\mathcal{C}_{u',\boldsymbol{\lambda}}$ be the coupler curve of u' w.r.t. the fixed triangle with vertices $\{v,u,w\}$ and an embedding $\boldsymbol{\rho}_{v,u,w}$. Let z_q be the altitude of q in the fixed triangle with lengths given by $\boldsymbol{\lambda}$. Then the set $\{y_q \colon ((x_{v'},y_{v'},z_{v'}))_{v'\in V'} \in \boldsymbol{S}_{\mathbb{R}}(G',\boldsymbol{\lambda},\boldsymbol{\rho}_{v,u,w})\}$ has only one element y'_p. If the parametric edge lengths $\boldsymbol{\lambda}'(t)$ are given by*

$$\lambda'_{u,w}(t) = ||(x_w, y_w - t, 0)||\,, \quad \lambda'_{u,q}(t) = ||(0, y'_q - t, z_q)||\,,$$
$$\lambda'_{u,v}(t) = t\,, \text{ and } \lambda'_e(t) = \lambda_e \text{ for all } e \in E_{G'} \setminus \{(u,v),(u,w),(u,q)\}\,,$$

then the coupler curve $\mathcal{C}_{u',\boldsymbol{\lambda}'(t)}$ of u' w.r.t. the fixed triangle is the same for all $t \in \mathbb{R}_+$, namely, it is $\mathcal{C}_{u',\boldsymbol{\lambda}}$. Moreover, if $(u',w) \in E$, then $\mathcal{C}_{u',\boldsymbol{\lambda}}$ is a spherical curve.

Proof: All coupler curves in the proof are w.r.t. the triangle defined above. Figure 5.2 illustrates the statement. Since G is minimally rigid, the set $S_{\mathbb{R}}(G',\boldsymbol{\lambda},\boldsymbol{\rho}_{v,u,w})$ is 1-dimensional. The coupler curve $\mathcal{C}_{q,\boldsymbol{\lambda}}$ of q is a circle whose axis of symmetry is the y-axis. Hence, the set $\{y_p \colon ((x_{v'},y_{v'},z_{v'}))_{v'\in V'} \in \boldsymbol{S}_{\mathbb{R}}(G',\boldsymbol{\lambda},\boldsymbol{\rho}_{v,u,w})\}$ has indeed only one element. The parametrized edge lengths $\boldsymbol{\lambda}'(t)$ are such that the position of v and w is the same for all t. Moreover, the coupler curve $\mathcal{C}_{q,\boldsymbol{\lambda}'(t)}$ of q is independent of t. Hence, the coupler curve $\mathcal{C}_{u',\boldsymbol{\lambda}'(t)}$ is independent of t, because the only vertices adjacent to u in G' are q,v and w. Thus, the positions of the other vertices are not affected by the position of u. □

Therefore, for every subgraph of G induced by vertices u,v,w,q,u' such that $\deg(u) = 4$ and $(q,v),(v,w),(u,v),(u,w),(u,q),(u,u') \in E$, we have a 2-parametric family of lengths $\boldsymbol{\lambda}(t,t')$ such that the coupler curve $\mathcal{C}_{u',\boldsymbol{\lambda}(t,t')}$ w.r.t. the fixed triangle vuw is independent of t and t'. Recall that the parameter t' represents the length of (u,u'), which corresponds to the radius of the sphere, and the parameter t determines the lengths of $(u,v),(u,w)$ and (u,p). Now, we aim to find t' and t such that $r_3(G,\boldsymbol{\lambda}(t,t'))$ is maximized.

Let us clarify that whereas [13] were also changing the coupler curve, our approach is different in the sense that the coupler curve is preserved within one step of our method, while only the position and radius of the sphere corresponding to the removed edge are changed in order to have as many intersections as possible. In the next step, we pick a different edge to be removed.

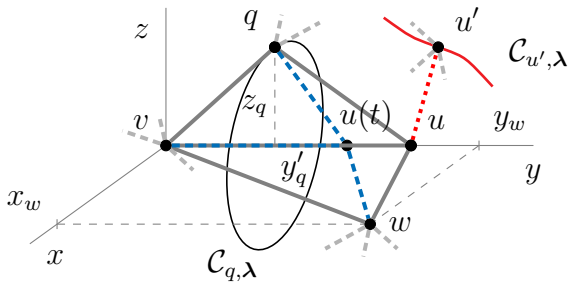

Figure 5.2: *Since the lengths of $\lambda_{u,q}$ and $\lambda_{u,w}$ are changed accordingly to the length of (u, v) (blued dashed edges), the coupler curves $\mathcal{C}_{q,\boldsymbol{\lambda}'(t)}$ and $\mathcal{C}_{u',\boldsymbol{\lambda}'(t)}$ are independent of t. The red dashed edge (u, u') is removed from G.*

In order to illustrate the method, let $\boldsymbol{\lambda}$ be edge lengths of G_{48} given by

$$\begin{aligned}
&\lambda_{1,2} = 1.99993774567597\,, && \lambda_{2,7} = 10.5360917228793\,, && \lambda_{2,3} = 0.99961432208948\,,\\
&\lambda_{1,3} = 1.99476987780024\,, && \lambda_{3,7} = 10.5363171636461\,, && \lambda_{3,4} = 1.00368644488060\,,\\
&\lambda_{1,4} = 2.00343646098439\,, && \lambda_{4,7} = 10.5357233031495\,, && \lambda_{4,5} = 1.00153014850485\,,\\
&\lambda_{1,5} = 2.00289249524296\,, && \lambda_{5,7} = 10.5362736599978\,, && \lambda_{5,6} = 0.99572361653574\,,\\
&\lambda_{1,6} = 2.00013424746814\,, && \lambda_{6,7} = 10.5364788463527\,, && \lambda_{2,6} = 1.00198771097407\,.
\end{aligned}$$

Using `Matplotlib` by [39], our program [8] can plot the coupler curve of the vertex v_6 of the graph $G_{48}\backslash(v_2, v_6)$ w.r.t. the fixed triangle $v_1v_2v_3$, see Figure 5.3 for the output. There are 28 embeddings for $\boldsymbol{\lambda}$. Following Lemma 7 for the subgraph given by $(u, v, w, q, u') = (v_2, v_3, v_1, v_7, v_6)$, one can find a position and radius of the sphere corresponding to the removed edge (v_2, v_6) such that there are 32 intersections. Such edge lengths are obtained by taking $\lambda_{1,2} = 4.0534\,,\ \lambda_{2,7} = 11.1069\,,\ \lambda_{2,6} = 3.8545\,,\ \lambda_{2,3} = 4.0519$.

Instead of finding suitable parameters for the position and radius of the sphere by looking at visualizations, we implemented a sampling procedure that tries to maximize the number of intersections [8]. The inputs of the function `sampleToGetMoreEmbd` are starting edge lengths $\boldsymbol{\lambda}$ and vertices u, v, w, q, u' satisfying the assumptions of Lemma 7, including the extra requirement that (u', w) is an edge. In order to count the real embedding number, we use the homotopy continuation package `phcpy` [68] for solving the algebraic systems.

5.2 Classification and Lower Bounds

A first upper bound on the number of embeddings is the mixed volume of systems of sphere and Cayley-Menger varieties. This bound is crucial for homotopy continuation system solving, as mentioned before. Let us remark that, in the case of sphere equations the mixed volume is also equal to the m-Bézout bound almost always (see Section 3.2.1). On the other hand, in the case of Cayley-Menger varieties these two bounds do not always coincide. The second natural bound of graph realizations is the number of

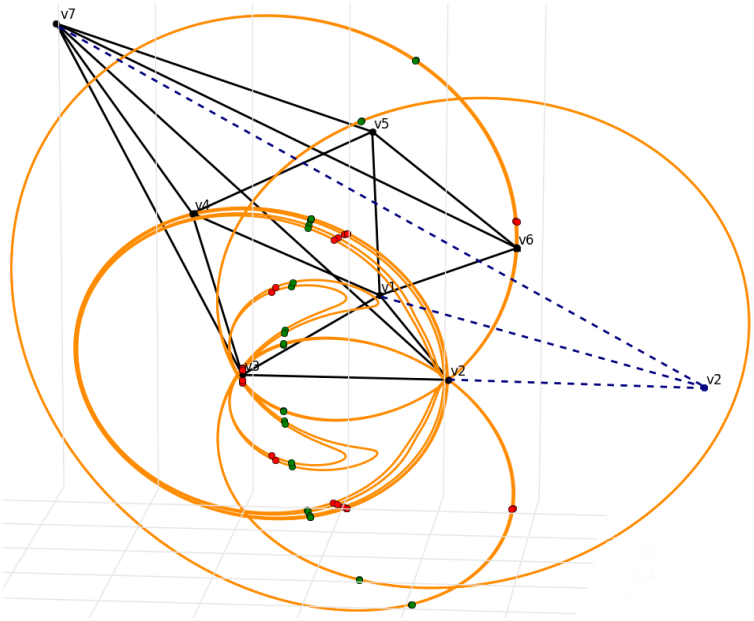

Figure 5.3: *The coupler curve $\mathcal{C}_{v_6,\boldsymbol{\lambda}}$ of G_{48} with the edge v_2v_6 removed. The 28 red points are intersections of $\mathcal{C}_{v_6,\boldsymbol{\lambda}}$ with the sphere centered at v_2 with the edge lengths $\boldsymbol{\lambda}$, whereas the 32 green ones are for the adjusted edge lengths (illustrated by blue dashed lines).*

complex embeddings. The numbers of complex embeddings for all Laman graphs up to 12 vertices are known from [16], while the numbers of complex embeddings of Geiringer graphs up to 10 vertices were computed by [35]. We computed the complex solutions of spherical embeddings of Laman graphs up to 8 vertices. For the last part, we were motivated by a remark of Josef Schicho, who had observed that the numbers of planar and spherical solutions differ for the Desargues graph.

In order to find parameters that can maximize the number of real embeddings, we applied the methods described in Section 5.1. Polynomial system solving during sampling was accomplished mainly via `phcpy`. We consider an embedding being real if the absolute value of the imaginary part of every coordinate is less than 10^{-15}. The final results were verified using Maple's `RootFinding` [Isolate]. Our results ameliorate significantly what was known about the bounds of real embeddings.

5.2.1 Embeddings of Laman Graphs on the plane

The numbers of realizations of all 6-vertex Laman graphs are known [13]. There are four non-trivial Laman graphs (requiring an H2 move in the last step of their construction- see Section 2.1) and the upper bound of real embeddings was computed in [24] for the graph with the maximal number of complex embeddings. Using stochastic and parametric methods, we were also able to maximize the number of embeddings for the other three

7-vertex graph with not trivial number of embeddings, completing a full classification for all 7-vertex Laman graphs according to their number of real embeddings [8].

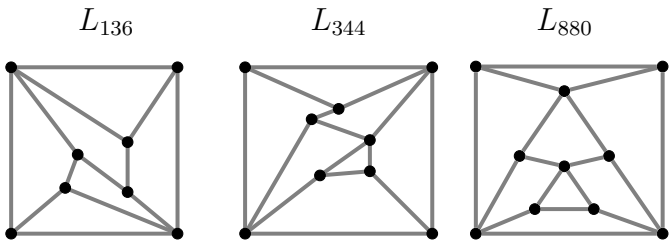

Figure 5.4: *Laman graphs with maximal numbers of complex embeddings with* $8 \leq |V| \leq 10$*. We have found tight bounds for* $|V| = 8$ *and* $|V| = 9$*.*

For bigger graphs, we focused on the graphs with the maximal number of complex embeddings, see Figure 5.4. The following table summarizes the bound on $r_2(G)$ as well as $c_2(G)$ and the mixed volume for the two different algebraic systems. Notice that it shows that there exist edge lengths such that all embeddings of the 8-vertex graph L_{136} and of the 9-vertex graph L_{344} are real.

$\|V\|$	**8**	**9**	**10**
	L_{136}	L_{344}	L_{880}
Mixed Volume of sphere eq.	192	512	1536
Mixed Volume of distance eq.	136	344	880
$c_2(G)$	136	344	880
$r_2(G) \geq$	136	344	860*

Now, we provide edge lengths giving the numbers of real embeddings in the table.

$\boldsymbol{L_{136}}$:
$\lambda_{1,2} = 1.000109994\,,\ \lambda_{1,4} = 1.000334944\,,\ \lambda_{1,8} = 1.000119993\,,$
$\lambda_{2,3} = 1.000174985\,,\ \lambda_{2,7} = 1.000379928\,,\ \lambda_{3,6} = 1.000459894\,,\ \lambda_{3,8} = 1.000099995\,,$
$\lambda_{4,5} = 1.000049999\,,\ \lambda_{4,7} = 1.000144989\,,\ \lambda_{5,7} = 1.000389924\,,\ \lambda_{5,8} = 1.000354937\,,$
$\lambda_{6,7} = 1.000244970\,,\ \lambda_{6,8} = 1.000289958\,,$

$\boldsymbol{L_{344}}$:
$\lambda_{1,4} = 1.00100\,,\ \lambda_{1,6} = 1.00046\,,\ \lambda_{1,9} = 1.00057\,,$
$\lambda_{2,3} = 1.00058\,,\ \lambda_{2,5} = 1.00075\,,\ \lambda_{2,8} = 1.00084\,,\ \lambda_{3,7} = 1.00073\,,$
$\lambda_{3,9} = 1.00042\,,\ \lambda_{4,7} = 1.00096\,,\ \lambda_{4,9} = 1.00015\,,\ \lambda_{5,7} = 1.00083\,,$
$\lambda_{5,8} = 1.00003\,,\ \lambda_{6,7} = 1.00086\,,\ \lambda_{6,8} = 1.00008\,,\ \lambda_{8,9} = 1.00039\,,$

$\boldsymbol{L_{880}}$:
$\lambda_{1,4} = 1.0002169\,,\ \lambda_{1,8} = 1.0001366\,,\ \lambda_{1,10} = 1.0004509\,,$
$\lambda_{2,3} = 1.000763\,,\ \lambda_{2,7} = 1.0000575\,,\ \lambda_{2,10} = 1.0006078\,,\ \lambda_{3,7} = 1.0001763\,,$
$\lambda_{3,9} = 1.00075\,,\ \lambda_{4,8} = 1.0008574\,,\ \lambda_{4,9} = 1.000536\,,\ \lambda_{5,7} = 1.000491\,,$
$\lambda_{5,8} = 1.0002946\,,\ \lambda_{5,10} = 1.0006778\,,\ \lambda_{6,7} = 1.0004699\,,\ \lambda_{6,8} = 1.0002724\,,$
$\lambda_{6,9} = 1.0005141\,,\ \lambda_{9,10} = 1.0003913\,.$

5.2.1.1 Spherical embeddings of Laman graphs

Maximal numbers of embeddings in S^2 have been not studied so far. We attempted to find edge lengths such that the number of realizations was the same as the number of complex solutions for graphs that do not have a trivial number of embeddings. We shall observe again that the $c_2(G)$ varies for certain graphs from $c_{S^2}(G)$.

We have found parameters such that all the embeddings are real for all non-trivial graphs with 6 and the 7-vertex graphs with the maximal number of complex embeddings(they can be found in [8]). The Desargues graph has the maximal number of embeddings among 6-vertex graphs, namely, it can have 32 realizations (instead of 24 on the plane). In the 7-vertex case, there are two non-trivial graphs with 64 realizations (instead of 48 and 56 respectively on the plane),see Figure 5.5. Let us indicate that 64 realizations can be also achieved by the 3 graphs constructed by applying an H1 move on L_{24}, since H1 doubles the number of embeddings. Observe that this contrasts the situation of the complex embeddings in the plane, since it is known that for $|V| \leq 12$ there is always a unique Laman graph with the maximal number of complex embeddings on the plane among all Laman graphs with the same number of vertices [16]. We have also found edge lengths that maximize the spherical embeddings of L_{136} (see Figure 5.4). It has 192 real spherical embeddings. We remark that there is again another 8-vertex graph with 192 complex spherical embeddings, but we have found edge lengths with only 136 real spherical embeddings.

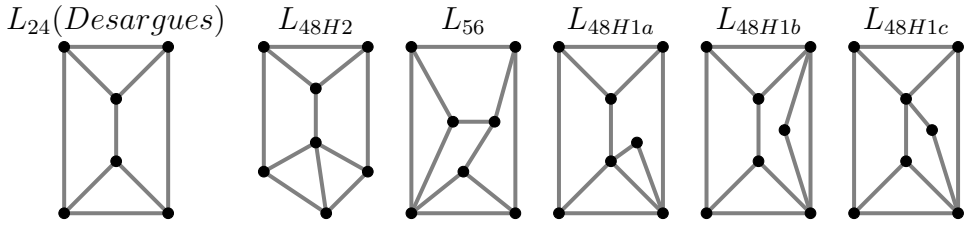

Figure 5.5: *Laman graphs with maximal numbers of spherical embeddings with 6 vertices (L_{24}- Desargues graph with 32 spherical embeddings) and 7 vertices (L_{48H1a},L_{48H1b},L_{48H1c},L_{48H2} and L_{56}- graphs with 64 spherical embeddings).*

This table gives upper bound and the number of real spherical embeddings for all graphs with $6 \leq |V| \leq 8$ that have the maximal number of embeddings.

$\|V$	**6**	**7**	**7**	**7**	**7**	**7**	**8**
	L_{24}	L_{48H2}	L_{56}	L_{48H1a}	L_{48H1b}	L_{48H1c}	L_{136}
Mixed Volume of sphere eq.	32	64	64	64	64	64	192
Mixed Volume of distance eq.	32	64	64	64	64	64	192
$c_{S^2}(G)$	32	64	64	64	64	64	192
$r_{S^2}(G)$	32	64	64	64	64	64	192

We present a list of lengths (using euclidean metric) that give maximal number of realizations for the non-trivial cases:

$\boldsymbol{L_{24}}$:
$\lambda_{1,2} = 1.43\,,\ \lambda_{1,4} = 1.39\,,\ \lambda_{1,6} = 1.055\,,$
$\lambda_{2,3} = 1.45\,,\ \lambda_{2,5} = 1.193\,,\ \lambda_{3,4} = 1.388\,,\ \lambda_{3,5} = 1.64\,,$
$\lambda_{4,6} = 1.691\,,\ \lambda_{5,6} = 1.386\,,$

$\boldsymbol{L_{48H2}}$:
$\lambda_{1,2} = 1.526433752\,,\ \lambda_{1,3} = 1.250599856\,,\ \lambda_{1,4} = 1.519868415\,,$
$\lambda_{2,5} = 1.772004515\,,\ \lambda_{2,6} = 1.371860051\,,\ \lambda_{2,7} = 1.019803903\,,\ \lambda_{3,4} = 1.475127113$
$\lambda_{3,7} = 1.363084737\,,\ \lambda_{4,6} = 1.314534138\,,\ \lambda_{5,6} = 1.754992877\,,\ \lambda_{6,7} = 1.054514106\,,$

$\boldsymbol{L_{56}}$:
$\lambda_{1,2} = 1.921665944\,,\ \lambda_{1,3} = 1.3\,,\ \lambda_{1,5} = 1.337908816\,,$
$\lambda_{2,5} = 1.058300524\,,\ \lambda_{2,6} = 1.306139349\,,\ \lambda_{2,7} = 1.468332387\,,\ \lambda_{3,4} = 1.2\,,$
$\lambda_{3,7} = 0.6693280212\,,\ \lambda_{4,5} = 1.370401401\,,\ \lambda_{4,6} = 1.630337388\,,\ \lambda_{6,7} = 1.994993734\,.$

$\boldsymbol{L_{136}}$:
$\lambda_{1,2} = 1.69431375697417\,,\ \lambda_{1,5} = 1.53147820126884\,,\ \lambda_{1,8} = 1.40741112578064\,,$
$\lambda_{2,3} = 1.46514833488809\,,\ \lambda_{2,5} = 1.43532284310132\,,\ \lambda_{2,7} = 1.3673675423030\,,\ \lambda_{3,4} = 1.35543641920214\,,$
$\lambda_{3,6} = 1.49080389256053\,,\ \lambda_{4,5} = 1.36622835551227\,,\ \lambda_{4,8} = 1.52724607627725\,,\ \lambda_{6,7} = 1.23765605522418\,.$
$\lambda_{6,8} = 0.871783052046995\,,\ \lambda_{7,8} = 1.76892528306539\,.$

5.2.2 Geiringer graphs

The method we introduced in Section 5.1.2 played a crucial role in increasing the number of embeddings of Geiringer graphs. We used our method for the only non-trivial graph with 6 vertices — the cyclohexane G_{16}. It was known that $r_3(G_{16}) = 16$, a result that can be verified by our method within a few tries with random starting lengths.

The case of $|V| = 7$ was the first open one. There are twenty trivial 7-vertex Geiringer graphs and six non-trivial ones. We computed the mixed volumes and the number of complex embeddings for each one of them. Then, using our code we were able to find edge lengths that give a full classification of all 7-vertex Geiringer graphs according to $r_3(G)$ [8].

We want to remark again at this point that G_{48} was the model for our coupler curve method. Using our implementation, we were able to find lengths that maximize the number of embeddings only after a few iterations. The structure of this graph fits perfectly to our method,

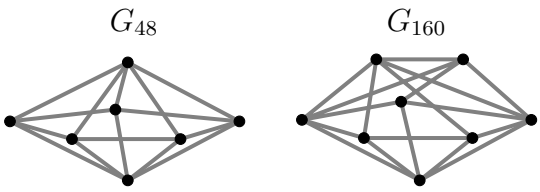

Figure 5.6: *The 7-vertex and 8-vertex graphs with the maximal number of embeddings (G_{48} and G_{160}).*

since there are 20 subgraphs of G_{48} given by vertices (u, v, w, q, u') satisfying the assumption in Lemma 7. Using tree search approach, we obtained edge lengths $\boldsymbol{\lambda}$ such that $r_3(G_{48}, \boldsymbol{\lambda}) = 48$:

$$\begin{array}{llll} \lambda_{1,2} = 1.9999, & \lambda_{1,6} = 2.0001, & \lambda_{4,5} = 7.0744, & \lambda_{4,7} = 11.8471, \\ \lambda_{1,3} = 1.9342, & \lambda_{2,6} = 1.0020, & \lambda_{5,6} = 4.4449, & \lambda_{5,7} = 11.2396, \\ \lambda_{1,4} = 5.7963, & \lambda_{2,3} = 0.5500, & d_{2,7} = 10.5361, & \lambda_{6,7} = 10.5365\,. \\ \lambda_{1,5} = 4.4024, & \lambda_{3,4} = 5.4247, & \lambda_{3,7} = 10.5245, & \end{array}$$

They can be found from the starting edge lengths given in Sec. 5.1.2 with 28 real embeddings in only 3 iterations, using the subgraphs $(v_5, v_6, v_1, v_7, v_4), (v_4, v_3, v_1, v_7, v_5)$ and $(v_3, v_2, v_1, v_7, v_4)$.

We repeated the same procedure for $|V| = 8$. In that case we can use the H1 doubling property for 311 graphs, while there are 63 graphs with a non-trivial number of embeddings. We computed complex bounds for all non-trivial graphs [8]. We subsequently found edge lengths that increase the number of real embeddings of G_{160}, which is the graph with the maximal number of complex embeddings $c_3(G_{160}) = 160$. We were able to find parameters $\boldsymbol{\lambda}$ such that $r_3(G_{160}, \boldsymbol{\lambda}) = 132$.

The following lengths give 132 real embeddings for G_{160}:

$$\begin{array}{llll} \lambda_{1,2} = 1.999, & \lambda_{2,3} = 1.426, & \lambda_{3,7} = 10.447, & \lambda_{5,8} = 4.279, \\ \lambda_{1,3} = 1.568, & \lambda_{2,6} = 0.879, & \lambda_{4,5} = 7.278, & \lambda_{6,8} = 0.398, \\ \lambda_{1,4} = 6.611, & \lambda_{2,7} = 10.536, & \lambda_{4,7} = 11.993, & \lambda_{7,8} = 10.474\,. \\ \lambda_{1,5} = 4.402, & \lambda_{2,8} = 0.847,, & \lambda_{5,6} = 4.321, & \\ \lambda_{1,6} = 1.994, & \lambda_{3,4} = 6.494, & \lambda_{5,7} = 11.239, & \end{array}$$

One may find a full list of Geiringer graphs with 7 and 8 vertices in [8].

5.2.3 Lower bounds

The maximal numbers of real embeddings that we found can serve to build an infinite class of bigger graphs. These frameworks can give us lower bounds on the maximum

Table 5.1: *Power basis of asymptotic lower bounds for minimally rigid graphs in all embedding spaces treated. The first line contains the existing lower bounds, while the second one the lower bounds presented here (there were previously no lower bounds for the real spherical case).*

embedding space	$\mathbb{R}^2$	S^2	$\mathbb{R}^3$
previous	2.3003	-	2.5198
new	2.3780	2.5198	2.6553

number of embeddings. To compute the lower bound, we will use the following theorem that combines caterpillar, fan and generalized fan constructions [35]:

Theorem 13 *Let $G = (V_G, E_G)$ be a generically rigid graph, with a generically rigid subgraph $G' = (V_{G'}, E_{G'})$. We construct a rigid graph using l copies of G, where all the copies have the subgraph G' in common. The new graph is rigid, has $|V| = |V_{G'}| + l(|V_G| - |V_{G'}|)$ vertices, and the number of its real embeddings is at least*

$$2^{(|V|-|V_{G'}|) \mod (|V_G|-|V_{G'}|)} \cdot r_d(G') \cdot \left(\frac{r_d(G)}{r_d(G')}\right)^{\left\lfloor \frac{|V|-|V_{G'}|}{|V_G|-|V_{G'}|} \right\rfloor}.$$

Remind that for a triangle T we have that $r_2(T) = r_{S^2}(T) = 2$, while $r_3(T) = 1$. For Laman graphs, the best asymptotic bound is derived from L_{880}:

Corollary 6 *The maximum number of real embeddings on the plane among Laman graphs with n vertices is bounded from below by*

$$2^{(|V|-3) \mod 7} \cdot 2 \cdot 430^{\lfloor (|V|-3)/7 \rfloor}.$$

The bound asymptotically behaves as $2.3780^{|V|}$.

The previous lower bound in that case was $2.3003^{|V|}$ by [24].

In the case of spherical embeddings, we may use L_{24}:

Corollary 7 *The lower bound for the maximum number of spherical embeddings among Laman graphs with $|V|$ vertices is*

$$2^{(|V|-3) \mod 7} \cdot 2 \cdot 16^{\lfloor (|V|-3)/3 \rfloor}.$$

This bound asymptotically behaves as $2.5198^{|V|}$.

We remark that L_{48H1a} and L_{48H2}, which have the 4-vertex Laman graph as a subgraph, can give the same asymptotic lower bound. The other 7-vertex graphs with $r_{S^2}(L) = 64$

can give only $2.3784^{|V|}$ as a lower bound, while the asymptotic bound from 8-vertex graph with 192 embeddings is $2.4914^{|V|}$.

Finally, using the fact that $r_3(G_{160}) \geq 132$, we obtain the following result:

Corollary 8 *The maximum number of real embeddings of Geiringer graphs with $|V|$ vertices can be bigger than*

$$2^{(|V|-3) \mod 5} 132^{\lfloor (|V|-3)/5 \rfloor},$$

indicating that $r_3(|V|) \in \Omega(2.6553^{|V|})$.

The previous lower bound for Geiringer graphs was $2.51984^{|V|}$ [25, 28]. Using the graph G_{48} yields $r_3(|V|) \in \Omega(2.6321^{|V|})$. Notice that we use a subgraph with one embedding and not with two, as we did in the cases of Laman graphs. This happens because there is no tetrahedron as a subgraph of the 8-vertex graphs that could give a better lower bound.

In Table 5.1, we compare the existing asymptotic lower bounds on the maximal real embedding number, with the improvements presented in this chapter.

6. CONCLUSION AND OPEN QUESTIONS

In this thesis we have developed various methods concerning bounds on the embedding number of minimially rigid graphs. We presented new methods to compute efficiently the m-Bézout bound of the complex embedings of minimally rigid graphs using graph orientations and matrix permanents. These bounds are graph-specific. We also compared our experimental results with existing ones indicating that some classes of graphs have tight m-Bézout bounds. Motivated by these results, we applied Bernstein's second theorem in the case of the m-Bézout bound for rigid graphs. Our findings in this topic can be generalized for every class of polynomial systems that have no zero solutions.

In order to improve general upper bounds on the embedding number, initially we exploited existing bounds on planar graph orientations and matrix permanents. This led to improvements on the asymptotic upper bounds of the embeddings for planar graphs in dimension 3 and for all graphs for $d \geq 5$. Then, we introduced a method that bounds the number of outdegree constrained eliminations that are related to the m-Bézout bound, as stated above. This method resulted in a new bound for the embeddings of all minimally rigid graphs with a given number of vertices, which was generalized as the first non-trivial upper bound in the cases of Laman and Geiringer graphs. It also improved bounds in all dimensions bigger than 3, including our own results.

Finally, we have developed and used efficient methods to maximize the number of real embeddings of rigid graphs in the case of planar, spherical and spatial embeddings. In this context a new technique inspired by coupler curves was introduced for Geiringer graphs. These methods led to a classification of certain Laman and Geiringer graphs up to their real embedding number and to an improvement of the asymptotic lower bounds on the maximal number of embeddings. These increased lower bounds combined with the ameliorated upper bounds found in this thesis, reduce the existing gap between them.

Several open questions rise from our results. First of all, the gap between upper and lower bounds remain (even in the case of lower bounds on the maximal complex embedding number which is easier to compute and was not treated in this thesis). In this context, it would be useful to investigate how sharp our upper bound is on the number of pseudograph orientations and, subsequently, on the maximal complex embedding number. Both of these may require large computational resources.

Besides that, finding the minimal m-Bézout bound requires the computation of bounds up to all possible choices for a fixed K_d. Thus, it would be convenient to find a method to select the K_d that attains the minimum without computing its bound. Another issue is that the elimination process may result to a more efficient algorithm for the computation of the outdegree-constrained orientations. The worst case scenario of our recursive algorithm is $\sim 2^{|E|}$, while the bound on orientations is in the order of $\sim \zeta_d^{|V|}$ (see Equation 4.10), which is much smaller.

Regarding the exactness of the m-Bézout bound and the application of Bernstein's second theorem, the first priority would be a possible proof (or refutation) of Conjecture 1.

This may help to investigate a possible relation between planarity and tight upper bounds, especially in the case of Geiringer graphs. Another issue is to optimize this method using the appropriate tools. A first idea is to construct resultant matrices that exploit the multi-homogeneous structure (see for example [27, 21]). The rank of the matrix could indicate which zero evaluations have solutions for our systems.

In the case of maximal real embeddings, the next step would be to ameliorate the maximal real bounds in all cases. One of the issues is the time needed to solve the systems of equations for bigger graphs, which is multiplied by the fact that more sampling iterations are necessary. For instance, our result for the 8-vertex Geiringer graph is the best one obtained from running the coupler curve method for several weeks, with various starting points. In the case of Laman graphs, we faced the problem that homotopy solvers like `phcpy` are not always able to track all solutions when $c_d(G)$ is very big (> 1000 solutions for minimally rigid graphs).

ABBREVIATIONS - ACRONYMS

B-M	Brègman-Minc bound
CAD	cylindrical algebraic decomposition
CM	Cayley-Menger matrix
dof	degrees of freedom
H1, H2, H3	Henneberg 1, 2, 3 (resp.)
mBe	m-Bézout
MV	mixed volume bound
Ε.Α.Γ.	ελαχιστικώς γενικά άκαμπτοι γράφοι
Θ.Α.Γ.	θεωρία Άκαμπτων Γράφων
Π.Φ. Bézout	πολυ-ομογενές φράγμα Bézout

Bounds on the maximal number of graph embeddings.

APPENDIX A. ALGEBRAIC BOUNDS.

In this Appendix we present the main algebraic bounds used in this thesis. These bounds are established for projective spaces, but can be also applied for affine polynomials. These are the Bézout bound, the m-Bézout bound and the mixed volume bound (also known as BKK bound). We also give Bernstein's second theorem on the exactness of mixed volumes.

For the rest of this Appendix we will consider square polynomial systems $\boldsymbol{f}(\boldsymbol{x}) = (f_1(\boldsymbol{x}), \ldots, f_m(\boldsymbol{x}))$, where $\boldsymbol{x} = (x_1, x_2, \ldots, x_m)$ is a vector of m variables $\boldsymbol{f}(\boldsymbol{x}) \in \mathbb{C}[\boldsymbol{x}]$.

The first (and simplest) bound is the well known Bézout bound. Here we give a version for 0-dimensional varieties in $\mathbb{C}^m$.

Theorem 14 (Bézout bound) *Let α_i be the total degree of a polynomial $f_i \in \boldsymbol{f}$. Then if the number of complex roots of $\boldsymbol{f}$ is finite, then it is bounded from above by $\prod_{i=1}^{m} \alpha_i$.*

This bound is a generalization of the fundamental theorem of algebra. Nevertheless, in many cases this bound is rather loose. We can have tighter bounds taking advantage of the particular structure of a polynomial system.

First let us define multihomogeneous polynomial systems that are the basis for the computation of the m-Bézout bound.

Definition 6 (Multihomogeneous polynomial) *Let $X_1 = (x_{1,1}, \ldots, x_{1,d_1})$, $X_2 = (x_{2,1}, \ldots, x_{2,d_2})$, $\ldots$, $X_n = (x_{n,1}, \ldots, x_{n,d_n})$ be a partition of the affine variables $\boldsymbol{x}$, with $|X_i| = m_i$, and $m_1 + \cdots + m_n = m$.*

Consider that every f_i is homogeneous in each variable set X_j, with homogenizing variable $x_{i,0}$ and multidegree specified by vector $\boldsymbol{\alpha_i} = (\alpha_{i,1}, \alpha_{i,2}, \ldots, \alpha_{i,n})$, where $\alpha_{i,j}$ denotes the degree of f_i in X_j. Then $\boldsymbol{f}$ is multihomogeneous of type

$$(m_1, \ldots, m_n; \boldsymbol{\alpha_1}, \ldots, \boldsymbol{\alpha_n}).$$

Given this definition, the classic theorem from algebraic geometry [62] can be used for the computation of the m-Bézout bound.

Theorem 15 *Consider the multihomogeneous system $\boldsymbol{f}(\boldsymbol{x})$ defined above. The coefficient of the monomial $Y_1^{m_1} \cdots Y_n^{m_n}$ in the polynomial defined by the product*

$$\prod_{i=1}^{m} (\alpha_{i,1} \cdot Y_1 + \cdots + \alpha_{i,n} \cdot Y_n). \tag{A.1}$$

bounds the number of roots of $\boldsymbol{f}(\boldsymbol{x})$ in $\mathbb{P}^{m_1} \times \cdots \times \mathbb{P}^{m_n}$, where Y_i are new symbolic parameters, and $\mathbb{P}^{m_i}$ is the m_i-dimensional projective space over $\mathbb{C}$. The bound is tight for generic coefficients of $\boldsymbol{f}(\boldsymbol{x})$.

A more delicate approach uses geometrical tools to establish upper bounds (see details in [19]).

Definition 7 (Newton Polytope) *Let a polynomial*

$$f(\boldsymbol{x}) = \sum_{\boldsymbol{\alpha} \in \mathbb{Z}^m} c_{\boldsymbol{\alpha}} \cdot \mathbf{x}^{\boldsymbol{\alpha}} \in \mathbb{C}[\boldsymbol{x}]$$

where $c_{\boldsymbol{\alpha}} \in \mathbb{C}^*$ *are the non-zero coefficients and* $\mathbf{x}^{\boldsymbol{\alpha}} = \prod_{i=1}^{m} x_i^{\alpha_i}$ *for a vector* $\boldsymbol{\alpha} = (\alpha_1, \ldots, \alpha_m)$. *Then the* Newton Polytope *of* f *is the convex hull of the exponent vectors* $\boldsymbol{\alpha}$ *and will be denoted with NP*(f).

A basic operation that forms a new polytope from two or more old ones is the Minkowski sum.

Definition 8 *Let* Q_1 *and* Q_2 *be two polytopes in* $\mathbb{R}^m$. *Then the minkowski sum* $Q_1 + Q_2$ *is a new polytope such that*

$$Q_1 + Q_2 = \{q_1 + q_2 : q_1 \in Q_1 \text{ and } q_2 \in Q_2\}$$

Notice that the Minkowski Sum of polytopes lying in complementary subspaces is the same as the cartesian product of these polytopes.

Minkowski sum is used to define the mixed volume for a collection of polytopes.

Definition 9 *The mixed volume of a collection of polytopes* $Q_1, Q_2, \ldots, Q_m \in \mathbb{R}^m$ *is defined by the coefficient of the monomial* $\mu_1 \cdot \mu_2 \cdots \mu_m$ *in the polynomial Vol*$_m(\mu_1 Q_1 + \cdots + \mu_m Q_m)$, *where Vol*$_m$ *is the* m*-dimensional volume and will be denoted by MV*$_m(Q_1, \ldots, Q_m)$.
An equivalent method to compute the mixed volume is the following formula:

$$MV_m(Q_1, \ldots, Q_m) = \sum_{j=1}^{m} (-1)^{m-j} \sum_{\substack{I \subset \{1,2,\ldots,m\} \\ |I|=j}} Vol_m \left(\sum_{i \in I} Q_i \right) \tag{A.2}$$

There is a connection between the mixed volume of Newton Polytopes and the number of roots for a polynomial in the corresponding toric variety. The toric variety is a projective variety defined essentially by the Newton Polytopes of the given system and contains the topological torus $(\mathbb{C}^*)^m$ as a dense subset. The set-theoretic difference of a toric variety and $(\mathbb{C}^*)^m$ is toric infinity in correspondence with projective infinity.

Theorem 16 (BKK theorem [9, 44, 46]) *Let* $\boldsymbol{f}(\boldsymbol{x})$ *as defined above, and let* $(NP(f_i))_{1 \le i \le m}$ *be the collection of Newton Polytopes for this polynomial system. Then, if the number of system's solutions in* $(\mathbb{C}^*)^m$ *is finite, it is bounded above by the mixed volume of these Newton Polytopes.*

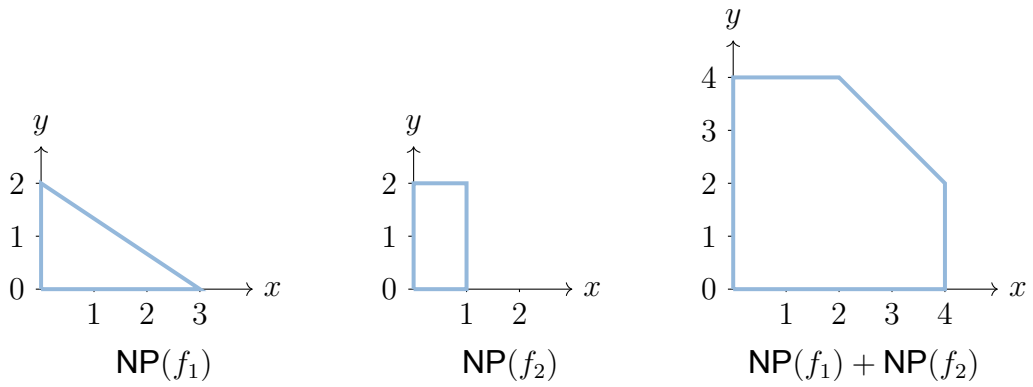

Figure A.1: *The Newton Polytopes of the polynomials in Example 7*

This relation was established by D.Bernshtein, A.Khovanskii and A.Kouchnirenko. Therefore this bound is known as *BKK bound* by their initials or simply *mixed volume bound*.

In general and without paying much attention to the underlying variety, we have the following relations as in [63]:

$$\#\text{real solutions} \leq \#\text{complex solutions} \leq \text{ mixed volume} \leq \text{ m-Bézout} \leq \text{ Bézout}.$$

On the other hand, the complexity of computing bounds goes in the opposite direction. More precisely, the computation of the m-Bézout bound is #P-hard by reduction to the permanent. The same hardness result holds for mixed volume, although for most polynomial systems the runtime in practice is much bigger than the m-Bézout computation. An additional problem in the case of the m-Bézout is to discover the optimal variable partition minimizing this bound for a given polynomial. This problem is not in APX, unless P=NP [52].

The Newton Polytopes capture the sparseness of the polynomials. In fact the Bézout and the m-Bézout bound can be also related with polytopes whose mixed volume gives these bounds. More precisely, the polytopes related to the Bézout bound are simplices, while the polytopes related to the m-Bézout bound are simplices or products of simplices (see [55] for details).

Let us give an example of the bounds and their polytopes.

Example 7 *We will consider the following polynomial system in two variables.*

$$f_1(x_1, x_2) = x_1^3 + x_2^2 - 3$$
$$f_2(x_1, x_2) = x_1 + x_2^2 x_1 + x_2^2 + 5$$

The Bézout bound of this system of equations is $3 \cdot 3 = 9$.

Let us compute the m-Bézout bound for the trivial partition $X_1 = \{x_1\}, X_2 = \{x_2\}$. *Obviously* $|X_1| = |X_2| = 1$, *so we need to find the coefficient of* $Y_1 \cdot Y_2$ *in the polynomial*

$$(3Y_1 + 2Y_2) \cdot (Y_1 + 2Y_2) = 3Y_1^2 + 8Y_1Y_2 + 4Y_2^2,$$

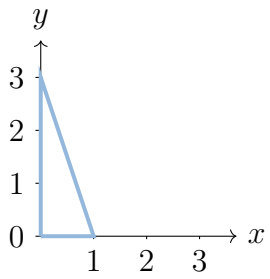

Figure A.2: *The Newton Polytope of a dense polynomial with total degree 3.*

indicating that the m-Bézout bound is 8*.*

Now, we will compute the mixed volume. We have

$$\textit{NP}(f_1) = Conv(\{(3,0),(0,2),(0,0)\}), \textit{NP}(f_2) = Conv(\{(1,0),(1,2),(2,0),(0,0)\}),$$

while their Minkowski sum is

$$\textit{NP}(f_1) + \textit{NP}(f_2) = Conv(\{(0,0),(4,0),(2,2),(1,4),(0,4)\})$$

(see Figure A.1).

Using Equation A.2 we get that the BKK bound is

$$Vol_2(\textit{NP}(f_1) + \textit{NP}(f_2)) - Vol_2(\textit{NP}(f_1)) = Vol_2(\textit{NP}(f_2)) = 8.$$

It is not a surprise that the BKK bound and the m-Bézout bound coincide. If we study the structure of the polytope NP(f_1) *we may see that it is a simplex, so it is related with dense polynomials and correspond also to both the Bézout and the m-Bézout bound. In the case of NP*(f_2) *we have the cartesian product of two 1-simplices* $\{(0,0),(1,0)\} \times \{(0,0),(0,2)\}$*, showing that the multidegree vector* $(1,2)$ *of this polynomial is equivalent with the Newton Polytope. On the other hand a dense polynomial with degree* 3 *would have as Newton Polytope the convex hull of a simplex, such that one of the coordinate for at least one vertex shall be* 3*, e.g.* $\{(0,0),(1,0),(0,3)\}$*, indicating that the Bézout bound shall be higher (See Figure A.2).*

It is obvious that if the polytopes associated with the Bézout or the m-Bézout bound coincide with the Newton Polytopes, then the bounds also coincide. On the other hand this is not a necessary condition for equal bounds, as in the case of sphere equations (see Section 3.2).

The exactness of the BKK bound can be verified by Bernstein's discriminant conditions. In order to state these conditions we first need the following definition.

Definition 10 (Initial form and face system) *Let* w *be a vector in* $\mathbb{R}^m$ *and* $f(\boldsymbol{x}) = \sum_{\boldsymbol{\alpha} \in \mathcal{A}} c_{\boldsymbol{\alpha}} \cdot \mathbf{x}^{\alpha}$ *be a polynomial in* $\mathbb{C}[\boldsymbol{x}]$*, where* $\mathcal{A}$ *consists of the exponent vectors of monomials with non-zero coefficients.*

Let $\mathcal{A}'$ be the subset of vectors in $\mathcal{A}$, such that $\boldsymbol{\alpha}' \in \mathcal{A}' \iff \langle \boldsymbol{\alpha}', w \rangle = \min_{\boldsymbol{\alpha} \in \mathcal{A}} (\langle \boldsymbol{\alpha}, w \rangle)$.

Then the initial form f^w *is a polynomial consisting of all the monomials whose exponent vectors belong in $\mathcal{A}'$:*

$$f^w(\boldsymbol{x}) = \sum_{\boldsymbol{\alpha}' \in \mathcal{A}'} c_{\boldsymbol{\alpha}'} \cdot \mathbf{x}^{\boldsymbol{\alpha}'}.$$

Since the initial form f^w contains precisely the monomials whose exponent vector minimizes the inner product with w and excluding the others, we can relate w to an inner vector of a face of NP(f). Hence, the algebraic system comprised of initial forms for a face normal w shall be called face system.

The necessary and sufficient condition of BKK exactness is stated below.

Theorem 17 (Bernstein's second theorem [9]) *Let $\boldsymbol{f}$ be a system of polynomials as defined above*

$$Q = \sum_{i=1}^{m} NP(f_i) \tag{A.3}$$

be the Minkowski sum of their Newton Polytopes. The number of solutions of $\boldsymbol{f}$ in $(\mathbb{C}^*)^m$ equals exactly its mixed volume (counted with multiplicities) if and only if, for all $w \in \mathbb{R}^m$, such that w is a face normal of Q, the system of equations $(f_i^w)_{1 \leq i \leq m}$ has no solutions in $(\mathbb{C}^*)^m$.

Let us note that although there is an infinite number of vectors that may appear as inner normals, Bernstein's condition can be verified choosing only one inner normal vector for every different face of Q. This theorem can also verify the exactness of the Bézout or the m-Bézout bound, if the Minkowski sum of polytopes related to these bounds is taken into account instead of the Minkowski sum of Newton polytopes (see Equation A.3).

Bounds on the maximal number of graph embeddings.

APPENDIX B. THE COMPUTATION OF THE EMBEDDING NUMBER USING SPHERE EQUATIONS IN THE ABSENCE OF K_d.

In Section 2.2 we introduce sphere equations and explain that the embedding number is the number of solutions derived from this system if all the coordinates of a complete graph in d vertices are fixed, following [28, 35]. Although in dimension 2 there can always be a fixed edge (or K_2), in bigger dimensions this condition is not guaranteed. For example, in most known cases of Geiringer graphs, there is a fixed triangle, but there exist minimally rigid graphs with no triangles: $K_{6,4}$ is the only instance with up to 10 vertices. We have not constructed as many graphs in bigger dimensions using Henneberg steps, as in dimensions 2 and 3 (see Table 2.1), but we can verify that the graphs with no complete subgraph K_d are more for $d \geq 4$. In this Appendix we will analyze how to compute the embedding number using sphere equations in the absence of a clique. Note that this case does not affect the asymptotic bounds presented in Chapter 4 and that all Geiringer graphs treated in Chapter 5 posses at least one triangle. We also remark that no such clarification is needed for the Cayley-Menger semialgebraic systems, since in that case the solutions of the system correspond to distance coordinates and not to usual euclidean ones.

Maxwell's condition subtracts the dof of trivial motions (rotations and translations) from the total number of coordinates for an embedding of a graph $G(V, E)$ in $\mathbb{R}^d$, as explained in Chapter 1. Fixing the number of coordinates corresponding to the dof yields already a $0-$dimensional algebraic system using Edge Equations 1.1, or the sphere equations. On the other hand, the solutions of such system correspond to multiple embeddings up to trivial motions. Before explaining that statement we need the following proposition.

Proposition 7 *The embedding number of a complete graph in d vertices up to rigid motions in $\mathbb{R}^d$ (or $\mathbb{C}^d$ and S^d) is 1.*

This proposition is trivial, since a graph K_d can be embedded as a $(d-1)-$dimensional simplex.

Let us now demonstrate how we treat the algebraic system in the case of Laman graphs, before generalizing this process to higher dimensions. Let K_2 be a complete graph with vertices $\{u, v\}$, or simply an edge, and $\lambda_{u,v}$ be an edge labeling. Maxwell's condition in dimension 2 indicates that we shall subtract 3 coordinates, so we can set $u(0, 0)$ and $v(0, y)$. Now it is clear that the y-coordinate of v can have two solutions, that are $y = \pm\lambda_{u,v}$ (See Figure B.1). These solutions evidently correspond to the same embedding, if we factor out rigid motions. Thus, if we also fix the second coordinate of v, then there is only one possible embedding for K_2 and by fixing the coordinates of that edge in a bigger Laman graph, the number of solutions of sphere equations is the same as the embedding number. Notice that the existence of the edge allows us to fix the additional coordinate.

For $d = 3$, Maxwell's condition removes 6 dof and the presence of a triangle removes 3 additional degrees of freedom, thus fixing the 9 coordinates of the triangle. If no triangle exists, 3 vertices, u, v, w , are selected such that 2 of them are the endpoints of an edge

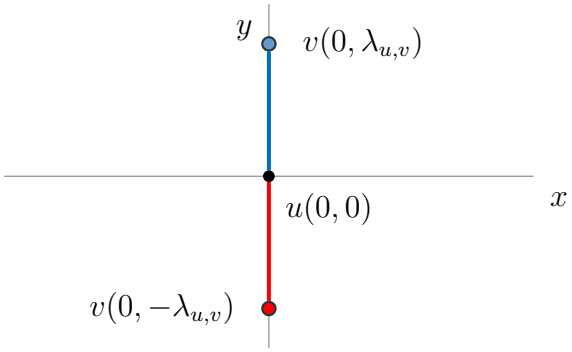

Figure B.1: *Fixing 2 coordinates for vertex u and 1 coordinate for vertex v, there are two possible embeddings for the latter. Both embeddings are equivalent up to trivial motions in $\mathbb{R}^2$.*

(u, v). Then, we use Maxwell's condition to remove 6 degrees of freedom as follows: first we define a plane on which all three vertices lie by fixing one of their coordinates e.g. $x = 0$ for all three, removing 3 dof, and then we fix the other 2 coordinates of u and 1 more coordinate of v removing the 3 remaining dof. An additional dof is removed using the edge, fixing the third coordinate of v. Now the first vertices u and v are ***fixed***, while w is *partially fixed*. The corresponding algebraic system counts every embedding twice (by reflection on the plane defined above). Notice that if we had not fixed the third coordinate of v, then there would be two solutions of the algebraic system for the embedding of the edge (u, v), as in the $2-$dimensional case, so in total this algebraic system would count every embedding four times.

Generally, if for a minimally rigid graph $G(V, E)$ in $d \geq 3$ no K_d exists, a maximal clique may be fixed with $d' < d$ vertices and for the rest $d - d'$ vertices one may fix an appropriate number of coordinates, thus factoring out rotations and translations according to Maxwell's condition. More precisely we can have the following cases:

- d' fixed vertices $v_1, \ldots, v_{d'}$ with no dof.
- $d - d'$ partially fixed vertices $v'_1, v'_2, \ldots, v'_{d-d'}$ with $d', d' + 1, \cdots, d - 1$ dof respectively.
- $|V| - d$ non-fixed vertices $u_1, \ldots, u_{|V|-d}$ with d dof.

Clearly, $d' \geq 2$ since an edge always exists. Let now $\boldsymbol{S}(G, \lambda, K_{d'}(\boldsymbol{\rho}))$ denote the solutions of sphere equations for the embedding of a graph in $\mathbb{C}^d$ and $\boldsymbol{S}_{\mathbb{R}}(G, \lambda, K_{d'}(\boldsymbol{\rho}))$ the real solutions in $\mathbb{R}^d$, up to a fixed embedding $K_{d'}(\boldsymbol{\rho})$ for a generic choice of edge lengths $\boldsymbol{\lambda}$. Then we have the following relations between the number of solutions and the embedding number:

$$|\boldsymbol{S}(G, \lambda, K_{d'}(\boldsymbol{\rho}))| = 2^{d-d'} \cdot c_d(G) \qquad \text{and} \qquad |\boldsymbol{S}_{\mathbb{R}}(G, \lambda, K_{d'}(\boldsymbol{\rho}))| = 2^{d-d'} \cdot r_d(G, \boldsymbol{\lambda}) \tag{B.1}$$

These relations can apply to the computation of a bound on the embeddings using the methods from Chapter 3 on a system of sphere equations as described above. More

precisely, let us denote with $\mathcal{B}(G, K_{d'})$ the orientations of a graph $G \backslash E(K_{d'})$ such that the outdegree of each vertex equals its dof, then the embedding number is bounded by

$$2^{|V|-d} \cdot \mathcal{B}(G, K_{d'}).$$

Notice that the number of vertices for the corresponding pseudograph are bounded by the inequality $|V| - d \leq n \leq |V| - 2$, since $n = |V| - d + d'$.

Similarly, we can construct the m-Bézout matrix A by adding blocks of rows associated to the partially fixed vertices. The number of each block equals to the dof of each one of these and the bound is computed by the following relation:

$$\left(\prod_{i=1}^{d-d'} \frac{1}{d' - 1 + i} \right) \cdot \left(\frac{2}{d!} \right)^{|V|-d} \cdot \text{per}(A).$$

In that case, the size of square matrix the A is $d \cdot n \times d \cdot n$, where n is the same as above.

Bounds on the maximal number of graph embeddings.

REFERENCES

[1] L. Asimow and B. Roth. The rigidity of graphs. *Transactions American Mathematical Society*, 245:279–289, 1978.

[2] J. Baglivo and J. Graver. *Incidence and Symmetry in Design and Architecture*. Cambridge Urban and Architectural Studies. Cambridge University Press, 1983.

[3] E. Bartzos, I. Z. Emiris, J. Legerský, and E. Tsigaridas. On the Maximal Number of Real Embeddings of Spatial Minimally Rigid Graphs. In *Proceedings of the 2018 ACM International Symposium on Symbolic and Algebraic Computation*, ISSAC '18, pages 55–62, New York, NY, USA, 2018. ACM.

[4] E. Bartzos, I. Z. Emiris, J. Legerský, and E. Tsigaridas. On the maximal number of real embeddings of minimally rigid graphs in $\mathbb{R}^2$, $\mathbb{R}^3$ and S^2. *J. Symbolic Computation*, 102:189–208, 2021.

[5] E. Bartzos, I. Z. Emiris, and J. Schicho. On the multihomogeneous Bézout bound on the number of embeddings of minimally rigid graphs. *J. Applicable Algebra in Engineering, Communication & Computing*, 31:325–357, 2020.

[6] E. Bartzos, I.Z. Emiris, and J. Schicho. Source code and examples for the paper "On the multihomogeneous Bézout bound on the number of embeddings of minimally rigid graphs". `https://doi.org/10.5281/zenodo.3542061`, 2019.

[7] E. Bartzos, I.Z. Emiris, and R. Vidunas. New upper bounds for the number of embeddings of minimally rigid graphs. *Discrete & Computational Geometry*, 2022.

[8] E. Bartzos and J. Legerský. Graph embeddings in the plane, space and sphere — source code and results. `https://doi.org/10.5281/zenodo.1495153`, 2018.

[9] D. N. Bernstein. The number of roots of a system of equations. *Functional Analysis and Its Applications*, 9(3):183–185, 1975.

[10] F. Bihan and F. Sottile. New fewnomial upper bounds from Gale dual polynomial system. *Moscow Mathematical Journal*, 7(3):387–407, 2007.

[11] S.J.L. Billinge, P.M. Duxbury, D.S. Gonçalves, C. Lavor, and A. Mucherino. Assigned and unassigned distance geometry: applications to biological molecules and nanostructures. *4OR*, 14(4):337–376, 2016.

[12] L.M. Blumenthal. Congruent Imbedding in Euclidean Space. In *Theory and Applications of Distance Geometry*, chapter 4, pages 90–121. Chelsea Publishing Company, New York, 1970.

[13] C. Borcea and I. Streinu. The number of embeddings of minimally rigid graphs. *Discrete & Computational Geometry*, 31:287–303, 2004.

[14] L. Brègman. Some properties of nonnegative matrices and their permanents. *Dokl. Akad. Nauk SSSR*, 211(1):27–30, 1973.

[15] L. Busé, I.Z. Emiris, B Mourrain, O Ruatta, and P Trébuchet. Multires, a Maple package for multivariate resolution problems. `http://www-sop.inria.fr/galaad/logiciels/multires`, 2002.

[16] J. Capco, M. Gallet, G. Grasegger, C. Koutschan, N. Lubbes, and J. Schicho. The number of realizations of a Laman graph. *SIAM J. Applied Algebra and Geometry*, 2(1):94–125, 2018.

[17] K. Clinch and D. Kitson. Constructing isostatic frameworks for the ℓ_1 and ℓ_∞ plane. *The Electronic Journal of Combinatorics*, 27(2), 2020.

[18] R. Connelly. Generic global rigidity. *Discrete Comput. Geom.*, 33:549–563, 2005.

[19] D.A. Cox, J. Little, and D. O'Shea. Polytopes, resultants, and equations. In *Using Algebraic Geometry*, chapter 7, pages 290–358. Springer-Verlag, 2005.

[20] M. Dattorro and J. Dattorro. Euclidean Distance Matrix. In *Convex Optimization & Euclidean Distance Geometry*, chapter 5, pages 337–411. 2005.

[21] A. Dickenstein and I.Z. Emiris. Multihomogeneous resultant formulae by means of complexes. *J. Symbolic Computation*, 36(3):317–342, 2003. ISSAC 2002.

[22] P. Dietmaier. The Stewart-Gough platform of general geometry can have 40 real postures. In J. Lenarčič and M.L. Husty, editors, *Advances in Robot Kinematics: Analysis and Control*, pages 7–16. Kluwer Academic Publishers, 1998.

[23] T. Duff, C. Hill, A. Jensen, K. Lee, A. Leykin, and J. Sommars. Solving polynomial systems via homotopy continuation and monodromy. *IMA J. Numerical Analysis*, 39(3):1421–1446, 2019.

[24] I. Z. Emiris and G. Moroz. The assembly modes of rigid 11-bar linkages. *IFToMM 2011 World Congress, Jun 2011, Guanajuato, Mexico*, 2011.

[25] I. Z. Emiris and B. Mourrain. Computer Algebra Methods for Studying and Computing Molecular Conformations. *Algorithmica 25*, pages 372–402, 1999.

[26] Ioannis Z. Emiris and Raimundas Vidunas. Root counts of semi-mixed systems, and an application to counting nash equilibria. In *Proceedings of the 2014 ACM International Symposium on Symbolic and Algebraic Computation*, ISSAC, pages 154–161. ACM, 2014.

[27] I.Z. Emiris and A. Mantzaflaris. Multihomogeneous resultant formulae for systems with scaled support. *J. Symbolic Computation*, 47(7):820–842, 2012. Special issue on: International Symposium on Symbolic and Algebraic Computation (ISSAC 2009).

[28] I.Z. Emiris, E. Tsigaridas, and A. Varvitsiotis. Mixed volume and distance geometry techniques for counting Euclidean embeddings of rigid graphs. In A. Mucherino, C. Lavor, L. Liberti, and N. Maculan, editors, *Distance Geometry: Theory, Methods and Applications*, pages 23–45. Springer-Verlag, 2013.

[29] D.G. Emmerich. *Structures Tendues et Autotendantes*. Ecole d'Architecture de Paris, la Villette, 1988.

[30] S. Felsner and F. Zickfeld. On the number of planar orientations with prescribed degrees. *Electronic J. Combinatorics*, 15:Research paper R77, 2008.

[31] M. Gallet, G Grasegger, and J Schicho. Counting realizations of Laman graphs on the sphere. *Electron. J. Comb.*, 27(2), 2020.

[32] M.E. Gáspár and P. Csermely. Rigidity and flexibility of biological networks. *Briefings in Functional Genomics*, 11(6):443–456, 2012.

[33] H. Gluck. Almost all simply connected closed surfaces are rigid. In Glaser L.C. and Rushing T.B., editors, *Geometric Topology*. Springer, Berlin, Heidelberg, 1975.

[34] S. Gortler, A. Healy, and D. Thurston. Characterizing generic global rigidity. *American Journal of Mathematics*, 132(4):897–939, 2010.

[35] G. Grasegger, C. Koutschan, and E. Tsigaridas. Lower bounds on the number of realizations of rigid graphs. *Experimental Mathematics*, 29(2):125–136, 2020.

[36] J. Graver, B. Servatius, and H. Servatius. *Combinatorial rigidity*, volume 2 of *Graduate studies in mathematics*. American Mathematical Society, 1993.

[37] F. Harary. *Graph Theory*. Addison-Wesley, 1969.

[38] J. Harris and L.W. Tu. On symmetric and skew-symmetric determinantal varieties. *Topology*, 23(1):71–84, 1984.

[39] J. D. Hunter. Matplotlib: A 2D graphics environment. *Computing In Science & Engineering*, 9(3):90–95, 2007.

[40] B. Jackson and J.C. Owen. Equivalent Realisations of Rigid Graphs. *10th Japanese-Hungarian Symposium on Discrete Mathematics and Its Applications*, pages 283–289, 2017.

[41] B Jackson and J.C. Owen. Equivalent realisations of a rigid graph. *Discrete Applied Mathematics*, 256:42–58, 2019. Special Issue on Distance Geometry: Theory & Applications (DGTA 16).

[42] T. Jordan and W. Whiteley. Global rigidity. In Jacob E. Goodman, Joseph O'Rourke, and Csaba D. Tóth, editors, *Handbook of Discrete and Computational Geometry*, chapter 63, pages 1657–1690. CRC Press LLC, 2017.

[43] Dieter Jungnickel. *Graphs, Networks and Algorithms*. Springer-Verlag, 2004.

[44] A.G. Khovanskii. Newton polyhedra and the genus of complete intersections. *Functional Analysis and Its Applications*, 12(1):38–46, 1978.

[45] A.G. Khovanskii. *Fewnomials*, volume 88 of *Translations of Mathematical Monographs*. American Mathematical Society, 1991.

[46] A.G. Kouchnirenko. Polyèdres de Newton et nombres de Milnor. *Inventiones mathematicae*, 32:1–32, 1976.

[47] L. Krick, M.E. Broucke, and B.A. Francis. Stabilisation of infinitesimally rigid formations of multi-robot networks. *International J. Control*, 82(3):423–439, 2009.

[48] G. Laman. On graphs and rigidity of plane skeletal structures. *J. Engineering Mathematics*, 4(4):331–340, 1970.

[49] A. Lee and I. Streinu. Pebble game algorithms and sparse graphs. *Discrete Mathematics*, 308(8):1425–1437, 2008. Special Issue on 3rd European Conference on Combinatorics.

[50] L. Liberti, B. Masson, J. Lee, C. Lavor, and A. Mucherino. On the number of realizations of certain Henneberg graphs arising in protein conformation. *Discrete Applied Mathematics*, 165:213–232, 2014. 10th Cologne/Twente Workshop on Graphs and Combinatorial Optimization (CTW 2011).

[51] H. Maehara. On Graver's Conjecture Concerning the Rigidity Problem of Graphs. *Discrete Comput Geom*, 6:339–342, 1991.

[52] G. Malajovich and K. Meer. Computing minimal multi-homogeneous bezout numbers is hard. *Theory of Computing Systems*, 40(4):553–570, 2007.

[53] J.C. Maxwell. On the calculation of the equilibrium and stiffness of frames. *The London, Edinburgh, and Dublin Philosophical Magazine and Journal of Science*, 27(182):294–299, 1864.

[54] H. Minc. Upper bounds for permanents of $(0, 1)$-matrices. *Bulletin of the American Mathematical Society*, 69:789–791, 1963.

[55] P. Mondal. How many zeroes? Counting the number of solutions of systems of polynomials via geometry at infinity. *arXiv:1806.05346v2 [math.AG]*, 2019.

[56] A. Nixon, J.C. Owen, and S. Power. A characterization of generically rigid frameworks on surfaces of revolution. *SIAM Journal on Discrete Mathematics*, 28(4):2008–2028, 10 2014.

[57] H. Pollaczek-Geiringer. Über die Gliederung ebener Fachwerke. *Zeitschrift für Angewandte Mathematik und Mechanik (ZAMM)*, 7(1):58–72, 1927.

[58] H. Pollaczek-Geiringer. Zur Gliederungstheorie räumlicher Fachwerke. *Zeitschrift für Angewandte Mathematik und Mechanik (ZAMM)*, 12(6):369–376, 1932.

[59] H. Robbins. A remark on Stirling's formula. *The American Mathematical Monthly*, 62(1):26–29, 1955.

[60] A. Schrijver. Bounds on the number of eulerian orientations. *Combinatorica*, 3(3):375–380, 1983.

[61] B. Schulze and W. Whiteley. Rigidity and scene analysis. In Jacob E. Goodman, Joseph O'Rourke, and Csaba D. Tóth, editors, *Handbook of Discrete and Computational Geometry*, chapter 61, pages 1593–1632. CRC Press LLC, 2017.

[62] I.R. Shafarevich. Intersection numbers. In *Basic Algebraic Geometry, vol. 1.*, pages 233–283. Springer, Berlin, Heidelberg, 2013.

[63] A.J. Sommese and C.W II Wampler. *The Numerical Solution of Systems of Polynomials Arising in Engineering and Science*. World Scientific Publishing, 2005.

[64] R. Steffens and T. Theobald. Mixed volume techniques for embeddings of Laman graphs. *Computational Geometry*, 43:84–93, 2010.

[65] Ileana Streinu and Louis Theran. Sparse hypergraphs and pebble game algorithms. *European J. Combinatorics*, 30(8):1944 – 1964, 2009. Special issue on Combinatorial Geometries and Applications: Oriented Matroids and Matroids.

[66] T.S. Tay and W. Whiteley. Generating isostatic frameworks. *Topologie Structurale*, (11):21–69, 1985.

[67] J.H. van Lint and R.M. Wilson. *A Course in Combinatorics*. Cambridge University press, 2001.

[68] J. Verschelde. Modernizing PHCpack through phcpy. In *Proceedings of the 6th European Conference on Python in Science (EuroSciPy 2013)*, pages 71–76, 2014.

[69] D. Walter and M. L. Husty. On a 9-bar linkage, its possible configurations and conditions for paradoxical mobility. *IFToMM World Congress, Besançon, France*, 2007.

[70] W. Whiteley. Cones, infinity and one-story buildings. *Topologie Structurale*, (8):53–70, 1983.

[71] W. Whiteley. Infinitesimally rigid polyhedra. i. statics of frameworks. *Transactions of the American Mathematical Society*, 285(2):431–465, 1984.

[72] D. Zelazo, A. Franchi, F. Allgöwer, H. H. Bülthoff, and P.R. Giordano. Rigidity maintenance control for multi-robot systems. *Robotics: Science and Systems*, 2012.

[73] Z. Zhu, A.M.-C. So, and Y. Ye. Universal rigidity and edge sparsification for sensor network localization. *SIAM Journal on Optimization, 20(6)*, pages 3059–3081, 2010.

[74] G. M. Ziegler. Fans, Arrangements, Zonotopes, and Tilings. In *Lectures on Polytopes*, pages 191–230. Springer-Verlag, 1995.